Aus dem Institut für Prophylaxe und Epidemiologie der Kreislaufkrankheiten

Klinikum der Ludwig-Maximilians-Universität München

Direktor: Prof. Dr. med. Christian Weber

The role of the proteasome in brown adipocyte development

Dissertation
zum Erwerb des Doktorgrades der Naturwissenschaften

an der Medizinischen Fakultät der

Ludwig-Maximilians-Universität München

vorgelegt von

Nienke Willemsen

aus

Zwolle (die Niederlande)

2024

Mit Genehmigung der Medizinischen Fakultät
der Universität München

Betreuer: Prof. Dr. rer. nat. Alexander Bartelt

Zweitgutachter: Prof. Dr. rer. nat. Jürgen Bernhagen

Dekan: Prof. Dr. med. Thomas Gudermann

Tag der mündlichen Prüfung: 06. November 2024

Affidavit

Affidavit

Willemsen, Nienke

_____

Surname, first name

_____

Street

_____

Zip code, town, country

I hereby declare, that the submitted thesis entitled:

The role of the proteasome in brown adipocyte development

……………………………………………………………………………………………….

is my own work. I have only used the sources indicated and have not made unauthorised use of services of a third party. Where the work of others has been quoted or reproduced, the source is always given.

I further declare that the dissertation presented here has not been submitted in the same or similar form to any other institution for the purpose of obtaining an academic degree.

Munich, 29/11/2023   Nienke Willemsen

_____   _____

place, date   Signature doctoral candidate

1. Table of contents

2.   List of abbreviations

Abbreviation	Definition
^{18}FDG	18-fluorodeoxyglucose
19S	Proteasome regulatory particle, also known as RP
20S	Proteasome core particle, also known as CP
26S	Constitutive proteasome
30S	Constitutive proteasome built out of one 20S and two 19S components
Atf3	Activating transcription factor 3
ATP	Adenosine triphosphate
BAT	Brown adipose tissue
BMI	Body mass index
cAMP	Cyclic adenosine monophosphate
CANDLE	chronic atypical neutrophilic dermatosis with lipodystrophy and elevated temperature
CL-316,243	Disodium 5-[(2R)-2-[[(2R)-2-(3-Chlorophenyl)-2-hydroxyethyl]amino]propyl]-1,3-benzodioxole-2,2-dicarboxylate hydrate
CNS	Central nervous system
Ddi2	DNA damage-inducible 1 homolog 2
DUB	Deubiquitinating enzyme
ER	Endoplasmic reticulum
FA	Fatty acid
FATP	Fatty acid transporter
Glut4	Glucose transporter type 4
Gpr3	G-coupled protein receptor 3
HSL	Hormone sensitive lipase
iBAT	Interscapular brown adipose tissue
MAPK	Mitogen activated protein kinases
MHC	Major histocompatibility complex
Myf5	Myogenic factor 5
NE	Norepinephrine
NEFA	Non-esterified fatty acid
Nfe2l1	Nuclear factor erythroid-2-like 1, also known as Nrf1 or TCF11

Ngly1	N-glycosylated by N-glycanase 1, also known as PNGase
NST	Non-shivering thermogenesis
PA	Proteasome activator
PKA	Protein kinase A
PRAAS	Proteasome-associated auto-inflammatory syndrome
Proteostasis	Protein homeostasis
Psm(x)	Proteasome subunit (x)
SCAT	Subcutaneous adipose tissue
Ub	Ubiquitin
Ucp1	Uncoupling protein 1
UPS	Ubiquitin proteasome system
WAT	White adipose tissue
β-AR	Beta-adrenergic receptor

3.   List of publications

Publications that are part of this thesis:

Publication I: <u>Willemsen N</u>, Arigoni I, Studencka-Turski M, Krüger E, Bartelt A. Proteasome dysfunction disrupts adipogenesis and induces inflammation via ATF3. *Mol. Metab*. May 2022, 101518.

Publication II: Koçberber Z*, <u>Willemsen N</u>*, Bartelt A. The role of proteasome activators PA28αβ and PA200 in brown adipocyte differentiation and function. *Frontiers in Endocrinology*. May 2023, 2;14:1176733.

Additional research articles:

Kotschi S, Jung A, <u>Willemsen N</u>, Ofoghi A, Proneth B, Conrad M, Bartelt A. NFE2L1-mediated proteasome function protects from ferroptosis. *Mol. Metab*. Jan 2022; 101436.

Reviews and comments:

<u>Willemsen N</u>, Bartelt A. Breathe and burn: Novel roles for myoglobin in thermogenesis. *Clinical and Translational Discover*. Dec 2022; 2 (4), e153.

<u>Willemsen N</u>*, Kotschi S*, Bartelt A. Fire up the pyre: inosine thermogenic signalling for obesity therapy. *STTT*. Dec 2022; 7(1), 1-2.

Lemmer IL*, <u>Willemsen N</u>*, Hilal N, Bartelt A. A guide to understanding endoplasmic reticulum stress in metabolic disorders. *Mol Metab*. 2021 Jan;101169

Pre-prints:

Ofoghi A, Kotschi S, Lemmer IL, Haas DT, <u>Willemsen N</u>, Bayer B, Moeller S, Haberecht-Mueller S, Krueger E, Krahmer N, Bartelt A. Activating the NFE2L1-ubiquitin-proteasome system by DDI2 protects from ferroptosis. *bioRxiv*, 2023.07. 04.547652

Lemmer IL, Haas DT, <u>Willemsen N</u>, Kotschi S, Toksoez I, Gjika E, Khani S, Rohm M, Diercksen N, Nguyen PBH, Menden MP, Egu DT, Waschke J, Larsen S, Ma T, Gerhart-Hines Z, Herzig S, Dyar K, Krahmer N, Bartelt A. Nfe2l1-mediated proteasome function controls muscle energy metabolism in obesity. *bioRxiv*, 2023.04. 20.537611

*shared first authorship

4.   Contribution to the publications

4.1 Contribution to Publication I: Willemsen et al. 2022

This section will outline my contribution to the publication "Proteasome dysfunction disrupts adipogenesis and induces inflammation van ATF3" **(1)**. The authors will be discussed with their initials.

A.B. initially proposed the project, acquired funding for the project, which included the grant application for the LMU medical faculty program FöFoLe for MD students. On this grant, I.A. was recruited. A.B. also established the collaboration with M.S.T. and E.K. in order to work with their established mouse model. During the project, A.B. provided supervision of both N.W. and I.A., and maintained communication with M.S.T. and E.K.

All experiments were performed by me or by I.A. under my supervision. I designed and wrote protocols for all experiments. Data acquired by I.A. were discussed with me. I.A. will use the data of her experiments for her monographic thesis (Thesis I.A., in preparation). She analysed her own data and prepared her own graphs for her thesis. However, for the publication, I re-analysed her data and prepared new graphs. The following figures were prepared with data from I.A.: 1A, 1D, 1E, 2I, and S3A-E.

I.A. also acquired data that were not used in the publication but laid the foundation for later experiments that were used for the publication and have therefore similar experimental set-ups. Some of that data will be used in her thesis.

I wrote the first draft of the manuscript. A.B. and I then edited the manuscript together, with input from I.A., M.S.T, and E.K. To prepare the manuscript for publication, A.B. and I responded to the reviewers' questions in a rebuttal and revised the manuscript, and I did the revision experiments and prepared the graphs with input from A.B.

4.2 Contribution to Publication II: Koçberber, Willemsen & Bartelt 2023

This section will outline my contribution to the publication "The role of proteasome activators PA28ab and PA200 in brown adipocyte differentiation and function" **(2)**. The authors will be discussed with their initials.

A.B. initially proposed the project and acquired funding for the project. A.B. and I designed the outline of the project together, and I designed the experiments with input from A.B. and Z.K.

All experiments were performed by me and/or Z.K. During this project, Z.K. was a master's student who fell under my daily supervision. All experiments were performed together at least once and then analysed by me. Z.K. performed replication experiments independently and analysed her data independently with input from me and A.B.

I designed the outline of the manuscript, Z.K. prepared the first draft of the graphs and of the "methods" section in the manuscript. I edited the graphs and prepared the draft for the manuscript. The manuscript was then edited by me and A.B.

For publication, I performed the revision experiments, revised the manuscript, and wrote the rebuttal letter with input from A.B.

5.   Introduction

In our modern society, obesity and related cardio-metabolic diseases are affecting a large portion of the population, and prevalence is rising **(3,4)**. Obesity, defined as having a body mass index (BMI) over 30 (kg/m^2), has given adipose tissue a bad reputation. However, adipose tissue plays a key role in our energy metabolism and is paramount for our metabolic health. The development of adipose tissue, the differentiation of pre-adipocytes into mature adipocytes is therefore vital for systemic metabolism. The research papers featured in this thesis have each investigated genes related to protein degradation, namely proteasome subunits, and their role in adipocyte differentiation and brown adipocyte function **(1,2)**. The introductory chapters leading up to these papers will discuss the function and mechanism of brown adipose tissue (BAT) **(Chapter 4.1)**, and the function and mechanism of the proteasome and its building blocks **(Chapter 4.2)**. Finally, I will briefly outline the primary research objectives of this thesis.

5.1 Introduction of brown adipose tissue (BAT)

Adipocytes, or fat cells, are specialized cells that store nutrient energy in the form of lipid droplets, and they are dispersed in specific adipose depots as well as in other organs **(4,5)**. The white adipocyte is the most abundant and most studied adipocyte subtype, characteristically with one large lipid droplet, with important functions in energy storage, nutrient homeostasis, and endocrine signalling, as well as in immunity, reproduction, and body temperature regulation **(5)**. In addition to white adipocytes, many mammals, including humans, possess thermogenic adipocytes: brown adipocytes that are mainly found in BAT depots and beige, or brite, adipocytes that are scattered in white adipose tissues (WAT). These thermogenic adipocytes have properties that do not only distinguish them from white adipocytes but gives them a unique role in energy and nutrient metabolism. This chapter will first outline the function and origin of BAT, before describing the cellular mechanisms that underlie non-shivering thermogenesis (NST). Finally, the implications of BAT in human health and disease are discussed.

5.1.1 The function and origin of BAT

Thermogenic adipocytes are remarkably dynamic cells that play a central role in the thermoregulation of many mammals. Thermogenic adipocytes have the capacity to produce heat independently of muscle tone or muscle activity, i.e. NST. This is particularly important for newborns and small mammals like rodents in order to maintain their core body temperature **(6,7)**. Thermogenic adipocytes are distinguishable from white adipocytes by their unique expression of Uncoupling protein 1 (*Ucp1*), their multilocular lipid droplets intracellular structure, and high amounts of mitochondria. In mice, most beige adipocytes are located in subcutaneous adipose tissue (SCAT). This thesis focusses on BAT and brown adipocytes, but most information on cellular processes is applicable for all thermogenic adipocytes. BAT consists of a variety of cells, most notably pre-adipocytes, brown adipocytes, endothelial cells, immune cells, and fibroblasts **(8)**. Pre-adipocytes originate from several distinct lineages, but classical brown pre-adipocytes stem from Myogenic factor 5 (Myf5)-positive progenitors, the same lineage that gives rise to skeletal myocytes **(9)**. Differentiation from Myf5 progenitors is driven by the transcription factor Prdm16 **(10,11)**. In mice, the largest BAT depot is interscapular BAT (iBAT). This and other BAT depots are highly innervated, which allows for the sympathetic activation by nervous system, as well as highly vascularized, which allows both for the fast supply of nutrients as well as the effective transfer of heat to the body. BAT already

develops in the fetus and is most active in newborns **(6,7)**. During aging, the number of thermogenic adipocytes decline, a process that is accelerated by high ambient temperatures and high-fat diets. However, thermogenic adipocytes are recruited upon cold exposure, which causes both the activation of brown and beige adipocytes, the increased browning of thermogenic adipocytes, and de novo differentiation of thermogenic adipocytes from pre-adipocytes **(6,12)**. There is evidence that white adipocytes are able to trans-differentiate into beige adipocytes under specific conditions **(11)**. In addition to cold exposure, other thermogenic factors have been identified over the years, like certain high-fat diets **(13,14)**, exercise **(15)**, and pharmaceutical drugs **(16)**. Regardless of the trigger, subsequent activation of thermogenic adipocytes leads to NST through Ucp1-dependent and independent futile cycling. Notably, this is a high energy- and nutrient-consuming process **(17,18)**. The capacity of massive nutrient clearance from circulation, gave BAT the name 'metabolic sink'. The energy consumption and the clearance of glucose and lipids by BAT strongly affect systemic energy metabolism. Although difficult to prove, researchers have argued that BAT has an evolutionary protective role against over-eating **(19)**. Increasing BAT activity protects mice against diet-induced obesity **(19–21)**. BAT may also impact systemic metabolism by secreting hormones or signaling peptides, collectively called batokines **(22)**. For example, the batokine Neuregulin 4 reduces fat storage in the liver, affecting lipid metabolism and insulin sensitivity in mice **(23)**. Finally, activation of thermogenic adipocytes leads to remodeling of the adipose depots and affects adipose-tissue residing immune cells **(5)**. In conclusion, BAT plays a prominent role in thermoregulation and modulates systemic energy metabolism.

5.1.2 The cellular mechanism of thermogenic adipocytes

As mentioned above, thermogenic adipocytes are activated upon cold exposure to produce heat. In the classical pathway, thermogenic cues like cold prompt the sympathetic nervous system to send norepinephrine (NE) to thermogenic adipocytes. NE binds to the beta-adrenergic receptors on the membrane of thermogenic adipocytes **(Figure 1)**. This results in increase of intracellular cyclic adenosine monophosphate (cAMP), which activates protein kinase A (PKA), which activates a cascade of lipases promoting lipolysis and increasing free fatty acids within the cells **(6)**. To supplement the intracellular fatty acid reserve, thermogenic adipocytes will produce non-esterified fatty acids (NEFAs) from triglycerides from the circulation **(17)**. NEFAs interact with Ucp1 in the mitochondrial membrane. Under thermoneutral conditions, Ucp1 is present in the mitochondrial membrane but constantly inhibited by purine nucleotides. Fatty acid binding undoes this inhibition, effectively activating Ucp1 **(24)**. Ucp1 is a carrier protein that shuttles protons back from the intermembrane space to the mitochondrial matrix. Consequently, oxidation is uncoupled from ATP synthesis, which results in "wasting" of chemical energy into heat. In parallel to lipolysis and Ucp1 activation, the cAMP-PKA pathway activates mitogen-activated protein kinases (MAPKs) which drive the increased transcription of thermogenic genes, including *Ucp1* and *Ppargc1a* **(25)**. Additionally, cAMP-PKA activates the mTOR pathway that leads to increased levels of glucose transport type 4 (Glut4) on the cell membrane **(26)**. These processes all take place acutely after cold exposure **(17,26)**. In order to meet the increased energetic demand of BAT, other tissues like WAT will also increase lipolysis **(27)**. After pro-longed cold exposure, i.e. over 24h in mice, BAT undergoes remodeling during which pre-adipocytes are differentiated into brown adipocytes, and brown adipocytes undergo increased browning **(6,12)**. Although Ucp1 was classically seen as the essential node for both acute and sustained NST, Ucp1 ablation does not completely disable cold adaption in mice, suggesting Ucp1-independent mechanisms of NST **(28)**. Futile cycles are cycles of two opposing metabolic reactions that dissipate chemical energy and, as a consequence, produce heat in adipocytes. Over the years, the creatine futile cycle **(29)**, the lipid futile cycle **(30)**, and calcium-ion (Ca^{2+})

futile cycle **(31)** were all described to contribute to NST. On top of that, NST could also be induced through non-sympathetic pathways, either amplifying or replacing adrenergic signaling. A recently emerged example of these 'alternative' agents is myoglobin **(32,33)**. Intriguingly, intracellular lipolysis can also activate thermogenesis, for example through G-coupled protein receptor 3 (*Gpr3*) expression **(21)**. In summary, the pathways leading to NST are intricate and likely interact with and amplify each other.
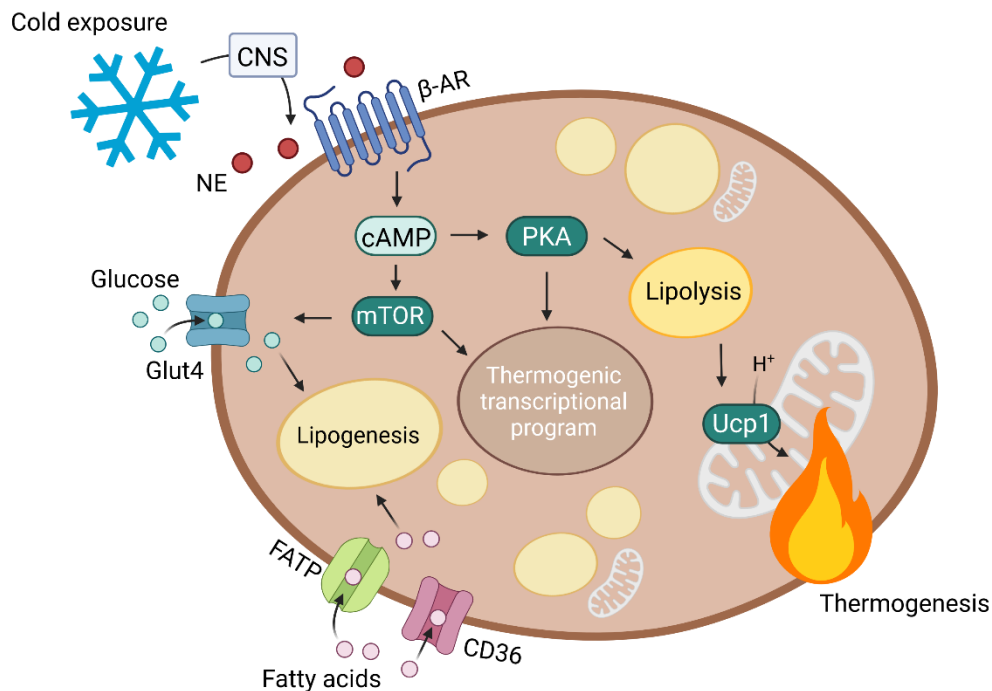
Figure 1: Simplified model of the thermogenic pathway. Cold exposure initiates NE-release by the CNS, which binds to β-ARs. This increases intracellular cAMP levels which induces several pathways leading to increased glucose and fatty acid uptake, increased transcription of thermogenic genes, and increased lipolysis. The released fatty acids activate Ucp1 on the membrane which uncouples proton transport from ATP production, resulting in thermogenesis. (CNS = central nervous system, NE = norepinephrine, β-AR = Beta-adrenergic receptor, cAMP = cyclic AMP, PKA = protein kinase A, Ucp1 = uncoupling protein 1, FATP = fatty acid transporter, Glut4 = glucose transporter type 4). The figure was created with Biorender.com

5.1.3 The role of human BAT in metabolic health

For a long time, it was thought that humans 'lose' all their BAT after newborn stage, but in 2009, PET-CT scanning revealed that BAT depots remain in adults **(34,35)**. Even though BAT is presumably not required to maintain body temperature, it remains functionally active in many adults **(34,36)**. Baseline BAT activity most likely only insignificantly contributes to energy expenditure **(37)**. However, calculations of human BAT activity could be underestimating the true activity, as the common measurement technique by 18-fluorodeoxyglucose (^{18}FDG) PET/CT scan might not adequately reflect BAT activity **(38)**. BAT can be activated in adults upon cold exposure, through "thermogenic" diet, or drugs, and this increases energy expenditure and nutrient consumption **(14,34,35,39,40)**. Furthermore, human BAT activity is positively associated with cardio-metabolic health **(36)**. An intervention study in mice shows that BAT transplantation is sufficient to reverse obesity **(41)**. Altogether, this makes BAT an attractive pharmaceutical target to treat (cardio)metabolic disorders. An important caveat here,

however, is that BAT is classically activated sympathetically. Activating agents that mimic norepinephrine will also act on adrenergic receptors on other tissues, like cardiac muscle, which brings cardiovascular risks **(42)**. As a consequence, there is interest in other therapeutic avenues, like activating thermogenic adipocytes in an alternative, non-sympathetic pathway **(21)**, by increasing diet-induced thermogenesis **(19)**, or by preventing age- and obesity- associated decline in BAT activity **(35,43)**. Unlocking the potential of NST, could substantially contribute to metabolic health.

5.2 Introduction of the proteasome

To maintain protein homeostasis (proteostasis), all cells including adipocytes undergo continuous surveillance and adaptive remodeling of their protein content through regulating protein synthesis and protein degradation. Appropriate protein degradation is vital to maintain cellular health **(44)**. In essence, protein degradation has four main roles: the removal of misfolded and erroneous proteins, the temporal regulation of proteins, the freeing of peptides and cofactors to be recycled for protein synthesis, and regulation of the immune response. To coordinate these processes, protein degradation is tightly regulated over two major axes: the ubiquitin-proteasome system (UPS) and lysosomal autophagy **(44,45)**. Any genetic malfunction in these processes lead to severe disease in humans. In this chapter, I will focus on the proteasome and its role in protein degradation. I will first discuss the broad mechanism of the UPS **(Chapter 4.2.1)**, and secondly non-constitutive proteasomes and their place in proteostasis **(Chapter 4.2.2)**, and finally proteasome associated auto-inflammatory syndromes (PRAAS) **(Chapter 4.2.3)**.

5.2.1 UPS and the constitutive proteasome

The proteasome is multi-subunit complex with a cylinder-shaped core particle with proteolytic activities, and can be found both in the cytosol as well as in the nucleus. This core particle (20S, or CP) is built of 28 proteasome subunits **(46)**. The constitutive 26S proteasome has one or two regulatory particles (19S, also known as RP, or PA700) attached to the core particle. These 19S particles are composed of 20 subunits and they regulate access to the catalytic core **(47,48)**. To select proteins for degradation by the proteasome, cells have an intrinsic tagging-system by Ubiquitin (Ub) in place **(Figure 2A)**. Ub conjugation to proteins is controlled by a cascade of enzymes. Briefly, there are three enzymatic steps leading to Ub binding. First, E1 ligases activate Ub in an adenosine triphosphate (ATP)-dependent manner. Secondly, Ub is transferred to an E2 ligase, and lastly, E3 ligases bind the ubiquitin to the targeted substrate **(45)**. Substrates are selected through the substrate specificity of the E3 ligases **(49)**. Classically, Ub was thought to only bind to lysine residues of substrates, but it was also found to bind to other residues **(49)**. If only one Ub binds to the substrate, the substrate is mono-ubiquitinated. However, frequently, more Ub attaches to one of seven lysine side chains of the initial Ub – Lys^6, Lys^{11}, Lys^{27}, Lys^{29}, Lys^{33}, Lys^{48}, or Lys^{63} – which leads to multi-ubiquitination. These polymeric Ub chains can occur in both single or branched chains, leading to a high variety of possible Ub chains **(49)**. The Ub tags will recruit proteins with ubiquitin-binding domains, some of which will initiate translocation of the Ub-substrate complex to the proteasome for degradation. However, it should be noted that Ub-tagging can also prime substrates for lysosomal-autophagy, influence protein location or protein-protein interaction, or initiate other signalling pathways **(45,49,50)**. When the Ub-substrate complex arrives at the proteasome, the proteasome initially binds to the ubiquitin chain. This process is reversible, and can be undone when deubiquitinating enzymes (DUBs) interfere

(51). The longer the Ub-chain, the higher the chance that the substrate will eventually be degraded by the proteasome **(52)**, but even mono-ubiquitin attachment to substrates increases its likelihood for degradation **(53)**. The window of reversible binding closes once the 19S particle of the constitutive proteasome binds to the substrate through binding by a ring-shaped complex of six ATPases **(54,55)**. The 19S particle will guide the substrate in the 20S cylinder. Once inside the cylinder, the substrate is exposed to three subunits with proteolytic active sites, namely Psmb6 (also known as β1, encoded by *Psmb6*), Psmb7 (also known as β2, encoded by *Psmb7*), and Psmb5 (also known as β5, encoded by *Psmb5*). These subunits are associated with caspase-like, trypsin-like, and chymotrypsin-like activity, respectively **(48)**. The catalytic activities break down the substrates to peptides that are let out again into the cytosol. UPS is required to adequately and timely terminate misfolded, erroneous or obsolete proteins. Under proteostatic conditions, the transcription factor Nuclear factor erythroid-2-like 1 (Nfe2l1, also known as Nrf1 or TCF11) is constantly degraded by the proteasome. However, when the UPS cannot meet the proteolytic demand of cell, ubiquitination levels rise and Nfe2l1 escapes degradation **(56,57)**. Nfe2l1 is an endoplasmic reticulum (ER) resident protein that gets de-N-glycosylated by N-glycanase 1 (Ngly1, also known as PNGase), ubiquitinated, and cleaved into its active form by protease DNA damage-inducible 1 homolog 2 (Ddi2) **(58–60)**. Consequently, Nfe2l1 transfers to the nucleus to amplify transcription of all constitutive proteasome subunits **(61)**. This feedback loop allows for an adaptive proteasome response in the cell. Ultimately, the UPS is a complex, tightly regulated system and its proper function is vital for cell and organism survival and function.
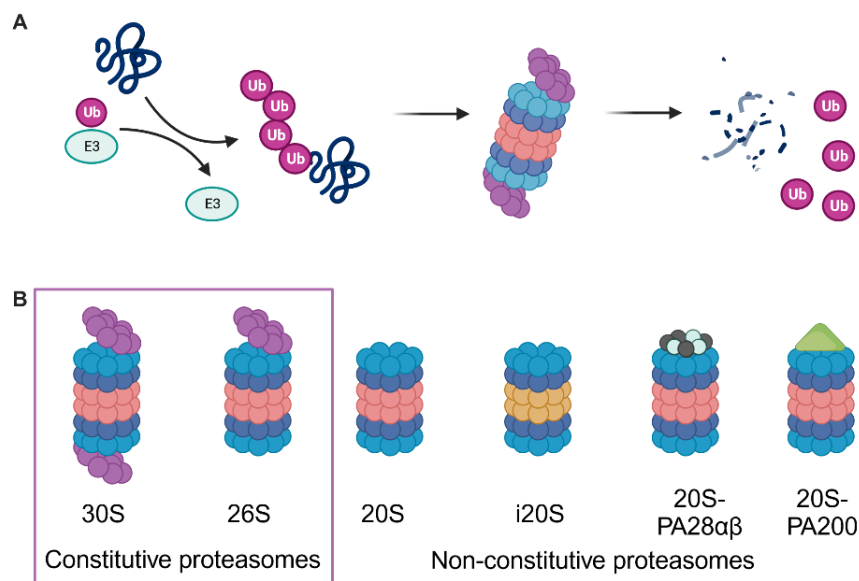

Figure 2. **(A)** A simplified model of UPS. E3 ligase bind the targeted substrate to ubiquitin. (Multi-)ubiquitinated proteins are translocated to the proteasome where they are degraded to peptides. **(B)** Different constitutive and non-constitutive proteasome subtypes. Made by Biorender.com

5.2.2 Non-constitutive proteasomes

As discussed above, the constitutive proteasome consists of a 20S core and one or two 19S lids, commonly called 26S or 30S, respectively. Access to the 26S or 30S proteasome is ubiquitin- and ATP-dependent. Aside

from these constitutive proteasomes, other subtypes of proteasomes have been identified, and their heterogeneity speaks to the variety of proteostatic needs within the cell **(Figure 2B)**. First, the 20S core particle can undergo structural changes. In response to interferon signalling, constitutive proteasome subunits can be exchanged for alternative immunoproteasome subunits (β1 to β1i, β2 to β2i, and β5 to β5i) **(62)**. The newly formed immunoproteasome performs a key step in the immune response by producing peptides for antigen presentation by the major histocompatibility complex (MHC) class I molecules **(63)**. Additionally, they are implicated to modulate cell differentiation **(64)**. Both the 20S as well as the immune-20S (i20S) can be found without attachments in the cell. Whereas previously thought as merely the building block for 26S or 30S, the 20S variant also functions independently **(65,66)**. Alternatively, 20S can bind to regulators different than 19S, namely proteasome activators (PAs) that function independently of ubiquitin and ATP **(67,68)**. ATP- and ubiquitin-independent proteolysis mainly seems to target unfolded proteins, for example proteins that denature due to oxidative stress **(69)**. There are three types of PAs classified: cytosolic PA28αβ (multi-subunit complex, also known as 11s or REG), nuclear PA28γ (also known as 11S or Psme3, encoded by *Psme3*), and PA200 (also known as Psme4 or Blm10, encoded by *Psme4*). The PA28αβ complex is built out of four PA28α (or Psme1, encoded by *Psme1*) and three PA28β (or Psme2, encoded by *Psme2*) subunits **(70)**. Functionally, PA28αβ is mostly associated with the immunoproteasome and oxidative stress **(71,72)**. PA28γ mediates nucleus proteostasis **(48)**. The function of PA200 is more elusive, but it may play roles in DNA repair and regulation of proteasome activity **(67,73,74)**. There are other proteasome subtypes and hybrid shapes that are not discussed here, but altogether they underscore the complexity of regulating protein degradation and peptide signalling.

5.2.3 Proteasome Associated Auto-inflammatory Syndromes (PRAAS)

Human diseases caused by mutations in genes coding for proteasome subunits or their transcription factors are rare, likely because loss-of-function of the constitutive proteasome is lethal for any cell or organism **(75,76)**. However, some patients with severe auto-inflammatory syndromes were found to have rare pathogenic mutations in proteasome subunit or proteasome assembly genes. These patients often present with developmental delay, joint contractures, muscle atrophy, lipodystrophy, bouts of fevers, and systemic inflammation **(77,78)**. Over the years, these diseases were described by different groups under different names, most notably as chronic atypical neutrophilic dermatosis with lipodystrophy and elevated temperature (CANDLE) **(77)**, Nakajo-Nishimura syndrome **(79)**, panniculitis-induced lipodystrophy (JMP), POMP-related auto-inflammation and immune dysregulation disease, and proteasome-associated auto-inflammatory syndrome (PRAAS) **(78,80)**. In this thesis, I will primarily use PRAAS as an overarching name for proteasome-subunit related disorders. There are several mutations identified in patients that lead to PRAAS, one of the more prevalent and most well-studied group of mutations are missense mutations in *PSMB8* (encoding for PSMB8, also known as β5i or LMP7) **(81,82)**. Other patients have mutations in *PSMB4* (encoding for PSMB4, also known as β7) **(82)**. As Psmb8 is exclusively part of the immunoproteasome, whereas Psmb4 is found in all proteasome variants, it is unclear whether mutations in their genes lead to the same disease mechanism. However, these mutations do all seem to lead to decreased proteasome activity, increased ubiquitination, and increased type I interferon (IFN) response **(78,82,83)**. This increased IFN type I response might be a response to intracellular proteasome impairment, and the dysregulated innate immune response is thought to result in most of the symptoms present in patients **(78)**. However, the precise disentanglement of affected pathways is still unclear. For example, it is unknown if lipodystrophy in patients is solely caused by dysregulated immune activity of immune cells, by proteasome impairment in adipocytes, or by a combination of both. There is currently no cure for PRAAS, but

patients often receive anti-inflammatory drugs like JAK inhibitors to alleviate their symptoms **(84)**. Determining the effects of (mutations in) proteasome subunits on different cell types would clarify the disease mechanisms in patients and could therefore contribute to disease management.

5.3 Research objectives

The observation that cold exposure increases proteasome activity in BAT led to the hypothesis that an adaptive proteasome response is required for NST **(85)**. Following on this, the transcription factor Nfe2l1 was shown to be required for NST, which linked fundamental UPS biology to BAT physiology **(85)**. In this thesis, I further explored the function of proteasome in both brown adipocyte differentiation and activation by zooming in on specific proteasome subunits. Firstly, I studied the role of proteasome subunits Psmb4 and Psmb8, as mutations in genes coding for these proteins cause PRAAS. Investigating the role of Psmb4 and Psmb8 in brown adipocytes can not only extend our knowledge on UPS biology in a physiological context, it could also improve our understanding of the observed lipodystrophy in PRAAS patients **(1)**. In the second research paper, I focused on PA28 and PA200 as their roles in UPS and cell biology are partially elusive and mainly studied in the context of yeast. Studying these PAs in the context of brown adipocyte differentiation and activation, will further enhance our understanding of their roles in proteostasis **(2)**. These research projects advance our basic comprehension of proteasome biology and the mechanisms underlying brown adipocyte differentiation and activation.

6.   Summary (in English)

Brown adipocytes are a specialized type of fat cells that can produce heat through uncoupling energy consumption from ATP production, which is referred to as non-shivering thermogenesis (NST). The development of mature brown adipocytes from pre-adipocytes already takes place in the placenta, but can be amplified later in life under the influence of environmental cues, like cold and diet. During differentiation into mature brown adipocytes, cells undergo extensive remodeling. Arguably, this remodeling requires appropriate protein degradation to remove faulty proteins and to free up amino acids for re-building new proteins. The bulk of intracellular protein degradation is done by the proteasome, a multi-subunit complex with a catalytic core. The two publications featured in this thesis explore the role of different proteasome subunits in the differentiation and activation of brown adipocytes.

In Willemsen et al. 2022 **(1)**, we studied the effects of loss of proteasome subunit beta 4 (Psmb4) and beta 8 (Psmb8, or Lmp7) on brown adipocyte development and activity in vitro. Loss-of-function mutations can cause rare proteasome associated auto-inflammatory syndromes (PRAAS), also known as Chronic Atypical Neutrophilic Dermatosis with Lipodystrophy and Elevated Temperature (CANDLE). As the name suggests, PRAAS/CANDLE patients suffer from lipodystrophy and fevers, which led to the hypothesis that loss of Psmb4/Psmb8 leads to impaired (brown) adipocyte development. We downregulated these genes through reverse transfection in immortalized mouse (brown) adipocyte cell-lines. The cells were then differentiated and analyzed with assays to measure ubiquitin proteasome system, adipogenesis, lipogenesis, lipolysis, inflammation and respiration. Surprisingly, loss of Psmb4 but not Psmb8 impaired proteostasis and adipogenesis. *Psmb4* knockdown (KD) disrupted proteasome assembly, and cells displayed high levels of stress and inflammation. We identified stress marker Activating transcription factor 3 (Atf3) as the link between disrupted proteasome activity and inhibited adipocyte development. *Atf3* KD prevented loss of adipogenesis and thermogenesis, without affecting the upstream *Psmb4* KD effects on protein degradation.

In Koçberber, Willemsen et al. 2023 **(2)**, we studied the effects of loss of proteasome activators (PAs) Pa28α (encoded by *Psme1*) and Pa200 (encoded by *Psme4*) on brown adipocyte development and activity, applying the same approach as in the previous study. PAs bind to the barrel-shaped 20S core structure of the proteasome and most likely act as selective gate-keepers to the proteolytic core. However, the physiological roles of PAs, especially in brown adipocytes, was unknown. In our experimental set-up, brown adipocytes did not require Pa28 and/or Pa200 for proteasome assembly or activity, nor for brown adipogenesis or NST.

In summary, the development of brown adipocytes requires a functional proteasome, but not all proteasome subunits are necessary to support in vitro adipogenesis. These works are linking fundamental proteasome biology and physiologic brown adipose tissue, contributing to our basic understanding of protein balance in cell and tissue development.

7.   Zusammenfassung (deutsch)[1]

Braune Adipozyten sind eine spezialisierte Art von Fettzellen, die durch Entkopplung des Energieverbrauchs von der ATP-Produktion Wärme erzeugen können, was als Nicht-zitternde Wärmebildung (Englisch: Non-Shivering-Thermogenesis (NST)) bezeichnet wird. Die Entwicklung differenzierter brauner Adipozyten aus Präadipozyten findet bereits in der Plazenta statt, kann aber später im Leben durch den Einfluss von Umwelt-faktoren wie Kälte und Ernährung verstärkt werden. Während der Differenzierung zu braunen Adipozyten wer-den die Zellen umfassend umgebaut. Dieser Umbau erfordert einen angemessenen Proteinabbau, um fehler-hafte Proteine zu entfernen und Aminosäuren für den Wiederaufbau neuer Proteine freizusetzen. Der Großteil des intrazellulären Proteinabbaus erfolgt durch das Proteasom, einem Komplex bestehend aus mehreren Un-tereinheiten mit einem katalytischen Kern. Die beiden in dieser Thesis vorgestellten Arbeiten untersuchen die Rolle verschiedener Proteasom-Untereinheiten bei der Differenzierung und Aktivierung von braunen Adipozyten.

In Willemsen et al. 2022 **(1)** untersuchten wir die Auswirkungen des Verlusts der Proteasom-Untereinheiten beta 4 (Psmb4) und beta 8 (Psmb8, oder Lmp7) auf die Entwicklung und Aktivität brauner Adipozyten in vitro. Funk-tionsverlust-Mutationen können seltene Proteasom-assoziierte autoinflammatorische Syndrome (PRAAS) ver-ursachen, die auch als chronische atypische neutrophile Dermatose mit Lipodystrophie und erhöhter Temperatur (CANDLE) bekannt sind. Wie der Name schon sagt, leiden PRAAS/CANDLE-Patienten an Lipodystrophie und Fieber, was zu der Hypothese führte, dass der Verlust von Psmb4/Psmb8 zu einer gestörten (braunen) Adipozy-tenentwicklung führt. Wir haben diese Gene durch reverse Transfektion in immortalisierten (braunen) Adipozy-ten-Zelllinien der Maus herunterreguliert. Die Zellen wurden dann differenziert und mit Assays zur Messung des Ubiquitin-Proteasom-Systems, der Adipogenese, der Lipogenese, der Lipolyse, der Entzündung und der Atmung analysiert. Interessanterweise beeinträchtigte der Verlust von Psmb4, nicht aber von Psmb8, die Proteostase und Adipogenese. Der Knockdown (KD) von *Psmb4* führte zu einer Unterbrechung der Proteasom-Assemblie-rung, und die Zellen zeigten ein hohes Maß an Stress und Entzündungen. Wir identifizierten den Stressmarker Aktivierender Transkriptionsfaktor 3 (Atf3) als Bindeglied zwischen der gestörten Proteasomaktivität und der gehemmten Adipozytenentwicklung. *Atf3* KD verhinderte den Verlust der Adipogenese und Thermogenese, ohne die vorgelagerten *Psmb4* KD-Effekte auf den Proteinabbau zu beeinträchtigen.

In Koçberber, Willemsen et al. 2023 **(2)** untersuchten wir die Auswirkungen des Verlusts der Proteasom-Aktiva-toren (PA) PA28α (kodiert durch *Psme1*) und PA200 (kodiert durch *Psme4*) auf die Entwicklung und Aktivität brauner Adipozyten, wobei wir den gleichen Ansatz wie in der vorherigen Studie verwendeten. PA binden an die zylinderförmige 20S-Kernstruktur des Proteasoms und fungieren höchstwahrscheinlich als selektive Einlasskon-trolleure für den proteolytischen Kern. Die physiologische Rolle der PA, insbesondere in braunen Adipozyten, war jedoch unbekannt. In unserem Versuchsaufbau benötigten braune Adipozyten weder Pa28 und/oder Pa200 für den Aufbau oder die Aktivität des Proteasoms noch für die braune Adipogenese oder NST.

Zusammenfassend lässt sich sagen, dass die Entwicklung von braunen Adipozyten ein funktionierendes Pro-teasom erfordert, dass aber nicht alle Proteasom-Untereinheiten notwendig sind, um die Adipogenese in vitro zu unterstützen. Diese Arbeiten stellen eine Verbindung zwischen der grundlegenden Proteasombiologie und der Physiologie des braunen Fettgewebes her und tragen zu unserem grundlegenden Verständnis des Protein-gleichgewichts bei der Zell- und Gewebeentwicklung bei.

---

[1]First draft was made with DeepL (https://www.deepl.com/en/translator)

8.   Publication I: Willemsen et al. 2022

Proteasome dysfunction disrupts adipogenesis and induces inflammation via ATF3

Nienke Willemsen[1], Isabel Arigoni[1], Maja Studencka-Turski[2], Elke Krüger[2] & Alexander Bartelt[1,3,4,5**]

[1]Institute for Cardiovascular Prevention (IPEK), Ludwig-Maximilians-University, Munich, Germany, [2]Institute of Medical Biochemistry and Molecular Biology, University Medicine Greifswald, Greifswald, Germany, [3]German Center for Cardiovascular Research, Partner Site Munich Heart Alliance, Technische Universität München, Munich, Germany, [4]Institute for Diabetes and Cancer (IDC), Helmholtz Center Munich, German Research Center for Environmental Health, Neuherberg, Germany, [5]Department of Molecular Metabolism & Sabri Ülker Center for Metabolic Research, Harvard T.H. Chan School of Public Health, Boston, USA

*Correspondence: Alexander Bartelt, alexander.bartelt@med.uni-muenchen.de

Keywords: brown adipose tissue, adipocytes, proteasome, ubiquitin, proteostasis, PSMB4, NFE2L1, ATF3.

Highlights

- PRAAS-associated PSMB4 is required for brown adipocyte differentiation
- Loss of PSMB4 activates NFE2L1 to counteract proteasome dysfunction
- The ATF3 pathway regulates adipocyte dysfunction and inflammation
- Loss of ATF3 restores adipogenesis in cells with loss of PSMB4

Graphical abstract
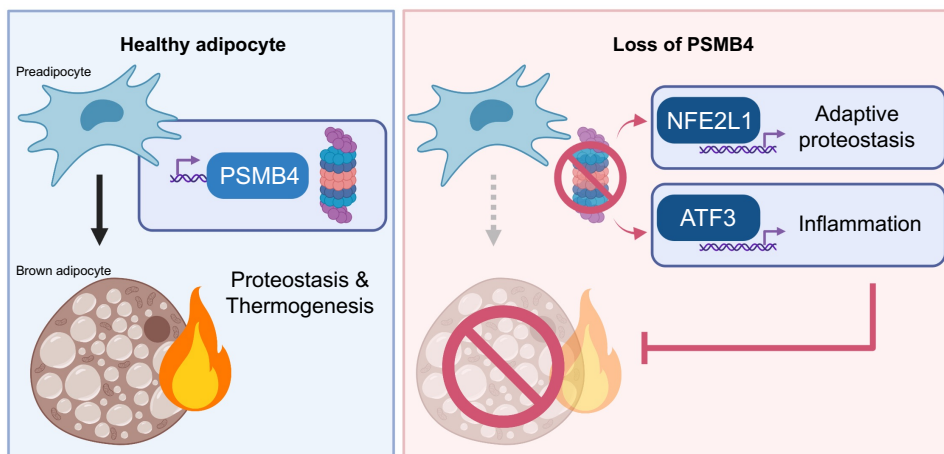
Abstract

Objective

Regulation of proteasomal activity is an essential component of cellular proteostasis and function. This is evident in patients with mutations in proteasome subunits and associated regulators, who suffer from proteasome-associated autoinflammatory syndromes (PRAAS). These patients display lipodystrophy and fevers, which may be partly related to adipocyte malfunction and abnormal thermogenesis in adipose tissue. However, the cell-intrinsic pathways that could underlie these symptoms are unclear. Here, we investigate the impact of two proteasome subunits implicated in PRAAS, Psmb4 and Psmb8, on differentiation, function and proteostasis of brown adipocytes.

Methods

In immortalized mouse brown pre-adipocytes, levels of *Psmb4*, *Psmb8*, and downstream effectors genes were downregulated through reverse transfection with siRNA. Adipocytes were differentiated and analyzed with various assays of adipogenesis, lipogenesis, lipolysis, inflammation, and respiration.

Results

Loss of Psmb4, but not Psmb8, disrupted proteostasis and adipogenesis. Proteasome function was reduced upon Psmb4 loss, but partly recovered by the activation of Nuclear factor, erythroid-2, like-1 (Nfe2l1). In addition, cells displayed higher levels of surrogate inflammation and stress markers, including Activating transcription factor-3 (Atf3). Simultaneous silencing of *Psmb4* and *Atf3* lowered inflammation and restored adipogenesis.

Conclusions

Our study shows that Psmb4 is required for adipocyte development and function in cultured adipocytes. These results imply that in humans with *PSMB4* mutations, PRAAS-associated lipodystrophy is partly caused by disturbed adipogenesis. While we uncover a role for Nfe2l1 in the maintenance of proteostasis under these conditions, Atf3 is a key effector of inflammation and blocking adipogenesis. In conclusion, our work highlights how proteasome dysfunction is sensed and mitigated by the integrated stress response in adipocytes with potential relevance for PRAAS patients and beyond.

1. Introduction

Maintenance and regulation of the proteome by the ubiquitin-proteasome system (UPS) is essential for cellular function and health. Degradation of unwanted, obsolete, or damaged proteins by UPS is critical for cells to respond to environmental cues such as nutrients, temperature, or other forms of stress. Failure of the UPS is associated with severe consequences for cellular and systemic health. Case in point, humans with mutations in genes coding for proteasomal subunits or their associated regulators, suffer from immuno-metabolic disorders. These diseases are characterized by a spectrum of rare auto-inflammatory syndromes known as proteasome associated auto-inflammatory syndromes (PRAAS), Chronic Atypical Neutrophilic Dermatosis with Lipodystrophy and Elevated Temperature (CANDLE) (1), Nakajo-Nishimura syndrome, or Joint Contractures-Muscular atrophy-microcytic anemia-Panniculitis-associated lipodystrophy (JMP) syndrome (2–4). The first discovered cause of PRAAS was a missense mutation in the gene coding for proteasome subunit beta 8 (*PSMB8,* also known as *LMP7*) (1), and since then, other loss-of-function mutations have been revealed as underlying causes, including proteasome subunit beta 4 (*PSMB4*) (5). The disease symptoms in patients, which include sterile inflammation by increased production of type I interferons (IFNs) and lipodystrophy, are likely a complex result of disturbed UPS and maladaptive activation of the unfolded protein response (UPR) (6).

The PRAAS-related genes *PSMB4* and *PSMB8* are coding for subunits of the proteasome, a complex that degrades obsolete or damaged proteins to peptides. PSMB4 and PSMB8 are subunits in the 20S core particle of the proteasome, which is a barrel-shaped structure of four heptameric rings of in total 28 subunits with a conserved modular architecture of $\alpha_{1-7}\beta_{1-7}\beta_{1-7}\alpha_{1-7}$. The active catalytic sites β1, β2, and β5 are located within this structure, which conceals them from the cytosol. The 20S core proteasome is associated with 19S regulator complexes to recognize, bind, and unfold ubiquitin-modified substrates for degradation. This allows for selective degradation of substrates that are translocated into the barrel (7). The modular structure of the proteasome is also evident in the diversity of isoforms with either alternative active sites or regulator complexes. The constitutive 26S proteasome is ubiquitously found in most cell types and is responsible for the bulk of protein degradation, as well as controls many cellular pathways including signaling, metabolism, and proliferation (8). Immunoproteasomes bear alternative active sites, and are permanently expressed in cells of hematopoietic origin, but can be induced in response to interferons in other cell types (9). Immunoproteasomes are implicated in MHC-class I antigen processing, but also in many processes beyond the immune response, such as cell differentiation (9). Whereas PSMB4/β7, is a subunit of all proteasome isoforms, PSMB8/β5i, is an inducible subunit that replaces β5 in the constitutive proteasome when the proteasome is being remodeled to an immunoproteasome (10).

PRAAS patients display several pathologies with varying degrees of severity, and aberrant inflammation and metabolic dysfunction are major hallmarks of the disease. Among these, the lipodystrophy phenotype is currently not well understood. Classically, lipodystrophy is caused by dysfunction of adipocytes, especially the ability to form healthy fat cells (11), but if PRAAS mutations cause cell-intrinsic differentiation defects or dysfunction of adipocytes has not been explored, yet. In addition, PRAAS patients suffer from recurrent fever flares, which are thought to be caused by inflammation in the central nervous system. However, body temperature is a result of several mechanisms, including adaptive thermogenesis, and it is possible that aberrant thermogenesis is involved in the pathology of PRAAS.

Brown adipose tissue (BAT) is a highly adaptive mammalian organ that is responsible for non-shivering thermogenesis (NST) (12). Stimulated by cold-induced norepinephrine (NE) and other stimuli, brown adipocytes generate heat through activity of uncoupling protein-1 (Ucp1) and other thermogenic mechanisms. The herewith associated oxidative respiration is highly energy demanding, and is fueled by intracellular and circulating nutrients (13). Prolonged cold exposure leads to remodeling of BAT (12), which induces proteotoxic pressure on brown adipocytes (14). We have previously shown that an adaptive increase in proteasomal activity was essential for the maintenance of NST (15). Adapting proteasomal activity to meet proteolytic demands is mediated by the transcription factor Nuclear factor erythroid-2, like-1 (Nfe2l1, also known as Nrf1 or TCF11). In most cell types, Nfe2l1 is continuously degraded by the proteasome, but it escapes its degradation when proteotoxic stress is increased in the cell, e.g., in the presence of chemical proteasome inhibitors. In that case, Nfe2l1 is cleaved from the ER membrane by the aspartyl protease DNA Damage Inducible 1 Homolog 2 (DDI2), translocates to the nucleus, and initiates the transcription of proteasome subunits, which results in restoration or heightening of proteasomal capacity (16,17). Lack of Nfe2l1 is associated with diminished NST, marked adipose tissue inflammation, and insulin resistance (15). Nfe2l1 was previously suggested to play a role in the disease mechanisms of PRAAS (6), but to the best of our knowledge no experimental evidence exists that Nfe2l1 is involved. Based on these findings, we hypothesized that compromised proteasome function, initiated by loss of PRAAS-related Psmb4 or Psmb8, impacts brown adipocyte proteostasis, development, function, and inflammation.

2. Materials and methods

2.1 Mice husbandry and tissue collection

All animal experiments were performed with approval of the local authorities (License: ROB-55.2-2532.Vet_02-30-32). Psmb8 whole-body knock-out mice were described previously (18,19). Animals were housed in individually ventilated cages at room temperature (22 °C), with a 12-h light–dark cycle, and fed chow-diet (Sniff) and water ad libitum. For cold exposure, wild-type C57BL/6J mice (Janvier) were housed at 30 °C or 4 °C for seven days. Mice were killed with cervical dislocation. Tissues were snap-frozen in liquid nitrogen and stored at −80 °C.

2.2 Cell culture, treatments, and reverse transfection

For cellular experiments, we used immortalized WT-1 mouse brown preadipocytes and 3T3-L1 mouse white preadipocytes. The cells were grown in DMEM Glutamax (Thermo Fisher, supplemented with 10 % v/v FBS (Sigma) and 1 % v/v PenStrep (Thermo), and incubated 37 °C, 5 % CO_2. They were continuously kept between 20-80 % confluency and split two or three times per week. Cells were used until their passage number exceeded 18. For differentiation, cells were grown to 90-100 % confluency. Then, WT-1 cells were differentiated in WT-1 induction medium (850 nM insulin (Sigma), 1 µM dexamethasone (Sigma), 1 µM T3 (Sigma), 1 µM rosiglitazone (Cayman), 500 nM IBMX (Sigma) and 125 nM indomethacin (Sigma)) from day 0 to day 2, and in WT-1 differentiation medium (1 µM T3 and 1 µM rosiglitazone) from day 2 up until day 5, with the medium being replaced every other day. 3T3-L1 cells were differentiated in 3T3-L1 differentiation medium (850 nM insulin (Sigma), 1 µM dexamethasone (Sigma), 1 µM rosiglitazone, and 500 nM IBMX) from day 0 up until day 5, with the medium replaced every other day. For in vitro treatments, differentiated cells were treated with DMSO, 100 nM Epoxomicin (Millipore) or 100 nM Bortezomib (Selleck) for

6 h, 100 nM ONX0914 (Adooq) for 6 h, 1 µM NE (Sigma) for 1 h, or 1 µM CL316,143 (Tocris) for 16 h. For in vitro gene silencing, mRNA levels of target genes were knocked down through reverse transfection with SMARTpool silencing RNA (siRNA, Dharmacon) in Lipofectamine RNAiMAX transfection reagent (Thermo Fisher), used according to manufacturer's instructions. siRNAs were added to the cells in 30 nM for single knock-down or two times 30 nM for double knockdown. Reverse transfection took place 1 day before induction. The transfection mix was replaced for standard induction medium 24 h after transfection. Cells were harvested as pre-adipocytes, early adipocytes, or mature adipocytes; on day 0, day 3 or day 5 of differentiation, respectively. If not further specified, assays were performed on mature adipocytes, i.e., day 5.

2.3   Gene expression analysis

We used NucleoSpin RNA kit (Macherey Nagel), according to the manufacturer's instructions, for RNA extraction. RNA concentrations were then measured with a NanoDrop spectrophotometer (Thermo Fisher). Complementary DNA (cDNA) was prepared by adding 2 µl Maxima H Master Mix (Thermo Fisher) to 500 ng RNA, adjusted with H_2O to 10 µl total. This cDNA mixture was diluted 1:40 in H_2O. Relative gene expression was measured with qPCR. Per reaction, 4 µL cDNA, 5 µL PowerUp™ SYBR Green Master Mix (Applied Biosystems) and 1 µL of 5 µM primer stock (Sigma, see Supplementary table 1 for sequences) were mixed. Expression was measured in a Quant-Studio 5 RealTime PCR system (Thermo Fisher, 2 min 50 °C, 10 min 95 °C, 40 cycles of 15 s 95 °C, 1 min 60 °C). Cycle thresholds (Cts) of genes of interest were normalized to *TATA-box binding protein (Tbp)* levels by the ΔΔCt-method. Relative gene expression is displayed as relative copies per *Tbp* or as fold change to the appropriate experimental control groups.

2.4   Protein isolation and analysis

The samples were lysed in RIPA buffer (50 mM Tris (Merck, pH = 8), 150 mM NaCl (Merck), 5 mM EDTA (Merck), 0.1 % w/v SDS (Carl Roth), 1 % w/v IGEPAL® CA-630 (Sigma-Aldrich), 0.5 % w/v sodium deoxycholate (Sigma-Aldrich)) freshly supplemented with protease inhibitors (Sigma-Aldrich) in a 1:100 ratio. Cell lysates were centrifuged for 30 min (4 °C, 21,000 *g*) and tissue lysates were centrifuged 3 times 30 min, before supernatant was collected. Protein concentrations were determined using the Pierce BCA assay (Thermo Fisher) according to the manufacturer's instructions. 15-30 µg protein per sample were denatured with 5 % vol/vol 2-mercaptoethanol (Sigma) for 5 min at 95 °C before they were loaded in Bolt™ 4–12 % Bis-Tris gels (Thermo Fisher). After separation, proteins were transferred onto a 0.2 µm PVDF membrane (Bio-Rad) using the Trans-Blot® Turbo™ system (Bio-Rad) at 12 V, 1.4 A for 16 min. The membrane was briefly stained with Ponceau S (Sigma) to verify protein transfer and consequently blocked in Roti-Block (Roth) for 1 h at room temperature. The membranes were incubated overnight in primary antibody dilutions (1:1000 in Roti-block) at 4 °C. The following primary antibodies were used: β-tubulin (Cell Signaling, 2146), Psmb4 (Santa Cruz, sc-390878), Psmb8 (Cell Signaling, 13635), Nfe2l1 (Cell Signaling, 8052), Ubiquitin/P4D1 (Cell Signaling, 3936), Ucp1 (Abcam, ab10983), and Proteasome 20S alpha 1+2+3+5+6+7 (Abcam, ab22674). After washing with TBS-T (200 mM Tris (Merck), 1.36 mM NaCl (Merck), 0.1 % v/v Tween 20 (Sigma)), the membranes were incubated in secondary antibody (Santa Cruz) solutions (1:10,000 in Roti-block) for 90 min at room temperature. The membranes were washed in TBS-T and developed using SuperSignal West Pico PLUS Chemiluminescent Substrate (Thermo Fisher) in a Chemidoc imager (Bio-Rad). The uncropped blot images can be found in the supplementary figure S1.

2.5   Oil Red O staining

We used Oil Red O (ORO) staining to measure lipid content in adipocytes. Cells were washed with cold DPBS (Gibco), fixed in zinc formalin solution (Merck) for 60 min at room temperature, and then again washed the cells with DPBS. After the samples had completely dried, they were stained with ORO mix (60 % v/v Oil-Red-O solution (Sigma), 40 % v/v H_2O) for 60 min. After the incubation time, the cells were washed several times with water. We took pictures to visualize lipid content. To quantify lipid content, the ORO staining was eluted with 100 % isopropanol, and the absorption was measured at 500 nm in a Tecan plate reader.

2.6   Free glycerol assay

To assess lipolysis, we used Free Glycerol Reagent (Sigma F6428) and Glycerol standard solution (Sigma G7793) to measure free glycerol concentrations in the cell culture supernatant. After treatment and just before harvesting the samples, we collected cell culture medium to measure free glycerol content. The kit was used according to manufacturer's instructions. For normalization, we measured protein content with Pierce BCA assay.

2.7   Proteasome activity

To prepare lysates for the proteasomal activity assay, cells were lysed in lysis buffer (40 mM TRIS pH 7.2 (Merck), 50 nM NaCl (Merck), 5 mM $MgCl_2$(6 H_2O) (Merck), 10 % v/v glycerol (Sigma), 2 mM ATP (Sigma), 2 mM 2-mercaptoethanol (Sigma). Activity was measured using the Proteasome Activity Fluorometric Assay II kit (UBPBio, J41110), according to manufacturer's instructions in a Tecan Plate reader. This assay allowed for measurements of chymotrypsin-like, trypsin-like, and caspase-like activity. The results were then normalized to either protein, using Bio-Rad Protein Assay Kit II (Bio-Rad), or DNA, using the Quant-iT PicoGreen dsDNA assay kit (Invitrogen, P7589), both according to manufacturer's instructions.

2.8   Native PAGE

The protocol for in-gel proteasome activity assay and subsequent immunoblotting was previously described in detail (20). In short, cells were lysed in Lysis buffer (50 mM Tris/HCl pH 7.5, 2 mM DTT, 5 mM $MgCl_2$, 10% glycerol (vol/vol), 2 mM ATP, 0.05% Digitonin (v/v)), with a phosphate inhibitor (PhosphoStop, Roche Diagnostics). The suspensions were kept on ice for 20 min and then centrifuged twice. Protein concentration was determined with Bio-Rad Protein Assay Kit II and 15 µg sample protein was loaded in a NuPAGE 3-8% Tris-Acetate gel (Thermo Fisher). The gel was run at a constant voltage of 150 V for 4 h. Afterwards, the gel was incubated in an activity buffer (50 mM Tris, 1 mM $MgCl_2$, 1 mM DTT) with 0.05 mM chymotrypsin-like substrate Suc-Leu-Leu-Val-Tyr-AMC (Bachem) for 30 min at 37 °C. The fluorescent signal was measured using ChemiDoc MP (Bio-Rad). The gel was then incubated in a solubilization buffer (2% SDS (w/v), 66 mM Na_2CO_3, 1.5% 2-Mercaptoethanol (v/v)) for 15 min to prepare the samples for blotting. Through tank transfer, the samples were transferred to a PVDF membrane by 40 mA, overnight and developed as described above. The uncropped images are in supplementary figure S1.

2.9   Extracellular flux analysis (Seahorse)

Mitochondrial respiration was measured with Seahorse Cell Mito Stress Test (Agilent) with some adjustments to the manufacturer's protocol. Briefly, WT-1 cells were cultured in a 24-well Seahorse plate until

day 3 of differentiation. Culture medium was then replaced for Seahorse medium (XF DMEM pH 7.4, 10 mM glucose, 1 mM Pyruvate, 2 mM L-glutamine) and the cells were incubated for 60 min at 37 °C without CO_2 before being placed in the Seahorse Analyzer XFe24. In the assay, the cells were treated with NE (final concentration in the well was 1 µM), oligomycin (1 µM), FCCP (4 µM) and µM rotenone–antimycin A (0.5 µM). The reagents were mixed for 3 min, followed by 3 min of incubation, and 3 min of measurements. Afterwards, total DNA was measured for normalization, with CyQUANT Cell Proliferation Assay Kit (Thermo Fisher), according to manufacturer's instructions.

2.10   Statistics

Data were analyzed with ImageLab, Microsoft Excel and Graphpad Prism. Unless otherwise specified, data are shown as mean ± standard error of the mean (SEM), including individual measurements. Multiple student's t-test was used for experiments when comparing two groups and one variable, one-way ANOVA with Tukey post-hoc test was used when comparing three or more groups, and two-ANOVA with Tukey post-hoc test was used for comparing two groups with two variables. P-values lower than 0.05 were considered significant. If groups are significantly different from each other, this is indicated in graphs either with an asterisk (*) or with different letters (a,b). If the same letter is used or nothing is indicated, the groups are statistically indifferent from each other.

3. Results

3.1   *Psmb4* is induced during adipocyte differentiation and regulated by cold

Proteasome function is an evolutionary conserved feature of every mammalian cell, but little is known about the relative presence of proteasome subtypes and subunits throughout the body. The PRAAS-linked subunits Psmb4 and Psmb8 are widely and robustly expressed in mouse tissues (Fig. S2A). To better understand expression dynamics in BAT physiology, we compared mice housed at 30 °C (thermoneutrality) and at 4 °C (cold). We found that both genes are robustly expressed in BAT of mice housed at 30 °C thermoneutrality (Fig. S2B). In response to cold, *Psmb4* was unchanged and *Psmb8* expression was lower at 4 °C compared to 30 °C (Fig. S2B). Next, we analyzed cultured brown adipocytes differentiated from immortalized preadipocytes. *Psmb4* mRNA levels were markedly higher in differentiated adipocytes compared to pre-adipocytes (Fig. S2C). In contrast, *Psmb8* expression was lower in differentiated adipocytes compared to pre-adipocytes (Fig. S2C). We also tested the response of these genes to pharmacological activation. In line with the in vivo data, *Psmb4* remained unchanged and *Psmb8* was lower in cells activated with NE or the β3-adrenergic agonist CL316,243 (Fig. S2D). In summary, these data show that both *Psmb4* and *Psmb8* are robustly expressed in adipocytes, but while *Psmb4* seems to be implicated in mature brown adipocyte function, *Psmb8* expression was diminished under these conditions. However, to rule out that Psmb8 might nevertheless have an important function we performed loss-of-function experiments. First, we collected adipose tissues from mice with whole-body deletion of Psmb8 (19) and analyzed gene expression and histology. Mice deficient in Psmb8 had no apparent BAT abnormalities, which also was reflected in unchanged gene expression (Fig. S3A). The notion that Psmb8 is dispensable was supported by in vitro experiments, as silencing of *Psmb8* neither in immortalized pre-adipocytes nor in mature adipocytes produced an impact on adipogenesis or stress markers (Fig. S3B-S3D). In addition, there was no difference in lipid content in mature adipocytes (Fig. S3E). In conclusion, loss of Psmb8 did not affect adipogenesis

or BAT phenotype in vitro or in vivo. The concomitant down-regulation of Psmb8 in response to β3-adrenergic stimulation may indicate that immunoproteasome function is dispensable in brown adipocytes.

3.2 Loss of Psmb4 disrupts adipogenesis and proteostasis

As *Psmb4* was induced during adipocyte differentiation and highly expressed in activated brown adipocytes and BAT, we next studied the role of Psmb4 in brown adipocyte adipogenesis and thermogenic function in more detail. We also investigated if loss of Psmb4 was associated with cellular stress, assessed by measuring surrogate markers of ER stress and inflammation. Loss of Psmb4 was achieved by silencing *Psmb4* expression through siRNA ("siPsmb4 cells"). Transfection one day before the start of differentiation successfully reduced mRNA levels and this effect remained stable during different stages of adipogenesis (Fig. 1A), resulting in lower protein levels (Fig. 1B, 1C). Silencing of Psmb4 led to lower levels of adipogenesis (*Adipoq, Fabp4, Pparg)* and thermogenesis markers (*Ucp1*) during the early phase of adipocyte differentiation (Fig. 1D). In mature adipocytes, these changes were less pronounced albeit detectable for *Pparg* and *Ucp1* (Fig. 1E). Instead, *Ccl2*, a surrogate marker for the adipocyte stress response (21), was markedly higher in siPsmb4 compared to control cells (Fig. 1E). However, ER stress markers *Ddit3* and *Hspa5* did not change upon Psmb4 knockdown (Fig. 1D, 1E). These alterations on transcription level translated to lower lipid content (Fig 1E) and lower lipolysis after treatment with CL316,243 (Fig. 1F). PRAAS patients suffer from lipodystrophy in white adipose tissue. Therefore, to complement our findings in WT-1 cells, we also studied the effects of loss of Psmb4 in white adipocytes. For this we used 3T3-L1 cells, immortalized murine white adipocytes, and knocked down *Psmb4.* Knock-down successfully lowered gene expression (Fig. S4A). si*Psmb4* cells had lower expression of adipogenesis marker *Adipoq* but not *Fabp4*, higher expression of stress markers *Ccl2* and *Cxcl1*, and lower expression of ER stress marker *Ddit3* (Fig. S4B). Silencing *Psmb4* lowered Psmb4 protein levels (Fig. S4C, S4D). Complementing the results in WT-1 cells, 3T3-L1 si*Psmb4* cells had higher Nfe2l1 and global ubiquitin levels (Fig. S4C, S4D). In addition, *siPsmb4* cells had lower lipid droplet content and lower baseline lipolysis (Fig. S4E, S4F). Overall, 3T3-L1 cells replicate the effects of loss of Psmb4 on adipogenesis. Altogether, loss of Psmb4 limited adipogenesis and adipocyte function in both brown and white adipocytes.

As Psmb4 is part of the constitutive proteasome, we hypothesized that loss of Psmb4 would disturb UPS and proteostasis. To determine proteasome function in these cells we performed native PAGE analysis, which allows examining activity and protein levels of macromolecular proteasome configurations, i.e., 30S, 26S, and 20S. Chymotrypsin-like peptide hydrolysis activity was lower in siPsmb4 compared to control cells (Fig. 2A). On protein level, there were less 20S and 26S complexes present in siPsmb4 cells, as well as an increase in various subcomplexes, including precursors of the 20S proteasome (Fig. 2A, 2B). However, the overall levels of proteasome subunits were unchanged (Fig. 2C, 2D), indicating an assembly deficit of the proteasome in the absence of Psmb4. This is further underscored by the increase in ubiquitin levels in siPsmb4 cells (Fig. 2E, 2F).. Notably, these changes in UPS were accompanied by higher levels of active Nfe2l1 in the siPsmb4 compared to control cells (Fig. 2G, 2H), indicating that the brown adipocyte mounts an adaptive response to overcome UPS dysfunction. Interestingly, in cell lysates of siPsmb4 compared to control cells, proteasomal activity was lower in immature adipocytes but higher in mature adipocytes (Fig 2I). In summary, loss of Psmb4 led to proteotoxic stress through proteasome dysfunction as well as limited adipogenesis and adipocyte function.

3.3 Activation of Nfe2l1 partially compensates for the loss of Psmb4

While loss of Psmb4 had a marked effect on proteasome function, it did not completely disable UPS. We hypothesized that the activation of Nfe2l1 mitigated some of the effects of Psmb4 silencing. Therefore, we tested whether the adipocyte phenotype was more severe in a double *Psmb4* and *Nfe2l1* knockdown model. Double knockdown successfully led to lower mRNA as well as protein levels of both Psmb4 and Nfe2l1 (Fig. 3A, 3B, 3CE). Double knockdown also inhibited the Nfe2l1-mediated increase in proteasome subunits on protein and gene expression level (Fig 3B, 3C, 3D). Indeed, double knockdown of both *Nfe2l1* and *Psmb4* led to lower proteasomal activity compared to control cells or single gene silencing (Fig. 3E). The effects of the double knockdown of *Psmb4* and *Nfe2l1* on adipogenesis markers compared to control or the single knockdown cells were minimal (Fig. 3F). However, *Psmb4* knockdown was associated with higher adipocyte inflammation surrogate markers compared to control cells, but this effect was not further amplified by additional *Nfe2l1* knockdown (Fig. 3G). In addition, loss of Psmb4 led to markedly higher mRNA levels of *Activating Transcription Factor-3 (Atf3)*, an important transcription factor linked to the integrated stress response, but not of other stress markers (Fig. 3H), an effect also seen in PRAAS patients (5). These changes were independent of *Nfe2l1* knockdown (Fig. 3H). In summary, activation of Nfe2l1 helps to sustain proteasome function upon loss of Psmb4, but this effect did neither restore adipogenesis nor reduce the adipocyte stress response under these conditions.

3.4 Atf3 links loss of Psmb4 to inflammation and adipogenesis

The fact that Atf3 expression was selectively induced in siPsmb4 cells caught our attention, as Atf3 is a stress-induced transcription factor that reportedly has been associated with adipogenesis and lipogenesis (22). To investigate the role of Atf3 in our model system, we silenced *Psmb4*, *Nfe2l1* or *Atf3* individually and in a paired fashion (Fig. 4A). This approach did not affect the viability of the adipocytes (Fig. 4B). Unlike targeting Nfe2l1, *Atf3* knockdown in addition to *Psmb4* knockdown did not affect proteasomal activity (Fig. 4C). However, *Atf3* knockdown in addition to *Psmb4* knockdown normalized the expression of the inflammation markers *Ccl2 and Cxcl1* compared to siPsmb4 and control cells (Fig. 4D). In line with this normalized gene expression pattern, double knockdown of both *Psmb4* and *Atf3* largely rescued lipogenesis and restored lipolysis as follows. Particularly, cells with double knockdown of *Psmb4* and *Atf3* displayed markedly higher lipid content compared to si*Psmb4* cells, and similar lipid content compared to control cells (Fig. 4E). Knockdown of only *Atf3* or *Nfe2l1* had no effect. Brown adipocytes with double knockdown of *Psmb4* and *Atf3* displayed higher NE-induced glycerol release compared to si*Psmb4* cells, cancelling out the effect of si*Psmb4* (Fig. 4F). Again, knockdown of only *Atf3* or *Nfe2l1* had no effect. (Fig. 4F). To verify whether the effects on lipolysis were caused by changes in lipogenesis or lipolysis, we measured expression of essential lipases involved in degradation of triglycerides. Expression levels of Adipose triglyceride lipase (Atgl, encoded by *Pnpla2*), Hormone sensitive lipase (Hsl, encoded by *Lipe),* and Monoglyceride lipase (Mgll, encoded by *Mgll*) were not affected by si*Psmb4* (Fig. 4G). Therefore, the effect of *Psmb4* knockdown on glycerol release was due to a lower triglyceride content, and not altered lipolysis activity. Finally, to assess NST, we measured NE-stimulated oxygen consumption followed by a mitochondrial stress test using a Seahorse Analyzer. In line with the finding that loss of Psmb4 diminishes brown adipocyte function, si*Psmb4* cells displayed abolished NE-stimulated and uncoupled respiration as well as lower maximal capacity compared to control cells. Double knockdown of both *Psmb4* and *Atf3* largely rescued these alterations in mitochondrial function (Fig. 4H, 4I). Knockdown of only *Atf3* or *Nfe2l1* had no effect

(Fig. 4H, 4I). In conclusion, loss of Psmb4 disrupts adipogenesis and thermogenesis through the activation of Atf3.

4. Discussion

The proteasome is considered a prerequisite for cellular proteostasis, but its remodeling in response to processes of physiologic adaptation remains largely unexplored. PRAAS syndrome has shed light on the relevance of the proteasome in human pathology, but the underlying molecular mechanisms linking disturbed proteasome function to e.g., inflammation and lipodystrophy remains unclear. Here, we show that in mouse brown adipocytes loss of Psmb4 disturbs proteostasis and protein quality control and, thus, impacts adipogenesis and thermogenesis. In contrast, *Psmb8* silencing had no effect. In these cells, *Psmb4* is a constitutively expressed gene that is upregulated during adipogenesis and states of thermogenic activation. *Psmb4* is a target gene of Nfe2l1 and this regulation is in line with the general requirement of increased proteasome function during cold adaptation (15). Contrasting this, *Psmb8* encodes for a subunit of the immunoproteasome subunit, which is induced by interferons. Psmb8 ablation was previously shown to disrupt proteostasis in immune response (5,19). As the role of the immunoproteasome is especially important in hematopoietic cells (23,24), it is perhaps logical that Psmb8 expression diminishes during differentiation, as there is little requirement for a mature adipocyte. Considering this, it is not surprising that Psmb8 is dispensable for brown adipocyte development and function.

PRAAS patients with mutations in *PSMB4* or *PSMB8* have a similar disease presentation (5) and suffer from lipodystrophy and fevers. Our data suggest that the intrinsic cellular pathways may vary in these patients. It is possible that lipodystrophy in patients with *PSMB8* mutations is a result of autoinflammation and its systemic effects on adipose tissue whereas lipodystrophy in patients with *PSMB4* mutations is caused by a combination of the autoinflammatory syndrome and intrinsically impaired adipogenesis. Our results do not suggest that hyperactivation of BAT is involved in the fever symptoms in patients, as loss of Psmb4 function in mouse brown adipocytes diminishes NST. Nevertheless, altered thermoregulation in the absence of NST might contribute to the symptoms. In addition, we are aware that silencing of genes by RNAi does not completely reflect the natural effects of missense, truncation, or deletion mutations in patients. However, our study warrants further investigation of *PSMB4* mutations on proteasome and adipocyte function. A more complete understanding of systemic as well as cell-specific effects, could improve treatment options for patients.

An interesting and potentially therapeutically relevant aspect of our work is the adaptive activation of Nfe2l1 in response to loss of Psmb4 in adipocytes. This recruitment of Nfe2l1 is most likely a response to insufficient turnover of ubiquitinated proteins caused by proteasome dysfunction, as seen in PRAAS patients (25) or by inhibiting proteasome activity with chemical inhibitors (12). While the activation of Nfe2l1 partly restored total proteasomal activity, we found that this activation of Nfe2l1 was insufficient to overcome the defects in adipogenesis and adipocyte function. Perhaps, while both the loss of Psmb4 and Nfe2l1 cause abnormal proteasomal function, a major difference between the two conditions is the presence of incomplete proteasome intermediates. Reduced total proteasomal activity in the absence of Nfe2l1 was not associated with incomplete proteasome intermediates, and, consequently, also not with a block in adipogenesis. More work is needed to characterize the complex remodeling of cellular proteasome function under

proteotoxic stress conditions. Nfe2l1 activation might serve as a therapeutic approach to overcome some of the pathologies associated with PRAAS.

A major finding of our study is that silencing of *Atf3* largely rescued the adipocyte defects caused by loss of Psmb4. Atf3 is a member of the mammalian activation transcription factor/cAMP responsive element-binding (CREB) protein family of transcription factors that responds to various stressors (22) and is a downstream target of Atf4 (26). Interestingly, Atf3 was previously shown to downregulate adipogenesis markers and to protect against diet-induced obesity in mice (27). In the context of our research, Atf3 could be viewed as a brake that responds to proteotoxic stress caused by loss of Psmb4. Atf3 does not seem to signal back to the UPS or predispose the cell death, yet its activation induces inflammatory pathways, potentially sending out "danger" and "help" signals. Removing Atf3 clears the path for adipogenesis, lipid metabolism and thermogenesis and might be of therapeutic interest to tackling symptoms associated with PRAAS.

More generally, in the broader context of metabolism, our data underscore the relevance of UPS-mediated protein quality control in maintaining cellular health and function, exemplified here in the context of adipocytes. We show that proteostasis and lipid metabolism are intricately linked in adipocytes and failure to secure proteostasis results in diminished adipogenesis. An important hallmark of obesity-induced adipocyte dysfunction is cellular stress and inflammation, which are tightly linked to aberrant lipid metabolism and insulin resistance. Our finding that maladaptation of UPS and the activation of stress sensors, including Atf3, impede adipogenesis should also be interpreted in the context of potentially hampering obesity-induced adipose tissue expansion or, as in the case of PRAAS, resulting in lipodystrophy. Identifying the key nodes linking proteostasis to cellular stress pathways will represent an important step towards understanding pathological alterations that result in aberrant metabolism, inflammation, premature ageing, and cancer.

5. Acknowledgments

6. Conflict of Interest

The authors declare no conflicts of interest.

7. Author Contributions

N.W. and I.A. performed the experiments and analyzed data. M.S.T. and E.K. provided the mouse model and mouse samples. N.W. and A.B. conceptually designed the study, interpreted the data, and wrote the manuscript. All authors read and commented on the manuscript.

8. Funding

9. References

1. Torrelo A, Patel S, Colmenero I, Gurbindo D, Lendínez F, Hernández A, et al. Chronic atypical neutrophilic dermatosis with lipodystrophy and elevated temperature (CANDLE) syndrome. J Am Acad Dermatol. 2010 Mar;62(3):489–95.

2. Agarwal AK, Xing C, DeMartino GN, Mizrachi D, Hernandez MD, Sousa AB, et al. PSMB8 Encoding the β5i Proteasome Subunit Is Mutated in Joint Contractures, Muscle Atrophy, Microcytic Anemia, and Panniculitis-Induced Lipodystrophy Syndrome. Am J Hum Genet. 2010 Dec;87(6):866–72.

3. Kanazawa N. Nakajo-Nishimura Syndrome: An Autoinflammatory Disorder Showing Pernio-Like Rashes and Progressive Partial Lipodystrophy. Allergol Int. 2012;61(2):197–206.

4. Kitamura A, Maekawa Y, Uehara H, Izumi K, Kawachi I, Nishizawa M, et al. A mutation in the immunoproteasome subunit PSMB8 causes autoinflammation and lipodystrophy in humans. J Clin Invest. 2011 Oct 3;121(10):4150–60.

5. Brehm A, Liu Y, Sheikh A, Marrero B, Omoyinmi E, Zhou Q, et al. Additive loss-of-function proteasome subunit mutations in CANDLE/PRAAS patients promote type I IFN production. J Clin Invest. 2015 Oct 20;125(11):4196–211.

6. Ebstein F, Poli Harlowe MC, Studencka-Turski M, Krüger E. Contribution of the Unfolded Protein Response (UPR) to the Pathogenesis of Proteasome-Associated Autoinflammatory Syndromes (PRAAS). Front Immunol. 2019 Nov 26;10:2756.

7. Finley D. Recognition and Processing of Ubiquitin-Protein Conjugates by the Proteasome. Annu Rev Biochem. 2009 Jun;78(1):477–513.

8. Collins GA, Goldberg AL. The Logic of the 26S Proteasome. Cell. 2017 May;169(5):792–806.

9. Kimura H, Caturegli P, Takahashi M, Suzuki K. New Insights into the Function of the Immunoproteasome in Immune and Nonimmune Cells. J Immunol Res. 2015;2015:1–8.

10. Huber EM, Basler M, Schwab R, Heinemeyer W, Kirk CJ, Groettrup M, et al. Immuno- and Constitutive Proteasome Crystal Structures Reveal Differences in Substrate and Inhibitor Specificity. Cell. 2012 Feb;148(4):727–38.

11. Mann JP, Savage DB. What lipodystrophies teach us about the metabolic syndrome. J Clin Invest. 2019 Aug 5;129(10):4009–21.

12. Cannon B, Nedergaard J. Brown Adipose Tissue: Function and Physiological Significance. Physiol Rev. 2004 Jan;84(1):277–359.

13. Bartelt A, Bruns OT, Reimer R, Hohenberg H, Ittrich H, Peldschus K, et al. Brown adipose tissue activity controls triglyceride clearance. Nat Med. 2011 Feb;17(2):200–5.

14. Lemmer IL, Willemsen N, Hilal N, Bartelt A. A guide to understanding endoplasmic reticulum stress in metabolic disorders. Mol Metab. 2021 Jan;101169.

15. Bartelt A, Widenmaier SB, Schlein C, Johann K, Goncalves RLS, Eguchi K, et al. Brown adipose tissue thermogenic adaptation requires Nrf1-mediated proteasomal activity. Nat Med. 2018 Mar;24(3):292–303.

16. Radhakrishnan SK, Lee CS, Young P, Beskow A, Chan JY, Deshaies RJ. Transcription Factor Nrf1 Mediates the Proteasome Recovery Pathway after Proteasome Inhibition in Mammalian Cells. Mol Cell. 2010 Apr;38(1):17–28.

17. Sha Z, Goldberg AL. Proteasome-Mediated Processing of Nrf1 Is Essential for Coordinate Induction of All Proteasome Subunits and p97. Curr Biol. 2014 Jul;24(14):1573–83.

18. Fehling HJ, Swat W, Laplace C, Kühn R, Rajewsky K, Müller U, et al. MHC Class I Expression in Mice Lacking the Proteasome Subunit LMP-7. Science. 1994 Aug 26;265(5176):1234–7.

19. Seifert U, Bialy LP, Ebstein F, Bech-Otschir D, Voigt A, Schröter F, et al. Immunoproteasomes Preserve Protein Homeostasis upon Interferon-Induced Oxidative Stress. Cell. 2010 Aug;142(4):613–24.

20. Yazgili AS, Meul T, Welk V, Semren N, Kammerl IE, Meiners S. In-gel proteasome assay to determine the activity, amount, and composition of proteasome complexes from mammalian cells or tissues. STAR Protoc. 2021 Jun;2(2):100526.

21. Rull A, Camps J, Alonso-Villaverde C, Joven J. Insulin Resistance, Inflammation, and Obesity: Role of Monocyte Chemoattractant Protein-1 (orCCL2) in the Regulation of Metabolism. Mediators Inflamm. 2010;2010:1–11.

22. Ku H-C, Cheng C-F. Master Regulator Activating Transcription Factor 3 (ATF3) in Metabolic Homeostasis and Cancer. Front Endocrinol. 2020 Aug 14;11:556.

23. Çetin G, Klafack S, Studencka-Turski M, Krüger E, Ebstein F. The Ubiquitin–Proteasome System in Immune Cells. Biomolecules. 2021 Jan 5;11(1):60.

24. Tubío-Santamaría N, Ebstein F, Heidel FH, Krüger E. Immunoproteasome Function in Normal and Malignant Hematopoiesis. Cells. 2021 Jun 22;10(7):1577.

25. Sotzny F, Schormann E, Kühlewindt I, Koch A, Brehm A, Goldbach-Mansky R, et al. TCF11/Nrf1-Mediated Induction of Proteasome Expression Prevents Cytotoxicity by Rotenone. Antioxid Redox Signal. 2016 Dec;25(16):870–85.

26. Forsström S, Jackson CB, Carroll CJ, Kuronen M, Pirinen E, Pradhan S, et al. Fibroblast Growth Factor 21 Drives Dynamics of Local and Systemic Stress Responses in Mitochondrial Myopathy with mtDNA Deletions. Cell Metab. 2019 Dec;30(6):1040-1054.e7.

27. Ku H-C, Chan T-Y, Chung J-F, Kao Y-H, Cheng C-F. The ATF3 inducer protects against diet-induced obesity via suppressing adipocyte adipogenesis and promoting lipolysis and browning. Biomed Pharmacother Biomedecine Pharmacother. 2022 Jan;145:112440.
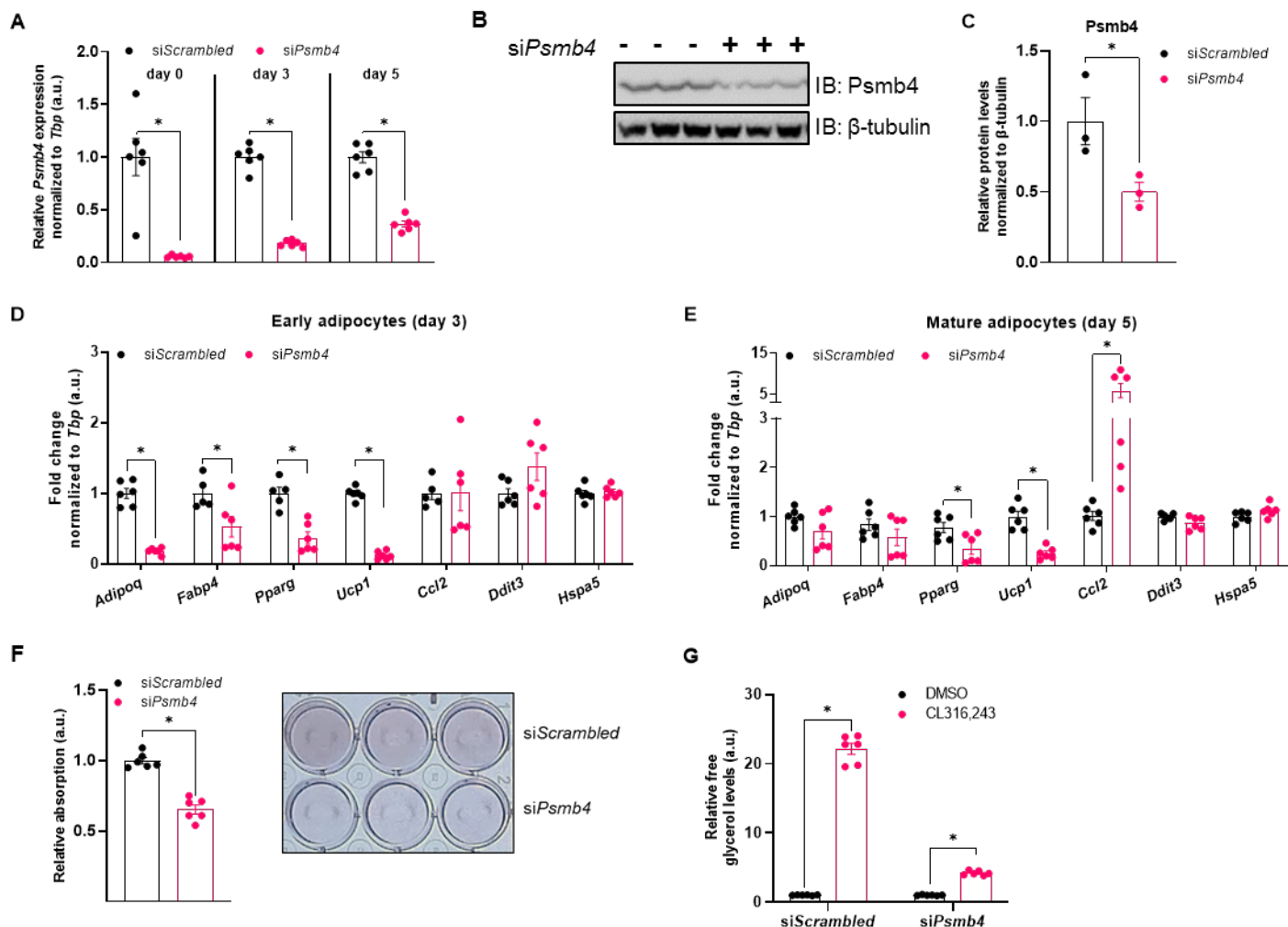
Fig. 1: Psmb4 controls adipogenesis and adipocyte health. (A) Relative gene expression of *Psmb4* at different time points after knockdown with scrambled or *Psmb4* siRNA. **(B, C)** Representative immunoblot of Psmb4 in siScrambled and siPsmb4 adipocytes with**(C)** protein quantification normalized to β-tubulin. **(D)** Relative gene expression of adipogenesis and stress markers adipocytes after *Psmb4* knockdown measured on day 3 of differentiation. **(E)** Relative gene expression of adipogenesis and stress markers adipocytes after *Psmb4* knockdown measured on day 5 of differentiation. **(F)** Representative Oil-Red-O staining and quantification (day 5). **(G)** Relative free glycerol levels in adipocyte supernatant (day 5) after DMSO or 1 µM CL316,243 treatment for 3 h. Data are mean ± SEM. Unless otherwise specified: n = 6 independent measurements from 2 separate experiments. Significant if *P* < 0.05, indicated by (*) or different letters.
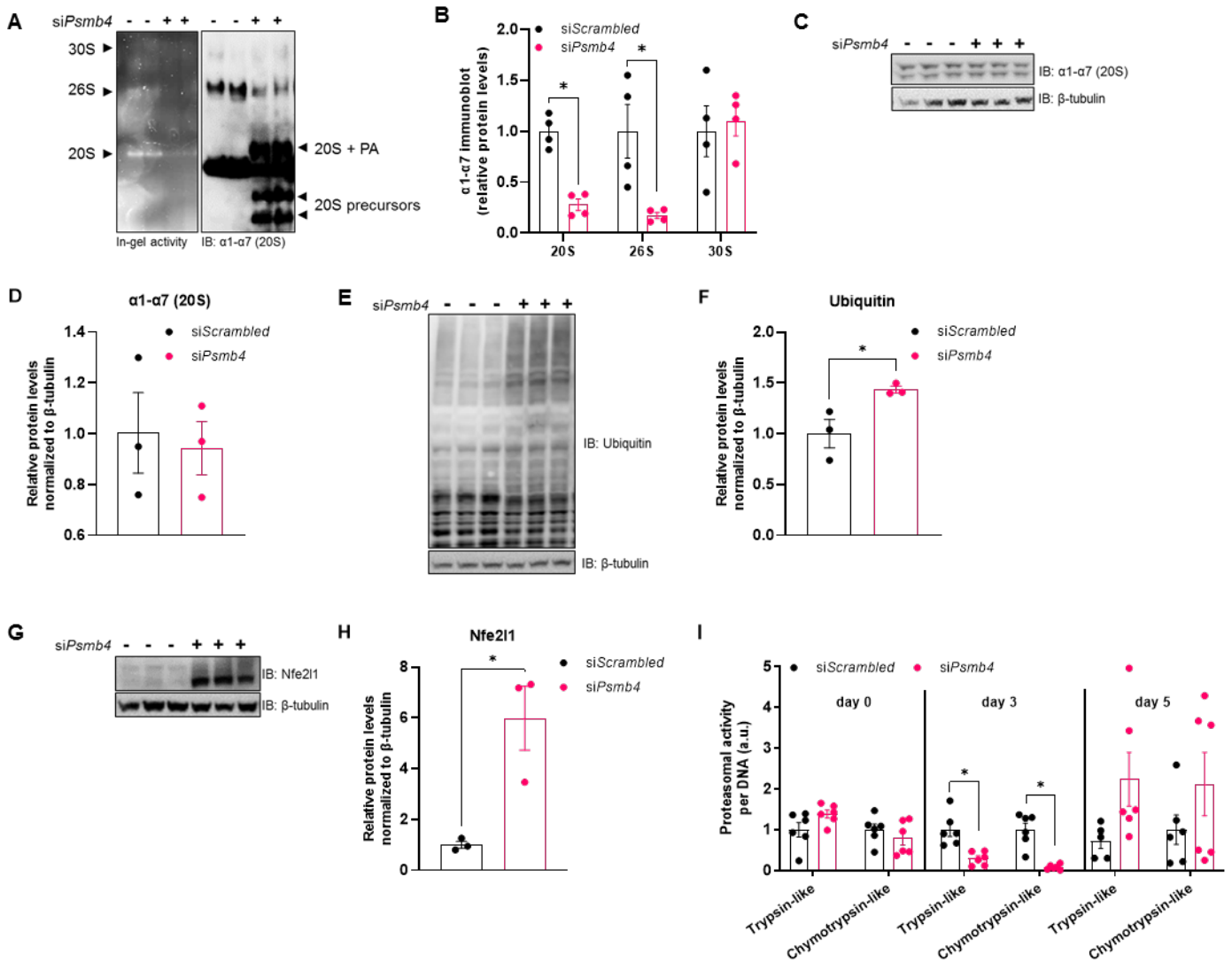
Fig. 2: Psmb4 controls UPS and proteostasis. (A) Representative Native PAGE with in-gel chymotrypsin-like proteasome activity and immunoblot of α1-α7 (20S) proteasome subunits. (PA: proteasome activators) **(B)** Relative protein levels α1-α7 (20S) proteasome subunits measured in Native PAGE immunoblots. **(C**, **D)**Representative immunoblot of α1-α7 (20S) proteasome subunits from adipocytes (day 5) with **(D)** protein quantification relative to β-tubulin. **(E, F)** Representative immunoblot of ubiquitin from adipocytes (day 5) with **(F)** protein quantification relative to β-tubulin. **(G, H)** Representative immunoblot of Nfe2l1 from adipocytes (day 5) with **(D)** protein quantification relative to β-tubulin. **(I)** Trypsin-like and chymotrypsin-like proteasome activity in adipocytes at different time points, normalized to DNA content. Data are mean ± SEM. Unless otherwise specified: n = 6 independent measurements from 2 separate experiments. Significant if $P < 0.05$, indicated by (*) or different letters.
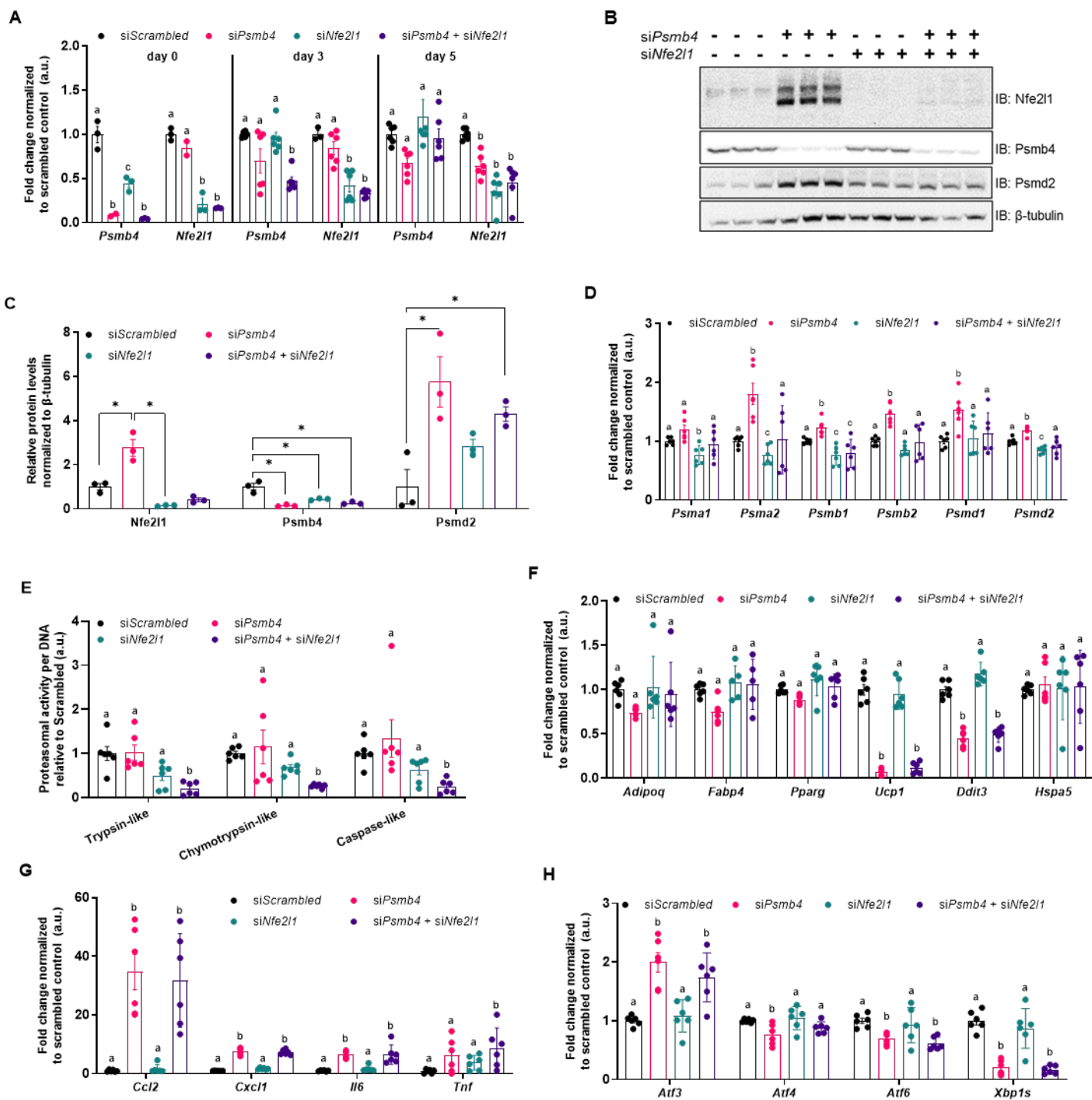
Fig. 3. Loss of Psmb4 initiates a proteostatic stress-response via Nfe2l1. (A) Relative gene expression of *Psmb4* and *Nfe2l1* at different time points after knockdown with scrambled, *Psmb4* and/or *Nfe2l1* siRNA. **(B, C)** Representative immunoblots of Nfe2l1, Psmb4, Psmd2 and β-tubulin in siScrambled, siPsmb4, siNfe2l1 or siPsmb4 + siNfe2l1 adipocytes (day 5) with **(C)** protein quantification levels normalized to β-tubulin.**(D)** Relative gene expression of various proteasome subunits. **(E)** Trypsin-like, chymotrypsin-like, and caspase-like proteasome activity in adipocytes (day 5), normalized to DNA content.

(Fig. 3 - continued from previous page). (F) Relative gene expression of adipogenesis and stress markers in adipocytes (day 5). **(G)** Relative gene expression of inflammation markers in adipocytes (day 5). **(H)** Relative gene expression of ER stress and unfolded protein response markers in adipocytes (day 5). Data are mean ± SEM. Unless otherwise specified: n = 6 independent measurements from 2 separate experiments. Significant if $P < 0.05$, indicated by (*) or different letters.
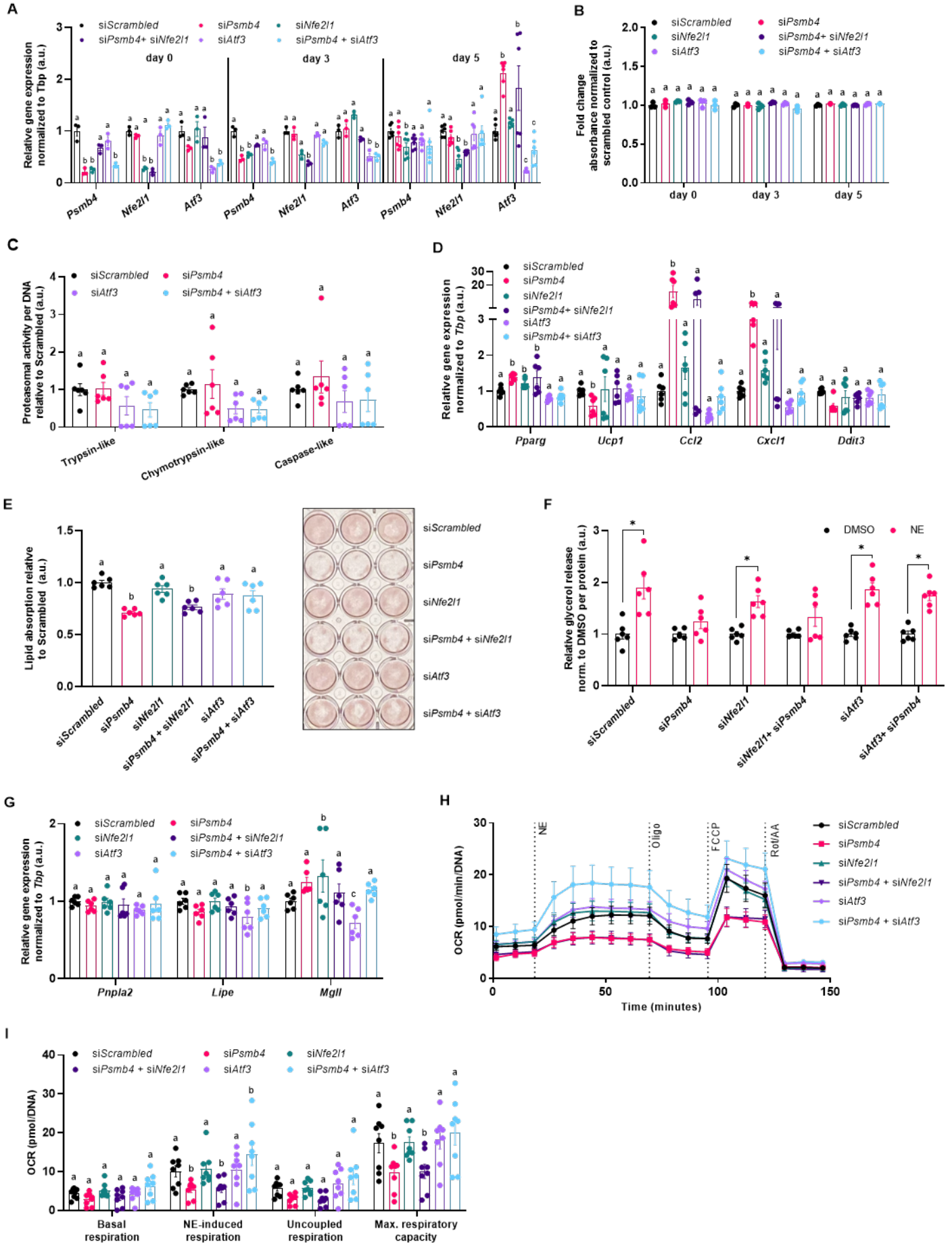
Fig. 4 (previous page). Loss of Psmb4 induces inflammation and blocks adipogenesis via Atf3. (A) Relative gene expression of *Psmb4*, *Nfe2l1*, and *Atf3*. **(B)** Viability in adipocytes. **(C)** Trypsin-like, chymotrypsin-like, and caspase-like proteasome activity in adipocytes (day 5), normalized to DNA content **(D)** Relative gene expression of adipogenesis and stress markers in adipocytes (day 5) after knockdown. **(E)** Oil-Red-O staining in adipocytes after knockdown. **(F)** Supernatant free glycerol levels after treatment with DMSO or 1 µM Norepinephrine (NE) for 1 h normalized to protein. **(G)** Relative gene expression of lipases in adipocytes (day 5). **(H, I)** Oxygen consumption rate (OCR) in adipocytes after knockdown, normalized to DNA levels (n = 8, from 2 experiments). Unless otherwise specified: n = 6 independent measurements from 2 separate experiments. Data are mean ± SEM. Significant if $P < 0.05$, indicated by (*) or different letters.
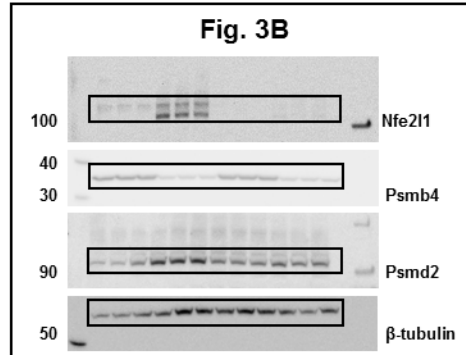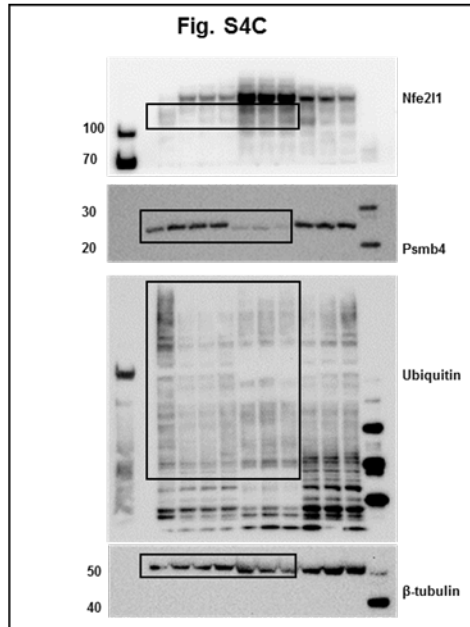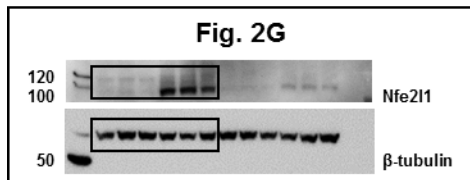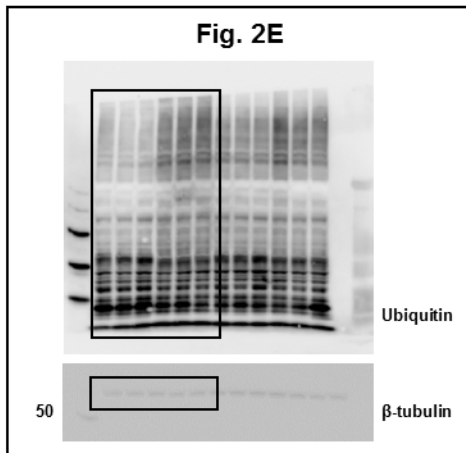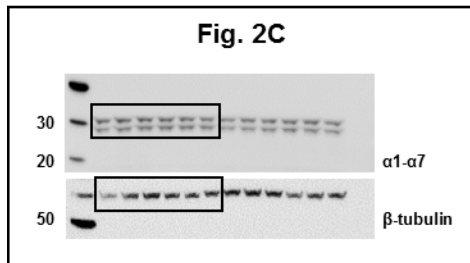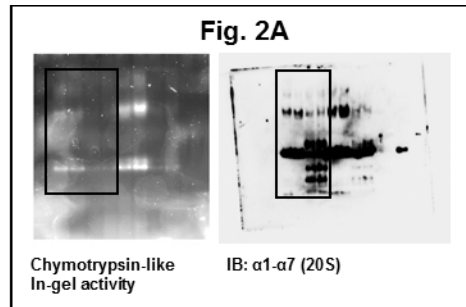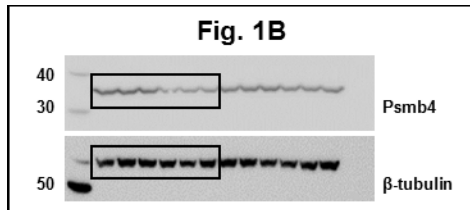
Fig S1: Uncropped pictures of immunoblots.
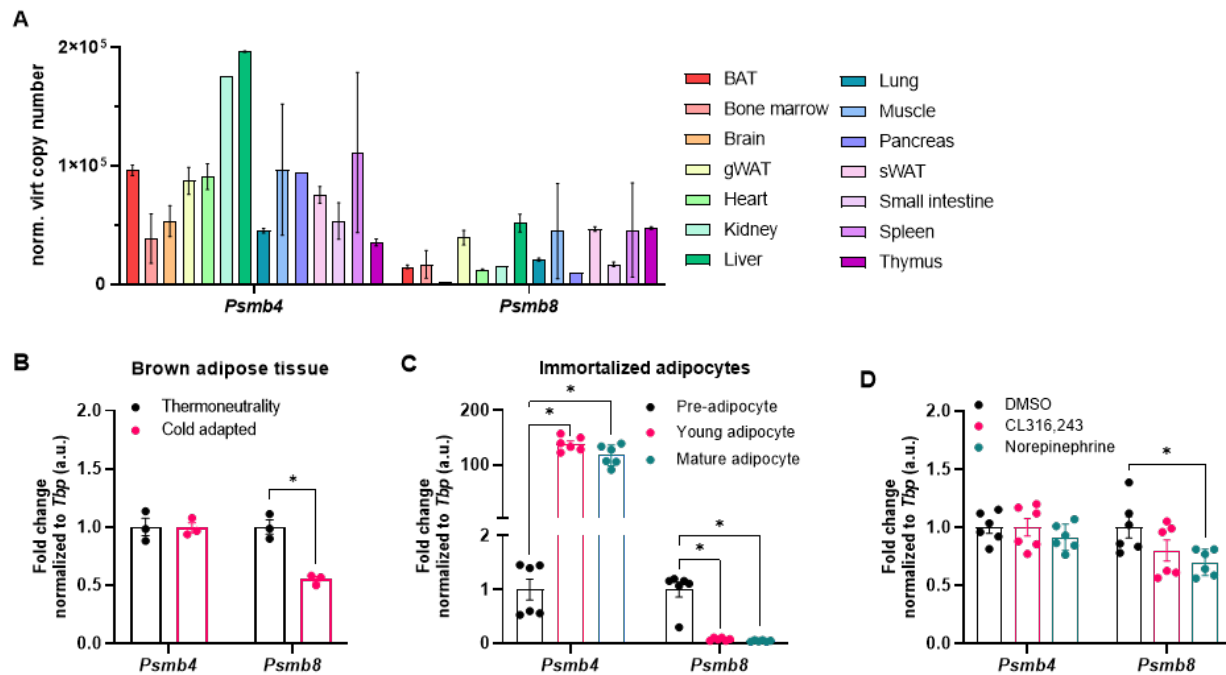
Fig. S2: Regulation of *Psmb4* and *Psmb8* expression in brown adipocytes. (A) Gene expression panel of *Psmb4* and *Psmb8* in a tissue library of WT mice (n=2). **(B)** Relative gene expression in BAT from mice housed at thermoneutrality (30 °C) or cold (4 °C) for 7 d (n = 3 biological replicates). **(C)** Relative gene expression in immortalized WT-1 brown adipocytes at day 0, day 3 (young) or day 5 (mature) of differentiation, or **(D)** in adipocytes (day 5) after treatment with DMSO, 1 μM CL316,243 (16 h) or 1 μM NE (1 h). Data are mean ± SEM. Unless otherwise specified: n = 6 independent measurements from 2 separate experiments. Groups are significantly different if $P < 0.05$, indicated by (*) or different letters.
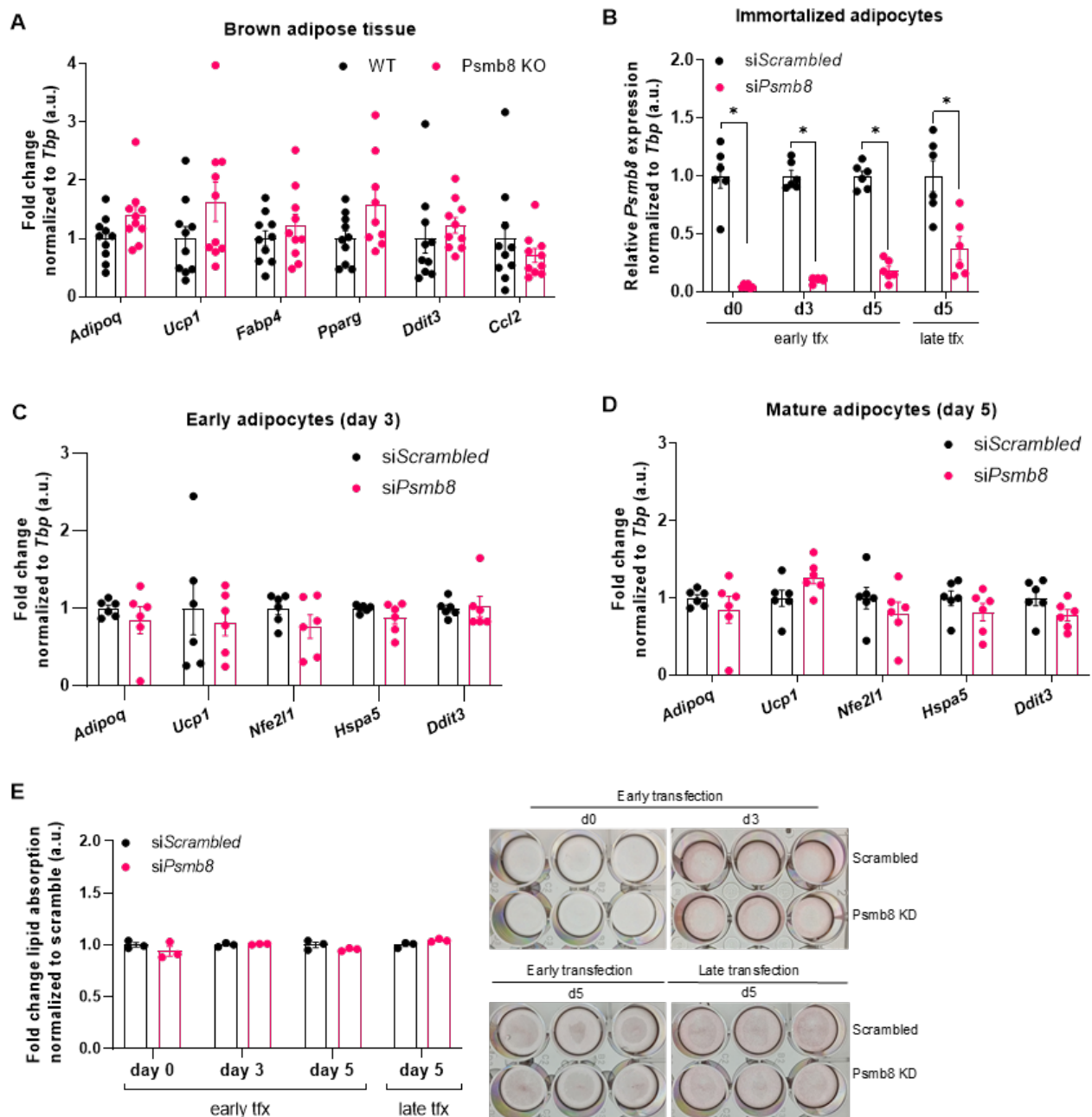
Fig. S3: Psmb8 does not affect adipogenesis or cellular function. (A) Relative gene expression of adipogenesis and stress markers in BAT from whole-body knock-out mice (n = 11 WT, n = 11 KO mice). **(B)** Relative gene expression of *Psmb8* in mature WT-1 cells after early transfection (day -1) or late transfection (day 3). (n = 6 from 2 independent experiments). **(C)** Relative gene expression of adipogenesis and stress markers in day 3 adipocytes after knockdown on day -1 (n = 6 from 2 independent experiments). **(D)** Relative gene expression of adipogenesis and stress markers in mature WT-1 cells after knockdown on day -1.(n = 6 from 2 independent experiments). **(E)** Oil Red O staining and lipid resorption in WT-1 cells after knockdown at day -1 or day 3 at different timepoints (n=3). Data are mean ± SEM. Significant if *P* < 0.05, indicated by (*) or different letters
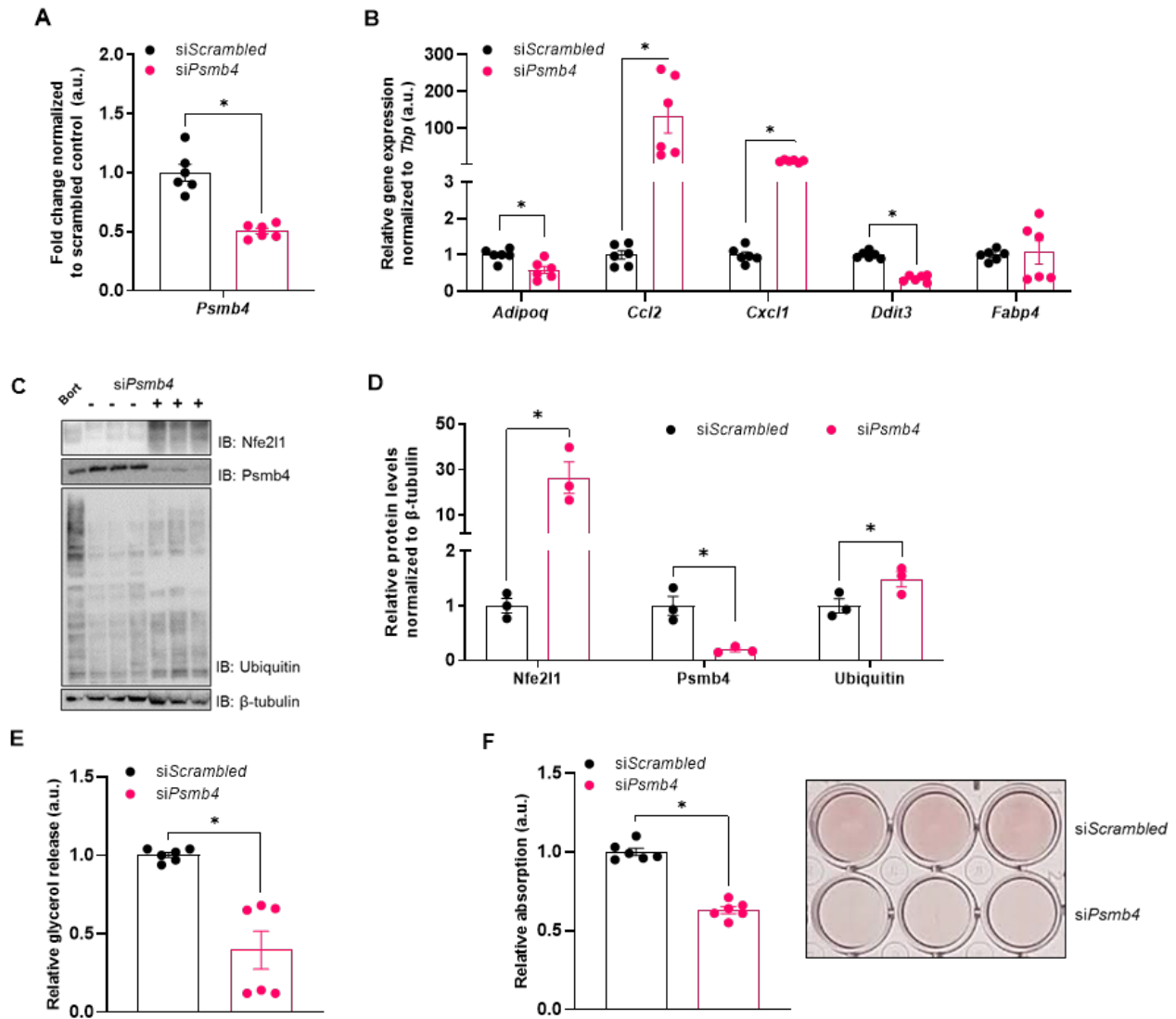
Fig. S4: Psmb4 controls adipogenesis in white adipocytes. (A) Relative expression of Psmb4 at differentiation day 5 after knockdown with siScrambled or siPsmb4 on day -1 in 3T3-L1 white adipocytes. **(B)** Relative gene expression of adipogenesis and inflammation markers in day 5 white adipocytes. **(C, D)** Immunoblot of Nfe2l1, Psmb4, Ubiquitin and β-tubulin. Bort = Bortezomib treated cells as positive control. **(D)** Protein quantification levels relative to β-tubulin. **(E)** Quantification of immunoblots normalized to β-tubulin. **(F)** Relative glycerol release in white adipocytes (day 5). **(G)** Lipid absorption and Oil-Red O staining in white adipocytes (day 5). Data are mean ± SEM. Unless otherwise specified: n = 6 independent measurements from 2 separate experiments. Groups are significantly different if $P < 0.05$, indicated by (*) or different letters.

Supplemental table. 1. List of primers used for quantitative real-time PCR.

Gene	Forward primer (5')	Reverse primer (5')
Adipoq	GGAGAGAAAGGAGATGCAGGT	CTTTCCTGCCAGGGGTTC
Atf3	GAGGATTTTGCTAACCTGACACC	TTGACGGTAACTGACTCCAGC
Atf4	CCTTCGACCAGTCGGGTTTG	CTGTCCCGGAAAAGGCATCC
Atf6	GGACGAGGTGGTGTCAGAG	GACAGCTCTTCGCTTTGGAC
Ccl2	TTAAAAACCTGGATCGGAACCAA	GCATTAGCTTCAGATTTACGGGT
Cxcl1	GACTCCAGCCACACTCCAAC	TGACAGCGCAGCTCATTG
Ddit3	CTGGAAGCCTGGTATGAGGAT	CAGGGTCAAGAGTAGTGAAGGT
Fabp4	GGATGGAAAGTCGACCACAA	TGGAAGTCACGCCTTTCATA
Hspa5	TCATCGGACGCACTTGGAA	CAACCACCTTGAATGGCAAGA
Il6	GCTACCAAACTGGATATAATCAGGA	CCAGGTAGCTATGGTACTCCAGAA
Lipe	GATTTACGCACGATGACACAGT	ACCTGCAAAGACATTAGACAGC
Mpll	TCGGAACAAGTCGGAGGT	TCAGCAGCTGTATGCCAAAG
Nfe2l1	GACAAGATCATCAACCTGCCTGTAG	GCTCACTTCCTCCGGTCCTTTG
Pnpla2	GAGCTTCGCGTCACCAAC	CACATCTCTCGGAGGACCA
Pparg	TCGCTGATGCACTGCCTATG	GAGAGGTCCACAGAGCTGATT
Psma1	TGCGTGCGTTTTTGATTTTAGAC	CCCTCAGGGCAGGATTCATC
Psma2	TGGCTGTGTTCCGACTTTC	AAGCTTACCAGATGGGCTGA
Psmb1	TTCCACTGCTGCTTACCGAG	CGTTGAAGGCATAAGGCGAAAA
Psmb2	CCCAGACTATGTCCTCGTCG	CCGTGTGAAGTTAGCTGCTG
Psmb4	ACTGGCCACTGGTTATGGTG	CAGCACTGGCTGCTTCTCTA
Psmb8	GTACTGGGAGAGGCTGTTGG	CAGCATCATGTTGGAAAGCA
Psmd1	GTGATAAAACACTTTCGAGGCCA	TGAATGCAGTCGTGAATGACTT
Psmd2	AATGGGAGATTCCAAGTCCA	AATGGGAGATTCCAAGTCCA
Tbp	AGAACAATCCAGACTAGCAGCA	GGGAACTTCACATCACAGCTC
Tnf	TCTTCTCATTCCTGCTTGTGG	GGTCTGGGCCATAGAACTGA
Ucp1	AGGCTTCCAGTACCATTAGGT	CTGAGTGAGGCAAAGCTGATTT
Xbp1s	GGTCTGCTGAGTCCGCAGCAGG	AGGCTTGGTGTATACATGG

9. Publication II: Koçberber, Willemsen & Bartelt 2023

The role of proteasome activators PA28αβ and PA200 in brown adipocyte differentiation and function

Zeynep Koçberber[1,†], Nienke Willemsen[1,†], Alexander Bartelt[1,2,3,4,*]

[1] Institute for Cardiovascular Prevention (IPEK), Ludwig-Maximilians-University Munich, Munich, Germany.
[2] German Center for Cardiovascular Research, Partner Site Munich Heart Alliance, Ludwig-Maximilians-University Hospital, Munich, Germany
[3] Institute for Diabetes and Cancer (IDC), Helmholtz Centre Munich, German Research Center for Environmental Health, Neuherberg, Germany
[4] Department of Molecular Metabolism & Sabri Ülker Center for Metabolic Research, Harvard T.H. Chan School of Public Health, Boston USA

[†]**First authorship:** These authors share first authorship

*Correspondence: Alexander Bartelt, alexander.bartelt@med.uni-muenchen.de

Abstract

Brown adipocytes produce heat through non-shivering thermogenesis (NST). To adapt to temperature cues, they possess a remarkably dynamic metabolism and undergo substantial cellular remodeling. The proteasome plays a central role in proteostasis and adaptive proteasome activity is required for sustained NST. Proteasome activators (PAs) are a class of proteasome regulators but the role of PAs in brown adipocytes is unknown. Here, we studied the roles of PA28α (encoded by *Psme1*) and PA200 (encoded by *Psme4*) in brown adipocyte differentiation and function. We found that *Psme1* and *Psme4* are expressed in brown adipocytes in vivo and in vitro. Through silencing of *Psme1* and/or *Psme4* expression in cultured brown adipocytes, we found that loss of PAs did not impair proteasome assembly or activity, and that PAs were not required for proteostasis in this model. Loss of *Psme1* and/or *Psme4* did not impair brown adipocyte development or activation, suggesting that PAs are neither required for brown adipogenesis nor NST. In summary, we found no role for Psme1 and Psme4 in brown adipocyte proteostasis, differentiation, or function. These findings contribute to our basic understanding of proteasome biology and the roles of proteasome activators in brown adipocytes**.**

1 Introduction

Thermogenic adipocytes produce heat through non-shivering thermogenesis (NST). Mammals - especially infants, small rodents, and hibernating animals - rely on NST for appropriate thermoregulation as it complements or substitutes shivering- or muscle-generated thermogenesis (1). The main class of thermogenic adipocytes are brown adipocytes, collectively forming brown adipose tissue (BAT) depots. Additionally, beige adipocytes with similar thermogenic capacity to brown adipocytes reside in white adipose tissue (WAT) (2,3).

The common denominator of these thermogenic adipocytes is their (potential) expression of Uncoupling-protein 1 (*Ucp1*), a fatty acid-activated proton carrier that uncouples the electron transport chain from ATP production, which is an exothermic reaction resulting in heat generation (1,3). Alternatively to Ucp1-mediated uncoupling, futile cycling of creatine, calcium, and fatty acids also lead to heat production in thermogenic adipocytes (4). In response to cold, the central nervous system initiates the release of norepinephrine (NE), which, through β-adrenergic receptors, acutely leads to lipolysis and Ucp1 activation. Over the years, several other thermogenic mediators have been identified to promote adipose tissue browning and NST (5–7). To fuel NST, BAT consumes large amounts of triglycerides and glucose (8,9), which is associated with a beneficial metabolic profile in mice and humans (8–11). In addition to acute activation, prolonged stimulation of NST results in BAT hyperplasia, mitochondrial biogenesis, as well as the emergence of beige adipocytes within certain white adipose depots (1,9). This cellular remodeling of oxidative capacity and lipid metabolism is regulated by a complex network of proteostasis mechanisms, including autophagy and the ubiquitin-proteasome system (UPS) (12–17). BAT activation and tissue remodeling are energy and resource costly processes (1,8), which is probably why thermogenic adipocytes have developed a remarkably dynamic metabolism, allowing them to shift between dormant and active metabolic state depending on the environmental temperature, diet, and hormonal status.

Protein degradation is a major pillar in maintaining proteostasis and metabolism, and appropriate protein turnover is essential in order to maintain healthy thermogenic adipocytes (12–14,17). The proteasome is important both for quality control of misshapen or damaged proteins as well as for determining the lifespan of proteins, and is, therefore, a key player in shaping the cellular proteome in response to nutritional and other environmental changes (18). The proteasome is a multi-meric complex composed of a 28-unit particle (20S, also called CP), which has a 'barrel-shaped' structure with a catalytic core, to which one or two regulatory particles can dock (19). The most common regulatory particle is the 19S particle (also called RP or PA700), which regulates substrate delivery to the 20S in an ubiquitin- and ATP-dependent manner (19,20). 20S associated with one or two 19S make up the constitutive 26S and 30S proteasome structures, respectively. The abundance of these complexes is partially under the transcriptional control of Nuclear factor erythroid 2-related factor-1 (Nfe2l1, also known as Nrf1 or TCF11) (21). 26S proteasome activity upheld and adapted by the transcriptional activity of Nfe2l1 is required for the matching proteasomal activity to the levels of ubiquitinated proteins generated by thermogenic adipocytes during cold and sustained NST (13). In addition to this transcriptional regulation, there also posttranslational mechanisms regulating proteasome activity. A class of regulatory proteins called proteasome activators (PAs) bind to 20S particles, giving rise to a variety of alternative proteasome complexes, whose functions are less well understood (22,23). The two cytosolic PAs are PA28αβ (also known as PA28, REG or 11S), and PA200 (also known as Blm10 in yeast). PA28αβ is a heptameric PA composed of four PA28α (encoded by *Psme1*) and three PA28β (encoded by *Psme2*) units (24), and are associated with the immune response and oxidative stress (23,25,26). PA200 (encoded by *Psme4*) is a large monomer (circa 200 kDa) that is implicated in the regulation of proteasome activity in the context of DNA repair (23,27–29). In previous work, we showed that Psme1 expression induces proteasome activity in mice (13).However, the function and importance of PAs for proteasome function and proteostasis in brown adipocyte is currently unknown. As the adaptive regulation of 26S proteasome activity is an essential part of NST and BAT function, we hypothesized that 20S-PAs structures play a role in this process. Here, we systematically investigate the roles of PA28αβ and PA200 in brown adipocytes by manipulating *Psme1* and *Psme4* expression in vitro.

2 Material & Methods

2.1 Mice husbandry and tissue collection

All animal experiments were performed with approval of the local authorities (License: ROB-55.2-22532.Vet_02-30-32). Mice were housed in individually ventilated cages at room temperature, with a 12-hour light/dark cycle, and fed chow diet (Sniff) and water ad libitum. For cold exposure, 12-week-old male C57BL/6J mice (purchased from Janvier) were exposed to 4 ℃ for seven days in a Memmert Climate Chamber HPP750 Life. For tissue collection, the afore-mentioned cold exposed mice and 16-week-old male mice with a C57BL/6J background were injected with a lethal dose of xylazine/ketamine (8/120 mg/kg mouse body weight). For primary cell collection, 6-week-old male C57BL/6J (Janvier) were killed by cervical dislocation. Interscapular and supraclavicular BAT was collected from the animals and freshly used for primary cell isolation.

2.2 Primary cell collection and culture

For primary cell culture, the collected BAT was first minced and then digested in DMEM/F-12 (Sigma-Aldrich, supplemented with 1.2 U/mL Dispase (Roche), 1 mg/mL collagenase type 2 (Worthington), 15 mg/mL fatty acid free BSA (Sigma-Aldrich), and 0.1 mg/mL DNase 1 (Roche)) at 37 ℃, on a shaker, for 30 minutes. The digestion was stopped by supplementing fetal bovine serum (FBS, Sigma-Aldrich). The suspension was filtered first through a 100 µM filter and then through a 30 µM filter. The stromal vascular fraction (SVF) was plated and cultured in DMEM/F-12 (supplemented with 10% v/v FBS and 1% v/v penicillin/streptomycin (Thermo Fisher Scientific)). The cells were incubated at 37 ℃, 5% CO_2. After reaching confluency, the pre-adipocytes were differentiated into mature brown adipocytes. From day 0 (confluence) to day 2, the cells received DMEM/F-12 supplemented with 1 µM dexamethasone (Sigma-Aldrich), 340 nM insulin (Sigma-Aldrich), 500 µM isobutylmethylxanthine (Sigma-Aldrich), 2 nM triiodothyronine (Sigma-Aldrich), and 1 µM rosiglitazone (Cayman). From day 2 until day 6, the cell received DMEM/F-12 supplemented with 10 nM insulin, 2 nM triiodothyronine, and 1 uM rosiglitazone. The medium was refreshed every other day.

2.3 Immortalised cell culture and treatment

The immortalised WT-1 mouse brown preadipocyte cell-line (kindly provided by Brice Emmanueli, University of Copenhagen) was grown in DMEM Glutamax (Thermo Fisher, supplemented with 10% v/v FBS and 1% v/v penicillin/streptomycin). After the pre-adipocytes reached confluency (day 0), their differentiation was induced with induction medium (DMEM Glutamax, supplemented with 860 nM insulin, 1 µM dexamethasone, 1 µM triiodothyronine, 1 µM rosiglitazone, 500 µM 3-isobutyl-1-methylxanthine, and 125 µM indomethacin (Sigma-Aldrich). After 48 hours, the induction medium was changed to differentiation medium (DMEM Glutamax, 1 µM triiodothyronine, 1 µM rosiglitazone). The differentiation medium was refreshed every other day. Cells were fully differentiated after 5-6 days. For target gene RNA inhibition (RNAi), cells received 30 nM SMARTpool silencing RNA (siRNA, Dharmacon) through reverse transfection with Lipofectamine RNAiMAX transfection reagent (Thermo Fisher) according to manufacturer's protocol. Transfection took place one day before induction (day -1). Cell treatments took place on day 5 of differentiation. Cells were treated with 100 nM Bortezomib (Sellect) for 6 or 24 hours, or 1 µM CL-316,143 (Tocris) for 3 hours, or dimethyl sulfoxide (DMSO) as control. Cells were harvested as pre-adipocytes (day 0), early brown adipocytes (day 3) or mature brown adipocytes (day 5-6). Unless mentioned otherwise, assays were performed on mature (day 5) adipocytes.

2.4   Gene expression analysis

RNA was extracted from tissues or cells with NucleoSpin RNA kit (Machery Nagel) according to the manufacturer's instructions, and RNA concentration was determined with NanoDrop (Thermo Fisher). RNA was synthesized into complementary DNA (cDNA) with Maxima H Master Mix (Thermo Fisher) according to the manufacturer's instructions. To measure gene expression, we combined 10 µg cDNA and 0.5 µM DNA primers with 5 µL PowerUp SYBR Green Master Mix (Applied Biosystems). To establish gene expression, the cycles thresholds (Ct) were calculated in Quant-Studio 5 RealTime PCR system (Thermo Fisher, standard conditions: 2 min on 50 °C, 10 min on 95 °C, 40 cycles of 15 s on 95 °C, and 1 min on 60 °C). Normalized virtual copy numbers were was calculated by normalizing the Cts of experimental genes to the Cts of the housekeeper gene *TATA-box binding protein* (*Tbp*) (Δ Ct). Relative gene expression was calculated by normalizing delta Ct of the experimental groups to the control groups (ΔΔ Ct). The primer sequences are listed in **Supplementary table 1**.

2.5   Protein isolation and analysis

The samples were collected in RIPA buffer (50 mM Tris (Merck, pH = 8), 150 mM NaCl (Merck), 0.1% w/v SDS (Carl Roth), 5 mM EDTA (Merck), and 0.5% w/v sodium-deoxycholate (Sigma–Aldrich)) freshly supplemented with a protease inhibitor (Sigma-Aldrich). Samples were lysed in a tissue lyser and then cells were centrifuged twice and tissue lysates were centrifuged three times for 30 min (4 °C, 21,000 *g*), to remove lipids and debris. Protein concentrations were determined with Pierce BCA assay (Thermo Fisher). Per sample, 15-30 µg proteins were denatured with 5 % v/v 2-mercaptoethanol (Sigma-Aldrich) for 5 min at 95 ℃. The denatured samples were loaded in a Bolt 4-12% Bis-Tris gel (Thermo Fisher). After separation, proteins were transferred onto a 0.2 µm PVDF membrane (Bio-Rad) using the Trans-Blot Turbo™ system (Bio-Rad, 25 V, 1.3 A for 7 min). The membrane was blocked in Roti-Block (Roth) for one hour at room temperature. The membranes were incubated overnight in primary antibody dilutions (1:1000 in Roti-block) at 4 ℃. The following primary antibodies were used: β-tubulin (Cell Signaling, 2146), Psmb4 (Santa Cruz, sc-390878), Psmd2 (Santa-Cruz, A-11), Psme1 (Abcam, ab3333), Psme4 (Thermo Fisher, PA1-1961), Nfe2l1 (Cell Signaling, 8052), Ubiquitin/P4D1 (Cell Signaling, 3936), Ucp1 (Abcam, ab10983), Hsp90 (Cell Signaling, 4877), and Proteasome 20S alpha 1+2+3+5+6+7 (Abcam, ab22674). The next day, the membrane was washed with TBS-T (200 mM Tris (Merck), 1.36 mM NaCl (Merck), 0.1% v/v Tween 20 (Sigma)), and incubated in secondary antibody (Santa Cruz) (1:10,000 in Roti-block) for 1h at room-temperature. The membranes were developed with SuperSignal West Pico PLUS Chemiluminescent Substrate (Thermo Fisher) in a Chemidoc MP imager (Bio-Rad). Full-size blot images are displayed in **Supplementary figure 2**.

2.6   Native PAGE: in-gel activity assay and immunoblot

The protocol for Native PAGE in-gel proteasome activity assay and subsequent immunoblotting was previously described in detail (15). Briefly, samples were lysed in OK-lysis buffer (50 mM Tris/HCl, pH = 7.5, 2 mM dithiothreitol, 5 mM $MgCl_2$ 10% v/v glycerol, 2 mM ATP, 0.05% v/v Digitonin (Thermo Fisher)), kept on ice for 20 minutes, and centrifuged thrice. 15 µg protein, determined with Bio-RAD Protein Assay Kit II, was loaded in a NuPAGE 3-8% Tris-Acetate gel (Thermo Fisher). The gel was run at a constant voltage of 150 V for four hours. The gel was then incubated in a reaction buffer (50 mM Tris, 1 mM $MgCl_2$, 1 mM dithiothreitol) for 30 minutes at 37 ℃. The fluorescence signal was measured in ChemiDoc MP. Next, the gel was prepared for protein transfer by 15 minutes incubation in a solubilization buffer (2% w/v SDS, 66 mM Na_2CO_3, 1.5% v/v

2-mercaptoethanol. The proteins were transferred to a PVDF membrane by 'wet' tank transfer (40 mA, overnight). The immunoblot was further treated as described above (see **2.5**). Full size blot images can be found in **Supplementary figure 2**.

2.7   Viability assay

AquaBlueR (MultiTarget Pharmaceuticals) was used to assess cell viability. Cells were incubated in 1:100 AquaBlueR for four hours at 37 ℃. Fluorescence was measured at 540/590 nm (excitation/emission) in a Spark 20M Plate reader (Tecan).

2.8   Lysate proteasome activity

Cells were lysed in lysis buffer (40 mM Tris (Merck, pH = 7.2), 50 nM NaCl (Merck), 5 mM $MgCl_2(6H_2O)$ (Merck), 10% v/v glycerol (Sigma), 2 mM ATP (Sigma), 2 mM 2-mercaptoethanol (Sigma)). Proteasome Activity Fluorometric Assay II Kit (UBPBio, J41110) was used according to the manufacturer's instructions to measure trypsin-like (T-L), chymotrypsin-like (CT-L), and caspase-like (C-L) proteasome activity. The fluorescent signaling was measured in the plate reader and the results were normalized to DNA with the Quant-iT PicoGreen dsDNA assay kit (Invitrogen, p7589), according to manufacturer's instructions.

2.9   Oil-Red-O (ORO) Staining

ORO staining was used to measure lipid content. Cells were washed with cold DPBS (Gibco), fixed in zinc formalin solution (Merck) for 15 minutes at room-temperature and again washed with 2-propanol (Merck). The cells were dried, incubated in 60% v/v ORO (Sigma) for 10 minutes at room-temperature followed by washing with water for 3-4 times. A picture of the plate was taken to visualize the lipid content. To measure absorption, ORO was eluted in 100% 2-propanol, and measured in the plate reader.

2.10   Free fatty acid release assay

To measure lipolysis in cell culture supernatants, Free Glycerol Reagent (Sigma F6428) and Glycerol standard solution (Sigma G7793) were used. Cell culture medium was collected to measure free glycerol content and the experiment was performed according to the manufacturer's instructions.

2.11   Extracellular Flux Analysis (Seahorse)

Oxygen consumption rate (OCR) was measured in a Seahorse XFe24 Analyzer (Agilent) and the assays performed as previously described (30). Briefly, we performed a Seahorse Cell Mito Stress Test (Agilent) largely according to manufacturer's instructions, but with the addition of a NE (1 μM) injection. There was no addition of BSA to the medium at any point. Two days before the assay, 20,000 adipocytes were seeded per well. During the assay, cells were consecutively treated with NE, oligomycin (1 μM), FCCP (4 μM), and Rotenone/Antimycin A (both 0.5 μM). Oxygen consumption was measured in intervals of 3 minutes. The results were normalized to total DNA levels which were measured with CyQuant Cell Proliferation Assay (C7026, Invitrogen) according to manufacturer's instructions. NE-induced respiration was calculated by subtracting maximum baseline OCR from maximum NE-induced OCR. Coupled respiration is baseline OCR minus OCR after oligomycin. Uncoupled respiration is OCR after oligomycin minus OCR after Rot/AA injection. Maximum respiration was calculated by subtracting minimum OCR, measured after Rot/AA injection, from maximum OCR, measured after FCCP injection.

2.12   Data analysis and visualization

All data was analyzed with Excel and GraphPad Prism. The raw data from the Seahorse was analyzed with Wave software (Agilent). Immunoblots were quantified with ImageLab (Bio-Rad). Data was visualized in GraphPad Prism. If not otherwise specified, data is represented as mean ± standard error of the mean (SEM). (Multiple) Student's t-test (with Bonferroni post-hoc test) was used to compare two groups with one variable. One-way ANOVA with Tukey post-hoc test was used to compare three groups with one variable. Two-ANOVA with Tukey post-hoc test was used to compare four groups with two different variables, i.e. for the double siRNA transfection experiments. Three-way ANOVA with Dunett's post-hoc test was used to compare more than four groups with more than two different variables, i.e. for the double siRNA transfection plus treatment experiments. P-values lower than 0.05 were considered significant. If groups are significantly different from each other, this is indicated in graphs either with an asterisk (*) or with different letters (a, b). If the same letter is used or if nothing is indicated, the groups are statistically indifferent from each other. The graphics were made in Biorender.com.

3.   Results

3.1   Proteasome activators are expressed in brown adipocytes

The remodeling of the constitutive proteasome is an essential component of brown adipocyte adaptation to sustained activation (13), but PAs are not part of the 26S/30S constitutive proteasome. Instead, they form hybrid shapes with the 20S core particle (22). It is unknown if PS are expressed in brown adipocytes, if proteasome hybrids are present in and if so, what their roles are in brown adipocyte biology. Therefore, we first assessed the levels of PAs in BAT, ex vivo and found that both *Psme1* and *Psme4* were abundantly expressed in the tissue (**Figure 1A**). Next, we measured *Psme1* and *Psme4* gene expression before and after brown adipocyte differentiation in primary cells obtained from the interscapular brown adipose tissue derived stromal fraction (SVF). Both genes were expressed in pre-adipocytes and mature brown adipocytes (**Figure 1B**). Following this, we determined if these genes were differentially expressed during states of BAT inactivity and BAT induction. Mice were exposed to either thermoneutrality (30 °C) or to cold (4 °C) for one week. Thermoneutrality initiates BAT whitening and cold activates non-shivering thermogenesis and promotes tissue browning. While *Psme1* and *Psme4* were expressed under both conditions, *Psme4* expression was highest in cold-exposed mice (**Figure 1C**). For the remainder of the experiments in this manuscript, we used an immortalized mouse brown pre-adipocyte cell line (Simplified model in **Figure 1D**). These pre-adipocytes differentiate into mature brown adipocytes within six days. After three days of induction, there was marked increase in expression of the adipogenesis markers *Adipoq*, *Cebpa*, *Fabp4,* and *Pparg*, as well as brown adipocyte marker *Ucp1* (**Figure 1E**). In these cells, we measured both gene expression and protein levels of Psme1 and Psme4 during different stages of cell differentiation. We found increased gene expression of *Psme1* and increased protein level of Psme1 during differentiation (**Figure 1F-G**). In contrast*, Psme4* expression did not change during differentiation, but protein Psme4 was only detectable in early and mature brown adipocytes, and not in pre-adipocytes. (**Figure 1F-G**). In summary, Psme1 and Psme4 are constitutively expressed in both pre-adipocytes and brown adipocytes, and Psme1 expression is induced during differentiation whilst Psme4 expression is induced with cold-induced activation in vivo.

47

3.2 The effect of loss of PAs on viability, stress, and inflammation

As the PAs Psme1 and Psme4 were present and regulated in brown adipocytes, we hypothesized that they could play a role in brown adipocyte function. In order to study their roles, we silenced *Psme1* and *Psme4* gene expression in brown adipocytes. We transfected cells before differentiation (day -1) with either *Psme1* siRNA, *Psme4* siRNA, or the combination of both. The knockdown successfully led to lower levels of gene expression and kept gene expression low even after differentiation (**Figure 2A**). This translated into an almost complete ablation of protein levels for both PAs (**Figure 2B**). First, we checked if silencing of PAs resulted in any impaired cell viability and found no effects of *Psme1* and/or *Psme4* gene silencing (**Figure 2C**). Additionally, we treated the cells with the chemical proteasome inhibitor bortezomib to measure bortezomib-induced cell death, as impairment of the proteasome or its regulation sensitizes cells to treatment with proteasome inhibitors (21,31). However, loss of Psme1 or Psme4 did not amplify bortezomib-induced cell death (**Figure 2D**). Finally, loss of PAs did not alter gene expression of *Ccl2*, a surrogate marker of adipocyte inflammation, nor that of *Atf3, Xbp1s, Herpud2*, or *Hspa5*, all surrogate markers of protein folding stress (**Figure 2E**) or in the transcription levels of the apoptosis marker *Ddit3* (**Figure 2E**). Overall, loss of Psme1 and or Psme4 did neither cause or enhance bortezomib-induced cell death nor provoke an overt stress response in the cells.

3.3 Loss of PAs does not impair UPS in brown adipocytes

PAs bind to 20S core particles, forming hybrid proteasomes, and, thus, PAs are implicated in regulating proteasome activity and substrate selection. To determine if manipulation of PAs impacts brown adipocyte proteostasis, we checked if *Psme1* and/or *Psme4* knockdown affected gene expression of proteasome transcription factor *Nfe2l1* or other proteasome subunits. We measured expression of several proteasome subunits to cover the different parts of the proteasome: *Psma3* and *Psmb6* as representative units of the 20S, *Psmd2* as part of the 19S regulatory particle, *Psme2* as part of the PA28αβ complex*, and *Psme3* for the nuclear PA28γ. We found no differences in any of these tested transcripts (**Figure 3A**). Correspondingly, we found no changes in protein levels of the seven α-subunits, ranging from Psma1 to Psma7, and of Psmb4 comparing controls cells and cells with *Psme1* and/or *Psme4* knockdown (**Figure 3B**). Additionally, both baseline and bortezomib-induced Nfe2l1 protein levels were unchanged, and both full-length and short-length forms were present in the brown adipocytes (**Figure 3C**). Global ubiquitin levels, as a marker for proteostatic stress and modulation of UPS, were similar between control and experimental groups (**Figure 3B**). To directly measure proteasome activity, we used two distinct methods. For the first approach, we measured trypsin-like, chymotrypsin-like, and caspase-like activity in whole-cell lysates after gene knockdown (**Figure 3D**). For the second approach, we loaded non-denatured proteins in a Native PAGE. This allowed us to visualize the 20S, 26S and 30S proteasome with in-gel proteasome activity and then subsequently quantify protein levels by immunoblotting. In line with the unchanged ubiquitin levels, we also found no impairment in proteasome activity, neither in in-gel chymotrypsin-like activity nor in α1-α7 protein levels (**Figure 3E**). We also investigated if stressing proteostasis with proteasome inhibitor bortezomib under knock-down conditions would result in altered respiration. While bortezomib treatment impaired mitochondrial respiration, this effect was not affected by silencing of Psme1 or Psme4 (**Supplementary Figure 1A-B**). Overall, this set of experiments demonstrated that Psme1 and Psme4 are dispensable for proteasome availability and function in brown adipocytes.

3.4 Loss of PAs does not affect adipogenesis or brown adipocyte function

Finally, to determine the effect of PAs on brown adipocyte-specific biology, we studied the effects of loss of PAs on brown adipocyte development and function. *Psme1* and/or *Psme4* knockdown did not affect expression of the adipocyte markers *Adipoq*, *Cebpa, Fabp4*, and *Pparg* (**Figure 4A**). However, there was a non-significant trend for lower *Ucp1* mRNA expression in cells with si*Psme4* (**Figure 4A**). Next, lipid content was measured as an indicator for net adipogenesis and lipogenesis. ORO staining showed that lipid content was not lower in the knock-down groups compared to the control groups (**Figure 4B-C**). As brown adipocytes induce lipolysis to fuel heat production (3), we measured cell culture supernatant glycerol levels before and after stimulation with the β3-adrenergic agonist CL-316,243. The glycerol release assay showed no effects upon loss of Psme1 and/or Psme4 (**Figure 4D)**. Finally, we measured oxygen consumption rate (OCR) to measure sympathetic response and global cellular respiration. NE-induced respiration was used to measure cellular NST-capacity in vitro. NE-induced respiration was not different between groups, nor was maximum respiratory capacity, suggesting that there were no significant changes in mitochondrial abundance and health (**Figure 4E-F**). Even stressing the system with Bortezomib treatment did not differentially affect knock-down groups compared to the control group (Figure 4 G). Taking these results together, we found no evidence that loss of PAs impaired adipocyte function.

4 Discussion

Brown adipocytes undergo cellular remodeling during thermogenic activation (1), and in order to sustain NST, an appropriate protein turnover is required (14). Although the role of the constitutive 26S proteasome in BAT and NST has been studied previously (13), the role of other proteasome types remains elusive. In this study, we investigated the roles of Psme1/PA28α and Psme4/PA200 in brown adipocyte differentiation and function. We found that *Psme1* and *Psme4* were constitutively expressed in brown pre-adipocytes and mature adipocytes, which alludes to a significant role in brown adipocyte proteostasis. However, in our model of cultured adipocytes, loss of Psme1 and/or Psme4 protein by RNAi did not affect viability or led to a marked stress response in the cells. Moreover, even though we saw minor effects on proteasome activity, UPS and proteostasis remained functional. Finally, neither differentiation nor activation of brown adipocytes was impaired after silencing of *Psme1* and/or *Psme4*. We conclude that in our experimental settings, Psme1 and Psme4 are dispensable for cultured brown adipocytes.

There are limitations to our model and approach that should be noted. Firstly, the experiments were performed in an immortalized brown adipocyte cell line, which cannot mimic the biological complexity and natural regulation of BAT activation or remodeling observed in vivo in mice or humans. An adipocyte-specific transgenic deletion mouse model could provide insight into the physiological roles of PAs, but these models have not yet been established. This cell model allowed for basic study of the role of PAs in adipocytes, but did not characterize PAs under different physiological conditions, e.g. nutrient deprivation, inflammation, nor did it take into account cell-cell interactions or systemic effects. Secondly, we limited our study to Psme1 and Psme4, leaving the other proteasome activators subunits Psme2 and Psme3 out of the scope of this study. Admittedly, as PA28αβ consists of Psme1 and Psme2 subunits, it is possible that sole loss of Psme1 would result in an alternative PA28 form with residual activity. However, this PA-variant is thought to be less stable and active, and it is unknown if there is a physiological relevance (24). Furthermore, there could also be compensation mechanism through Psme3 activation, but as Psme3 is a nuclear PA instead of cytosolic, we estimated this chance as low (22). Finally, we used siRNA to knockdown gene expression and this method

does not completely ablate protein levels. Even though we observed marked near to complete loss of protein for both Psme1 and Psme4, it is possible that a remaining low expression of *Psme1/Psme4* was sufficient to sustain a residual activity. However, we have previously shown that the same experimental strategy resulted in efficient ablation of 20S subunit Psmb4, which disrupted proteostasis, adipocyte differentiation, and thermogenesis (30). In addition, a separate study showed that siRNA-mediated manipulation of Psme4 affected myofibroblast differentiation (32). This indicates that the experimental RNAi strategy is capable of targeting both constitute and adaptive proteasome subunits and investigate their role for brown adipocyte differentiation and activity.

Regardless, the roles of Psme1 and Psme4 in regulating proteasome function and protein degradation are not well-established. Based on their structures, both PA28αβ and PA200 are thought to stimulate the insertion of unfolded proteins or peptides into the 20S proteasomes (22,23). Also, PA28αβ is associated with the immunoproteasome, a specific type of proteasome that specifically degrades proteins for antigen-presentation (25,26). However, mice lacking Psme1/Psme2 display no growth abnormalities or obvious health problems (33). In a study with triple-knockout mice, ablation of Psme1, Psme2 and nuclear Psme3/PA28γ (gene: *Psme3*), the researchers found reduced proteasome activity and exacerbated high-fat diet-induced hepatic dysfunction (34), even though the cause of this metabolic phenotype remains unclear. Also, the function of Psme4 is still being debated, but it is associated with the process of DNA repair (27,28) and was shown to play a role in myofibroblast differentiation (32). Whole-body Psme4 knock-out did not result in an overt phenotype, but showed impaired spermatogenesis and infertility (35,36). These studies with whole-body knock-out mouse models did not investigate or report any BAT or NST phenotype (32–36), leaving it as an open question if they participate in adipocyte biology in vivo. Although we found that Psme1 and Psme4 were not required in brown adipocytes in vitro under standard conditions, they may play a role in specific cellular stress responses. Based on its implication of immunoproteasome regulation, Psme1 may play a role in the immune response of the adipocyte, but the role of immunoproteasome formation in adipocytes is unknown, too. Alternatively, Psme1 and or Psme4 could be recruited in response to specific stressors, for example in the adaptive proteasome response against oxidative stress, proteasome autophagy or ferroptosis (37). Interestingly, it was observed that overexpression of Psme1 enhances proteasome activity in obese mouse models when proteasome function was compromised (13). Further scrutiny of the PAs in different contexts will contribute to our understanding of their functions and mechanisms and should determine if and how PAs play a role in adipocytes in vivo. In conclusion, our data reveal that, even though expressed high robust levels, Psme1 and Psme4 are dispensable for proteostasis, adipogenesis, and thermogenesis in cultured brown adipocytes.

5   Conflict of Interest

The authors declare that the research was conducted in the absence of any commercial or financial relationships that could be construed as a potential conflict of interest.

6   Author Contributions

AB and NW designed and supervised the study. ZK and NW performed the experiments, analyzed the data, and prepared the figures. AB supervised the study and analyzed the data. The authors wrote the manuscript together.

7 Funding

8 Acknowledgments

9 Contribution to the field statement

Brown adipocytes in brown adipose tissue (BAT) and beige adipocytes in white adipose tissue are thermogenic adipocytes that generate heat by uncoupling mitochondrial activity from ATP production. In response to sustained cold, these cells undergo remodeling to meet the thermogenic demand of the organism. In humans, BAT activity is associated with increased energy expenditure and improved cardio-metabolic health. Here, to elucidate the cellular remodeling that underlies BAT activity, we study protein degradation via the proteasome. The proteasome is a barrel-like structure with catalytic activity that can bind to proteasome regulators and activators that regulate the access of proteins to this barrel. We determined the relevance of proteasome activators 28α (PA28α, encoded by *Psme1*) and 200 (Pa200, encoded by *Psme4*) in brown adipocytes. Both the mechanistic and physiological functions of PAs are unclear, and their roles in (brown) adipocytes have not been studied until now. We studied PA28α/Psme1 and PA200/Psme4 by manipulating their expression in cultured brown adipocytes. We found that loss of *Psme1* and/or *Psme4* did not disrupt protein metabolism or proteasome activity. Additionally, we found that PAs are not required for brown adipocyte development or activity. Altogether, our data contributes to the basic understanding of PAs in brown adipocyte cell biology.

10 Abbreviations

Abbreviation	Definition
BAT	Brown adipose tissue
DMSO	Dimethyl sulfoxide
FCCP	Carbonyl cyanide p-trifluoro-methoxyphenyl hydrazone
NE	Norepinephrine
Nfe2l1	Nuclear factor erythroid 2-related factor 1

NST	Non-shivering-thermogenesis
Omy	Oligomycin
ORO	Oil-Red O
PA	Proteasome activator
Psm	Proteasome subunit
Psme1-4	Proteasome activator complex subunit 1-4
Rot/AA	Rotenone/Antimycin A
Ucp1	Uncoupling protein 1
UPS	Ubiquitin proteasome system

11 Reference list

1. Cannon B, Nedergaard J. Brown Adipose Tissue: Function and Physiological Significance. Physiol Rev. 2004 Jan;84(1):277–359.

2. Wu J, Boström P, Sparks LM, Ye L, Choi JH, Giang AH, et al. Beige Adipocytes Are a Distinct Type of Thermogenic Fat Cell in Mouse and Human. Cell. 2012 Jul;150(2):366–76.

3. Giroud M, Jodeleit H, Prentice KJ, Bartelt A. Adipocyte function and the development of cardiometabolic disease. J Physiol. 2022 Mar;600(5):1189–208.

4. Roesler A, Kazak L. UCP1-independent thermogenesis. Biochem J. 2020 Feb 14;477(3):709–25.

5. Li Y, Schnabl K, Gabler SM, Willershäuser M, Reber J, Karlas A, et al. Secretin-Activated Brown Fat Mediates Prandial Thermogenesis to Induce Satiation. Cell. 2018 Nov 29;175(6):1561-1574.e12.

6. Sveidahl Johansen O, Ma T, Hansen JB, Markussen LK, Schreiber R, Reverte-Salisa L, et al. Lipolysis drives expression of the constitutively active receptor GPR3 to induce adipose thermogenesis. Cell. 2021 Jun;184(13):3502-3518.e33.

7. Christen L, Broghammer H, Rapöhn I, Möhlis K, Strehlau C, Ribas-Latre A, et al. Myoglobin-mediated lipid shuttling increases adrenergic activation of brown and white adipocyte metabolism and is as a marker of thermogenic adipocytes in humans. Clin Transl Med [Internet]. 2022 Dec [cited 2023 Feb 27];12(12). Available from: https://onlinelibrary.wiley.com/doi/10.1002/ctm2.1108

8. Bartelt A, Bruns OT, Reimer R, Hohenberg H, Ittrich H, Peldschus K, et al. Brown adipose tissue activity controls triglyceride clearance. Nat Med. 2011 Feb;17(2):200–5.

9. Jung SM, Sanchez-Gurmaches J, Guertin DA. Brown Adipose Tissue Development and Metabolism. In: Pfeifer A, Klingenspor M, Herzig S, editors. Brown Adipose Tissue [Internet]. Cham: Springer International Publishing; 2018 [cited 2020 Aug 26]. p. 3–36. (Handbook of Experimental Pharmacology; vol. 251). Available from: http://link.springer.com/10.1007/164_2018_168

10. Cypess AM, Lehman S, Williams G, Tal I, Rodman D, Goldfine AB, et al. Identification and Importance of Brown Adipose Tissue in Adult Humans. N Engl J Med. 2009 Apr 9;360(15):1509–17.

11. Becher T, Palanisamy S, Kramer DJ, Eljalby M, Marx SJ, Wibmer AG, et al. Brown adipose tissue is associated with cardiometabolic health. Nat Med. 2021 Jan;27(1):58–65.

12. Altshuler-Keylin S, Shinoda K, Hasegawa Y, Ikeda K, Hong H, Kang Q, et al. Beige Adipocyte Maintenance Is Regulated by Autophagy-Induced Mitochondrial Clearance. Cell Metab. 2016 Sep;24(3):402–19.

13. Bartelt A, Widenmaier SB, Schlein C, Johann K, Goncalves RLS, Eguchi K, et al. Brown adipose tissue thermogenic adaptation requires Nrf1-mediated proteasomal activity. Nat Med. 2018 Mar;24(3):292–303.

14. Bartelt A, Widenmaier SB. Proteostasis in thermogenesis and obesity. Biol Chem [Internet]. 2019 Dec 1 [cited 2020 Feb 20];0(0). Available from: http://www.degruyter.com/view/j/bchm.just-accepted/hsz-2019-0427/hsz-2019-0427.xml

15. Foley KP, Chen Y, Barra NG, Heal M, Kwok K, Tamrakar AK, et al. Inflammation promotes adipocyte lipolysis via IRE1 kinase. J Biol Chem. 2021 Jan;296:100440.

16. Chen Y, Wu Z, Huang S, Wang X, He S, Liu L, et al. Adipocyte IRE1α promotes PGC1α mRNA decay and restrains adaptive thermogenesis. Nat Metab. 2022 Sep 19;4(9):1166–84.

17. Madhavan A, Kok BP, Rius B, Grandjean JMD, Alabi A, Albert V, et al. Pharmacologic IRE1/XBP1s activation promotes systemic adaptive remodeling in obesity. Nat Commun. 2022 Dec;13(1):608.

18. Goldberg AL. Protein degradation and protection against misfolded or damaged proteins. Nature. 2003 Dec;426(6968):895–9.

19. Finley D. Recognition and Processing of Ubiquitin-Protein Conjugates by the Proteasome. Annu Rev Biochem. 2009 Jun;78(1):477–513.

20. Martinez-Fonts K, Davis C, Tomita T, Elsasser S, Nager AR, Shi Y, et al. The proteasome 19S cap and its ubiquitin receptors provide a versatile recognition platform for substrates. Nat Commun. 2020 Dec;11(1):477.

21. Radhakrishnan SK, Lee CS, Young P, Beskow A, Chan JY, Deshaies RJ. Transcription Factor Nrf1 Mediates the Proteasome Recovery Pathway after Proteasome Inhibition in Mammalian Cells. Mol Cell. 2010 Apr;38(1):17–28.

22. Stadtmueller BM, Hill CP. Proteasome Activators. Mol Cell. 2011 Jan;41(1):8–19.

23. Coux O, Zieba BA, Meiners S. The Proteasome System in Health and Disease. In: Barrio R, Sutherland JD, Rodriguez MS, editors. Proteostasis and Disease [Internet]. Cham: Springer International Publishing; 2020 [cited 2023 Jan 23]. p. 55–100. (Advances in Experimental Medicine and Biology; vol. 1233). Available from: http://link.springer.com/10.1007/978-3-030-38266-7_3

24. Huber EM, Groll M. The Mammalian Proteasome Activator PA28 Forms an Asymmetric α4β3 Complex. Structure. 2017 Oct;25(10):1473-1480.e3.

25. Pickering AM, Koop AL, Teoh CY, Ermak G, Grune T, Davies KJA. The immunoproteasome, the 20S proteasome and the PA28αβ proteasome regulator are oxidative-stress-adaptive proteolytic complexes. Biochem J. 2010 Dec 15;432(3):585–95.

26. Seifert U, Bialy LP, Ebstein F, Bech-Otschir D, Voigt A, Schröter F, et al. Immunoproteasomes Preserve Protein Homeostasis upon Interferon-Induced Oxidative Stress. Cell. 2010 Aug;142(4):613–24.

27. Burris A, Waite KA, Reuter Z, Ockerhausen S, Roelofs J. Proteasome activator Blm10 levels and autophagic degradation directly impact the proteasome landscape. J Biol Chem. 2021 Jan;296:100468.

28. Ustrell V. PA200, a nuclear proteasome activator involved in DNA repair. EMBO J. 2002 Jul 1;21(13):3516–25.

29. Yazgili AS, Ebstein F, Meiners S. The Proteasome Activator PA200/PSME4: An Emerging New Player in Health and Disease. Biomolecules. 2022 Aug 20;12(8):1150.

30. Willemsen N, Arigoni I, Studencka-Turski M, Krüger E, Bartelt A. Proteasome dysfunction disrupts adipogenesis and induces inflammation via ATF3. Mol Metab. 2022 Aug;62:101518.

31. Sha Z, Goldberg AL. Proteasome-Mediated Processing of Nrf1 Is Essential for Coordinate Induction of All Proteasome Subunits and p97. Curr Biol. 2014 Jul;24(14):1573–83.

32. Welk V, Meul T, Lukas C, Kammerl IE, Mulay SR, Schamberger AC, et al. Proteasome activator PA200 regulates myofibroblast differentiation. Sci Rep. 2019 Dec;9(1):15224.

33. Murata S. Immunoproteasome assembly and antigen presentation in mice lacking both PA28alpha and PA28beta. EMBO J. 2001 Nov 1;20(21):5898–907.

34. Otoda T, Takamura T, Misu H, Ota T, Murata S, Hayashi H, et al. Proteasome Dysfunction Mediates Obesity-Induced Endoplasmic Reticulum Stress and Insulin Resistance in the Liver. Diabetes. 2013 Mar 1;62(3):811–24.

35. Khor B, Bredemeyer AL, Huang CY, Turnbull IR, Evans R, Maggi LB, et al. Proteasome Activator PA200 Is Required for Normal Spermatogenesis. Mol Cell Biol. 2006 Apr 15;26(8):2999–3007.

36. Huang L, Haratake K, Miyahara H, Chiba T. Proteasome activators, PA28γ and PA200, play indispensable roles in male fertility. Sci Rep. 2016 Mar 22;6(1):23171.

37. Kotschi S, Jung A, Willemsen N, Ofoghi A, Proneth B, Conrad M, et al. NFE2L1-mediated proteasome function protects from ferroptosis. Mol Metab. 2022 Mar;57:101436.
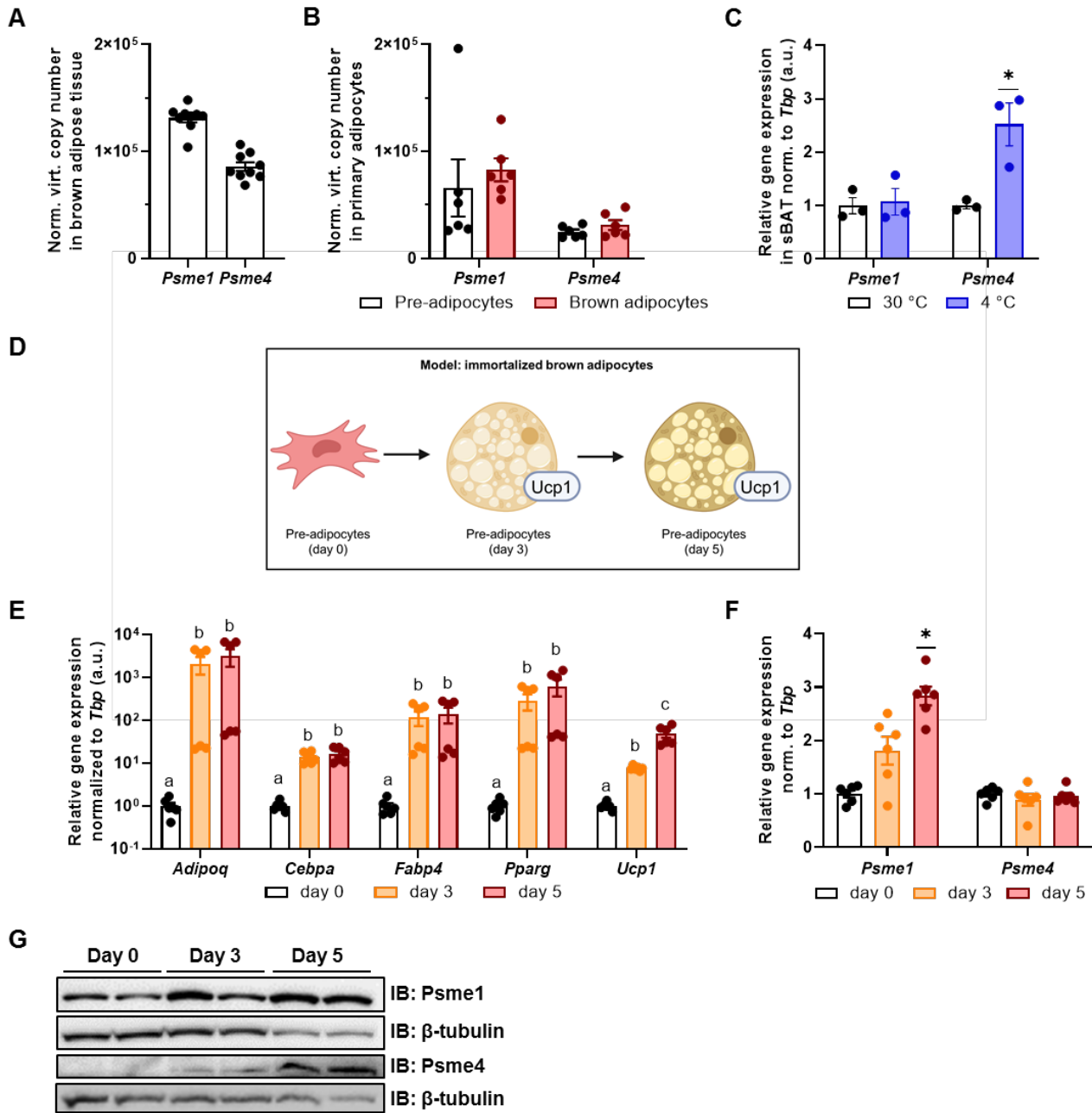
Figure 1: Psme1 and Psme4 expression in brown fat and brown adipocytes. **A-B)** Normalized gene expression of *Psme1* and *Psme4* in **(A)** brown adipose tissue (BAT) (n = 9 biological replicates), and **(B)** primary brown pre-adipocytes and mature adipocytes (n = 6 biological replicates). **C)** Relative gene expression of Psme1/Psme4 in BAT after cold exposure (1 week at 4 °C) (n = 3 biological replicates). **D)** Summary of experimental model made in Biorender.com. **E)** Relative gene expression of *Adipoq, Cebpa, Fabp4, Pparg* and *Ucp1* in immortalized brown adipocytes in different stages of development: pre-adipocytes (day 0), early adipocytes (day 3), and mature adipocytes (day 5). (n = 6 measurements pooled from two independent experiments). **F)** Relative gene expression of *Psme1* and *Psme4* in immortalized brown adipocytes in different stages of development: pre-adipocytes (day-0), early adipocytes (day 3), and mature adipocytes (day 5). (n = 6 measurements pooled from two independent experiments). **G)** Representative immunoblots showing Psme1, Psme4 and β-tubulin. Data are represented as mean ± SEM. Data are significant if $P < 0.05$, which is indicated with an asterisk (*) or by different letters (a, b).

55
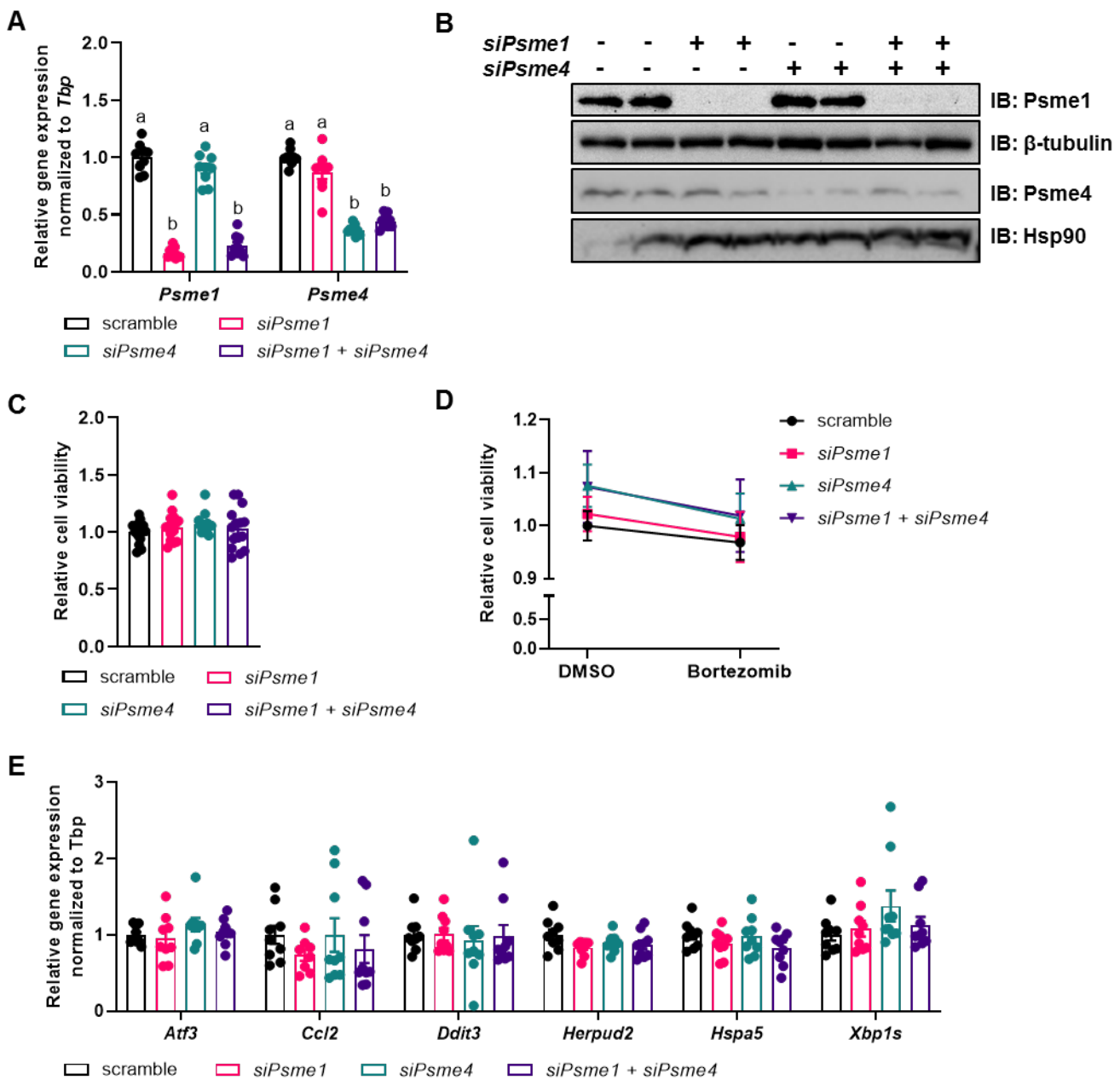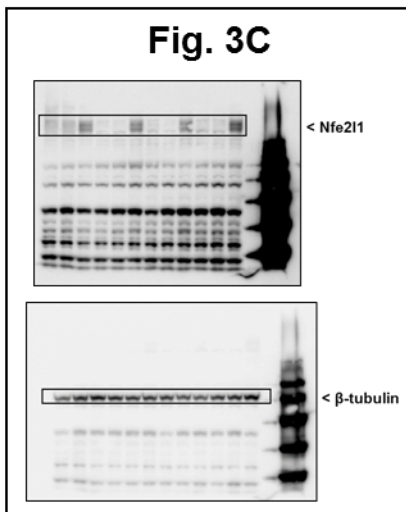
Figure 2: Silencing of Psme1 and/or Psme4 had no effect on viability. **A)** Relative gene expression of *Psme1* and *Psme4* after transfection with si*Psme1* and/or si*Psme4*. **B)** Representative immunoblots showing Psme1, Psme4, β-tubulin and Hsp90. **C)** Relative cell viability after transfection measured with AquaBlueR (n = 15 measurements pooled from three independent experiments). **D)** Relative survival after treatment with DMSO or Bortezomib (100 nM for 16 h) measured with AquaBlueR. (Mean of n = 15 measurements pooled from three independent experiments). **E)** Relative gene expression of inflammation and stress markers. Genes measured are *Atf3*, *Ccl2*, *Ddit3*, *Herpud2*, *Hspa5*, *Xbp1s.* Graphs show. Unless indicated otherwise, n = 9 measurements pooled from three independent experiments. Data are represented as mean ± SEM. Data are significant if $P < 0.05$, which is indicated with an asterisk (*) or by different letters (a, b).
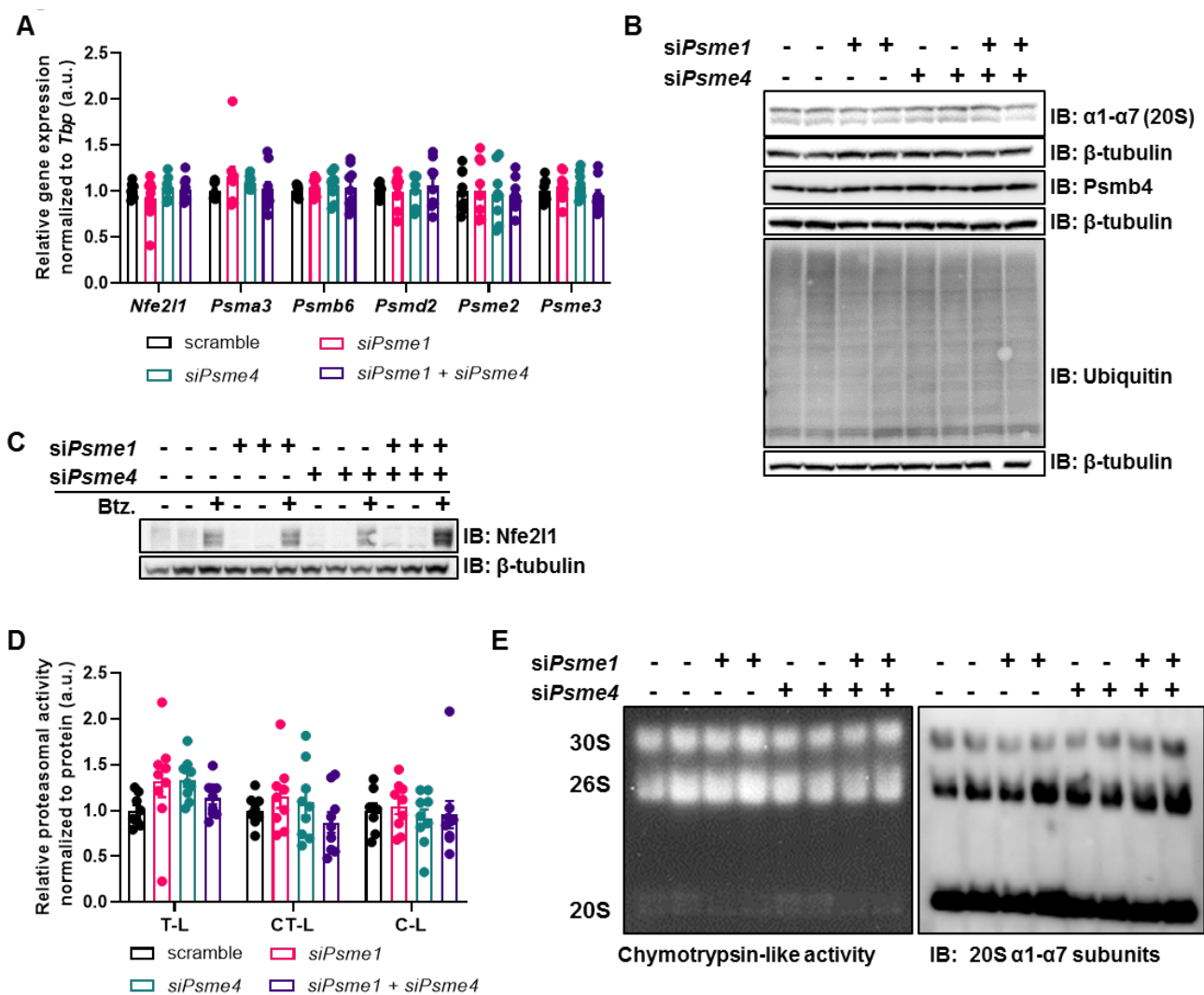
Figure 3: The effects of Psme1/Psme4 knockdown on proteasome activity. A) Relative gene expression of *Nfe2l1* and proteasome subunits *Psma3*, *Psmb6*, *Psmd2*, and *Psme3*, in brown adipocytes after transfection with si*Psme1* and/or si*Psme4*. **B)** Representative immunoblots with protein levels of Psmd2, Psmb4, α1-α7, and β-tubulin. **C)** Representative immunoblots with protein levels of Nfe2l1 and β-tubulin after treating cells with DMSO or Bortezomib (100 nM, 6 h). **D)** Proteasome activity of chymotrypsin-like (CT-L), trypsin-like (T-L) and caspase-like (C-L) activity. **E)** Representative native PAGE with in-gel CT-L-activity and immunoblot with α1-α7 (20S) staining. Unless indicated otherwise, n = 9 measurements pooled from three independent experiments. Data are represented as mean ± SEM. Data are significant if $P < 0.05$, which is indicated with an asterisk (*).
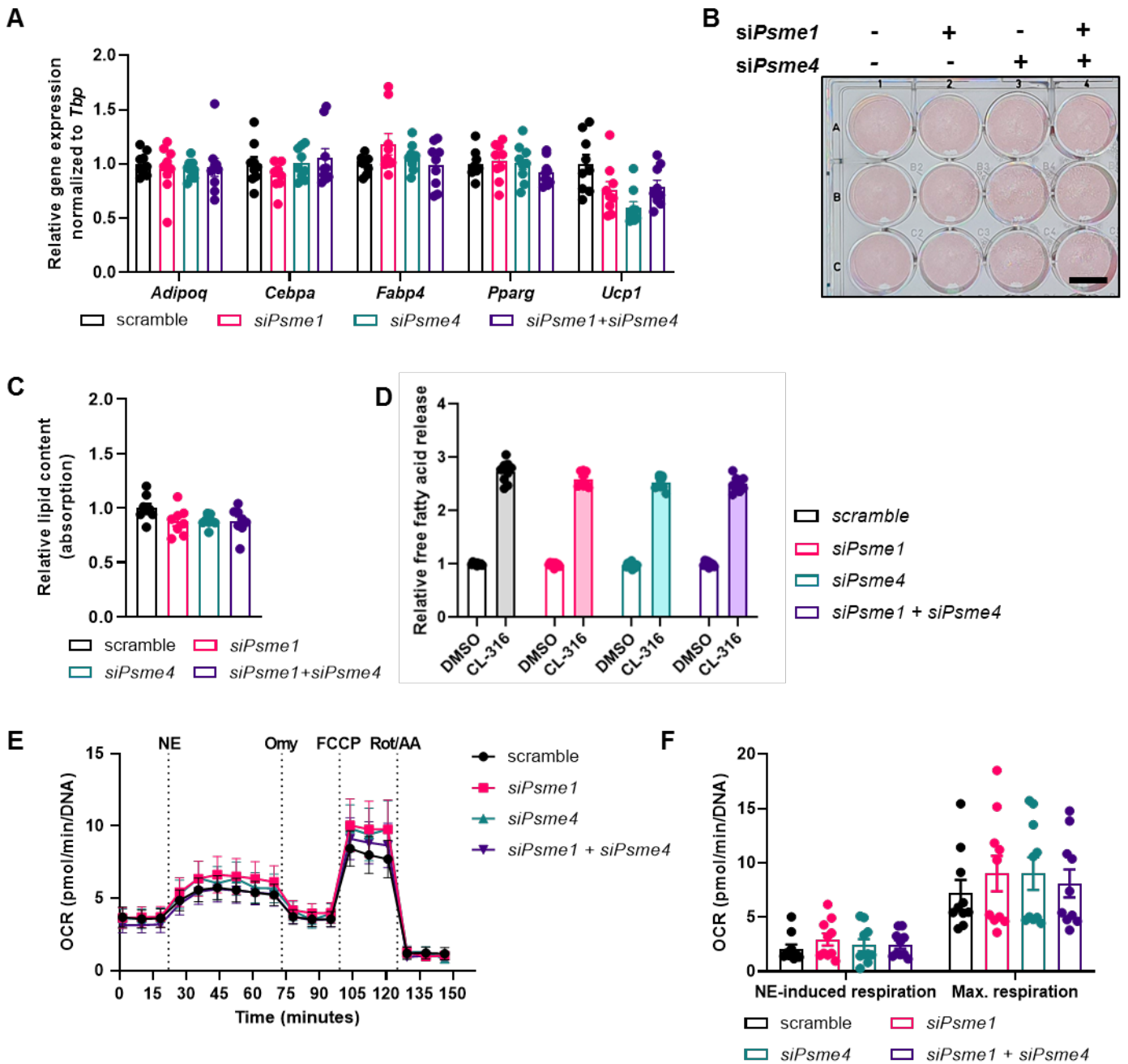
Figure 4: Loss of Psme1/Psme4 did not impair adipocyte function. **A)** Relative gene expression of adipocyte markers in brown adipocytes after transfection with si*Psme1* and/or si*Psme4*. Genes: measured: *Adipoq, Cebpa, Fabp4, Pparg* and *Ucp1*. **B)** Representative Oil-Red-O staining and **(C)** relative lipid content measured as absorption. Scale bar in image equals 1 cm. **D)** Relative free fatty acid levels in medium after cell treatment with DMSO or CL-316,243 (CL-316) (1 µM, 3 hours). **E-F)** Oxygen consumption rate (OCR) during NE treatment and mitochondrial stress test, normalized to DNA levels (n = 8 measurements pooled from two independent experiments). NE: norepinephrine, Omy: oligomycin, FCCP: carbony cyanide p-trifluoro-methoxyphenyl hydrazone, Rot/AA: rotenone/ antimycin A. Unless indicated otherwise, n = 9 measurements pooled from three independent experiments. Data are represented as mean ± SEM. Data are significant if *P* < 0.05, which is indicated with an asterisk (*).
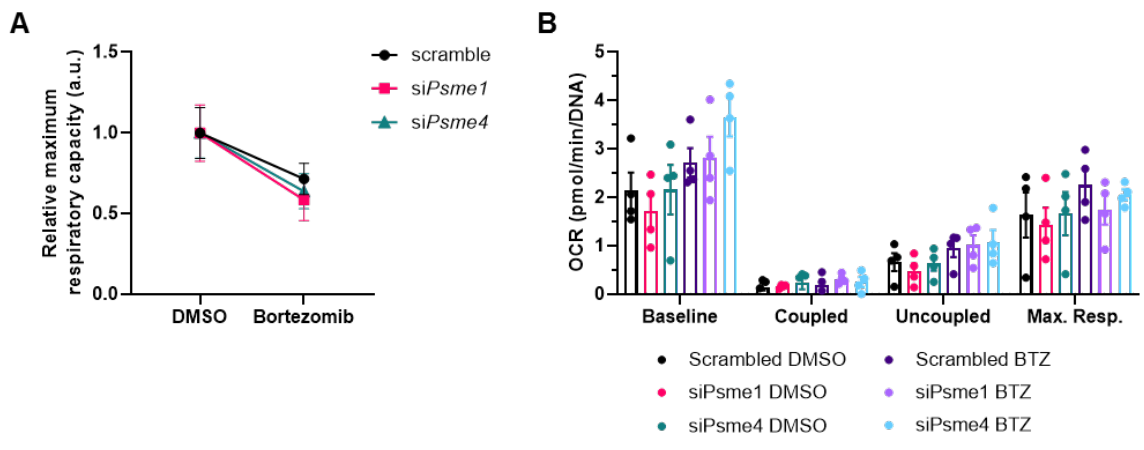
Supplementary figure 1: A) Relative maximum respiratory capacity of Bortezomib treated cells compared to DMSO treated cells. Treatment was either DMSO or 100 nM Bortezomib for 16 hours pre-ceding the mitochondrial stress test. Maximum respiratory capacity is maximum OCR measured after FCCP treatment minus OCR after Rot/A treatment, before DNA normalization (n = 4). **B)** Oxygen consumption rate (OCR) from mitochondrial stress test, normalized to DNA levels (n = 4). Max. Resp. = Maximum Respiratory capacity. Data are represented as mean ± SEM. Data are significant if $P < 0.05$, which is indicated with an asterisk

Fig. 1G
< Psme1
< β-tubulin
< Psme4
< β-tubulin

Fig. 2B
< Psme1
< β-tubulin
< Psme4
< Hsp90

Fig. 3B
< Psmb4
< β-tubulin
< β-tubulin
< α1-α7 (20S)
Ubiquitin
< β-tubulin

Fig. 3C
< Nfe2l1
< β-tubulin

Fig. 3E
α1-α7 (20S)
Chymotrypsin-like activity
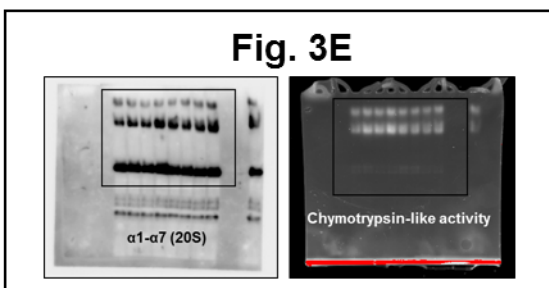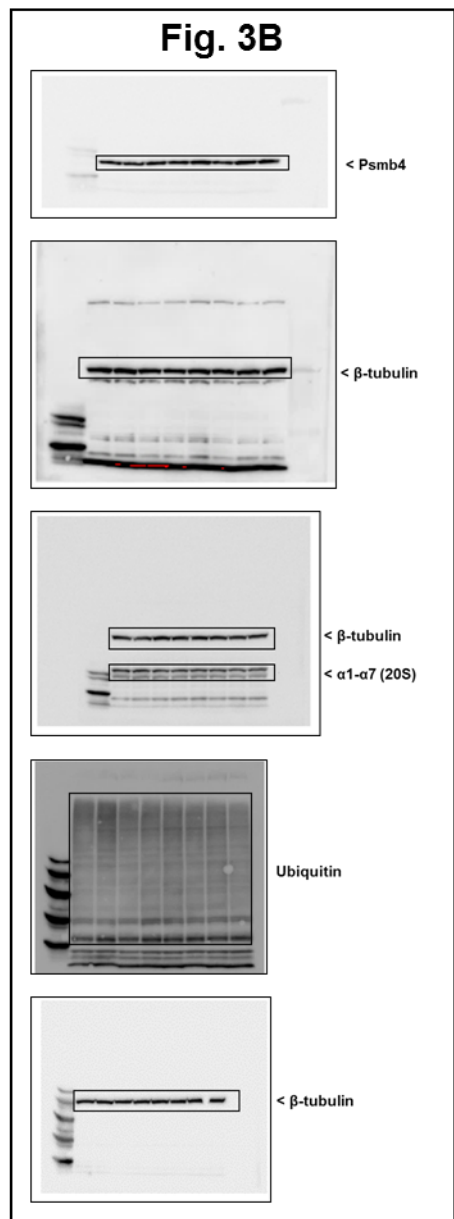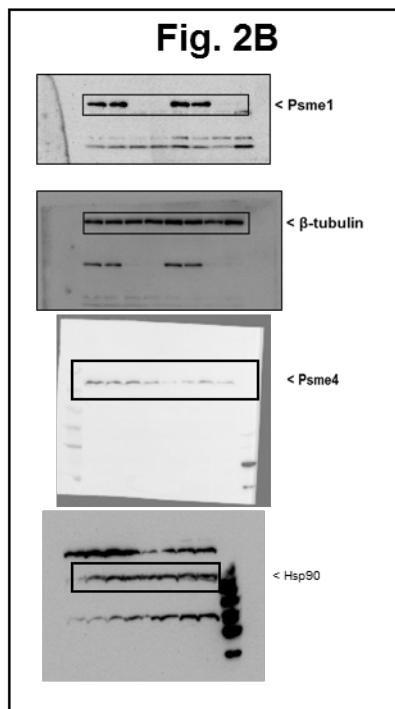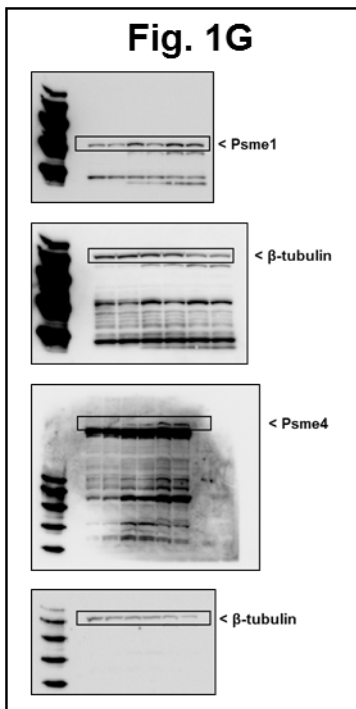
Supplementary figure 2: Uncropped pictures from immunoblots.

Supplementary table 1: Primers used for qPCR.

Primer	Forward sequence (5' to 3')	Reverse sequence (5' to 3')
Adipoq	GGAGAGAAAGGAGATGCAGGT	CTTTCCTGCCAGGGGTTC
Atf3	GAGGATTTTGCTAACCTGACACC	TTGACGGTAACTGACTCCAGC
Ccl2	TTAAAAACCTGGATCGGAACCAA	GCATTAGCTTCAGATTTACGGGT
Cebpa	AAACAACGCAACGTGGAGA	GCGGTCATTGTCACTGGTC
Ddit3	CTGGAAGCCTGGTATGAGGAT	CAGGGTCAAGAGTAGTGAAGGT
Fabp4	GGATGGAAAGTCGACCACAA	TGGAAGTCACGCCTTTCATA
Herpud2	ATGGACCAAAGTGGGATGGAG	TCAATGGTTTGCTAGGGTACAC
Hspa5	TCATCGGACGCACTTGGAA	CAACCACCTTGAATGGCAAGA
Nfe2l1	GACAAGATCATCAACCTGCCTGTAG	GCTCACTTCCTCCGGTCCTTTG
Pparg	TCGCTGATGCACTGCCTATG	GAGAGGTCCACAGAGCTGATT
Psma3	GAAGCAGAGAAATATGCCAAGG	GCAACTGTTACAGAAATGTAAACCA
Psmb6	GAAAACCGGGAAGTCTCCAC	CTCGATTGGCGATGTAGGAC
Psmd2	AATGGGAGATTCCAAGTCCA	TGACATCTCCATTGCAGGAC
Psme1	ATAATTTTGGCGTGGCTGTC	TGGAGATCTGCGTGTGGA
Psme2	GGGTGGCAATTCAGGAGA	CTACAGCGTCCCCTCGTTC
Psme3	CACTGTCACAGAGATTGATGAGAA	GGATCATGTCATGGAGAGTGAC
Psme4	CCTCACACAATGTTCCAAAGAC	GAAACAGAAAAGTTAAAGACCTTCTGA
Tbp	AGAACAATCCAGACTAGCAGCA	GGGAACTTCACATCACAGCTC
Ucp1	AGGCTTCCAGTACCATTAGGT	CTGAGTGAGGCAAAGCTGATTT
Xbp1s	GGTCTGCTGAGTCCGCAGCAGG	AGGCTTGGTGTATACATGG

10. References

The figures in this manuscript were made with Biorender.com and the first draft of the German summary was made with DeepL algorithm.

1. Willemsen N, Arigoni I, Studencka-Turski M, Krüger E, Bartelt A. Proteasome dysfunction disrupts adipogenesis and induces inflammation via ATF3. Mol Metab. 2022 Aug;62:101518.

2. Koçberber Z, Willemsen N, Bartelt A. The role of proteasome activators PA28αβ and PA200 in brown adipocyte differentiation and function. Front Endocrinol. 2023 May 2;14:1176733.

3. Hruby A, Hu FB. The Epidemiology of Obesity: A Big Picture. PharmacoEconomics. 2015 Jul;33(7):673–89.

4. Giroud M, Jodeleit H, Prentice KJ, Bartelt A. Adipocyte function and the development of cardiometabolic disease. J Physiol. 2022 Mar;600(5):1189–208.

5. Rosen ED, Spiegelman BM. What We Talk About When We Talk About Fat. Cell. 2014 Jan;156(1–2):20–44.

6. Cannon B, Nedergaard J. Brown Adipose Tissue: Function and Physiological Significance. Physiol Rev. 2004 Jan;84(1):277–359.

7. Oelkrug R, Polymeropoulos ET, Jastroch M. Brown adipose tissue: physiological function and evolutionary significance. J Comp Physiol B. 2015 Aug;185(6):587–606.

8. Sun W, Dong H, Balaz M, Slyper M, Drokhlyansky E, Colleluori G, … Wolfrum C. snRNA-seq reveals a subpopulation of adipocytes that regulates thermogenesis. Nature. 2020 Nov 5;587(7832):98–102.

9. Sanchez-Gurmaches J, Guertin DA. Adipocytes arise from multiple lineages that are heterogeneously and dynamically distributed. Nat Commun. 2014 Sep;5(1):4099.

10. Seale P, Bjork B, Yang W, Kajimura S, Chin S, Kuang S, … Spiegelman BM. PRDM16 controls a brown fat/skeletal muscle switch. Nature. 2008 Aug;454(7207):961–7.

11. Wang W, Seale P. Control of brown and beige fat development. Nat Rev Mol Cell Biol. 2016 Nov;17(11):691–702.

12. Bartelt A, Heeren J. Adipose tissue browning and metabolic health. Nat Rev Endocrinol. 2014 Jan;10(1):24–36.

13. Von Essen G, Lindsund E, Cannon B, Nedergaard J. Adaptive facultative diet-induced thermogenesis in wild-type but not in UCP1-ablated mice. Am J Physiol-Endocrinol Metab. 2017 Nov 1;313(5):E515–27.

14. Li Y, Schnabl K, Gabler SM, Willershäuser M, Reber J, Karlas A, … Klingenspor M. Secretin-Activated Brown Fat Mediates Prandial Thermogenesis to Induce Satiation. Cell. 2018 Nov 29;175(6):1561-1574.e12.

15. Xu X, Ying Z, Cai M, Xu Z, Li Y, Jiang SY, … Sun Q. Exercise ameliorates high-fat diet-induced metabolic and vascular dysfunction, and increases adipocyte progenitor cell population in brown adipose tissue. Am J Physiol-Regul Integr Comp Physiol. 2011 May;300(5):R1115–25.

16. Martins FF, Marinho TS, Cardoso LEM, Barbosa-da-Silva S, Souza-Mello V, Aguila MB, Mandarim-de-Lacerda CA. Semaglutide (GLP-1 receptor agonist) stimulates browning on subcutaneous fat adipocytes and mitigates inflammation and endoplasmic reticulum stress in visceral fat adipocytes of obese mice. Cell Biochem Funct. 2022 Dec;40(8):903–13.

17. Bartelt A, Bruns OT, Reimer R, Hohenberg H, Ittrich H, Peldschus K, … Heeren J. Brown adipose tissue activity controls triglyceride clearance. Nat Med. 2011 Feb;17(2):200–5.

18. Park G, Haley JA, Le J, Jung SM, Fitzgibbons TP, Korobkina ED, … Guertin DA. Quantitative analysis of metabolic fluxes in brown fat and skeletal muscle during thermogenesis. Nat Metab. 2023 Jun 19;5(7):1204–20.

19. Nedergaard J, Von Essen G, Cannon B. Brown adipose tissue: can it keep us slim? A discussion of the evidence for and against the existence of diet-induced thermogenesis in mice and men. Philos Trans R Soc B Biol Sci. 2023 Oct 23;378(1888):20220220.

20. Bachman ES, Dhillon H, Zhang CY, Cinti S, Bianco AC, Kobilka BK, Lowell BB. βAR Signaling Required for Diet-Induced Thermogenesis and Obesity Resistance. Science. 2002 Aug 2;297(5582):843–5.

21. Sveidahl Johansen O, Ma T, Hansen JB, Markussen LK, Schreiber R, Reverte-Salisa L, … Gerhart-Hines Z. Lipolysis drives expression of the constitutively active receptor GPR3 to induce adipose thermogenesis. Cell. 2021 Jun;184(13):3502-3518.e33.

22. Gavaldà-Navarro A, Villarroya J, Cereijo R, Giralt M, Villarroya F. The endocrine role of brown adipose tissue: An update on actors and actions. Rev Endocr Metab Disord [Internet]. 2021 Mar 12;

23. Wang GX, Zhao XY, Meng ZX, Kern M, Dietrich A, Chen Z, … Lin JD. The brown fat–enriched secreted factor Nrg4 preserves metabolic homeostasis through attenuation of hepatic lipogenesis. Nat Med. 2014 Dec;20(12):1436–43.

24. Jung SM, Sanchez-Gurmaches J, Guertin DA. Brown Adipose Tissue Development and Metabolism. In: Brown Adipose Tissue [Internet]. Cham: Springer International Publishing; 2018. p. 3–36. (Handbook of Experimental Pharmacology; vol. 251).

25. Cao W, Daniel KW, Robidoux J, Puigserver P, Medvedev AV, Bai X, Floering LM, Spiegelman BM, Collins S. p38 Mitogen-Activated Protein Kinase Is the Central Regulator of Cyclic AMP-Dependent Transcription of the Brown Fat Uncoupling Protein 1 Gene. Mol Cell Biol. 2004 Apr 1;24(7):3057–67.

26. Olsen JM, Csikasz RI, Dehvari N, Lu L, Sandström A, Öberg AI, Nedergaard J, Stone-Elander S, Bengtsson T. β 3 -Adrenergically induced glucose uptake in brown adipose tissue is independent of UCP1 presence or activity: Mediation through the mTOR pathway. Mol Metab. 2017 Jun;6(6):611–9.

27. Heine M, Fischer AW, Schlein C, Jung C, Straub LG, Gottschling K, … Heeren J. Lipolysis Triggers a Systemic Insulin Response Essential for Efficient Energy Replenishment of Activated Brown Adipose Tissue in Mice. Cell Metab. 2018 Oct;28(4):644-655.e4.

28. Keipert S, Kutschke M, Ost M, Schwarzmayr T, Van Schothorst EM, Lamp D, … Jastroch M. Long-Term Cold Adaptation Does Not Require FGF21 or UCP1. Cell Metab. 2017 Aug;26(2):437-446.e5.

29. Kazak L, Chouchani ET, Jedrychowski MP, Erickson BK, Shinoda K, Cohen P, … Spiegelman BM. A Creatine-Driven Substrate Cycle Enhances Energy Expenditure and Thermogenesis in Beige Fat. Cell. 2015 Oct;163(3):643–55.

30. Oeckl J, Janovska P, Adamcova K, Bardova K, Brunner S, Dieckmann S, … Klingenspor M. Loss of UCP1 function augments recruitment of futile lipid cycling for thermogenesis in murine brown fat. Mol Metab. 2022 Jul;61:101499.

31. Ikeda K, Kang Q, Yoneshiro T, Camporez JP, Maki H, Homma M, … Kajimura S. UCP1-independent signaling involving SERCA2b-mediated calcium cycling regulates beige fat thermogenesis and systemic glucose homeostasis. Nat Med. 2017 Dec 1;23(12):1454–65.

32. Christen L, Broghammer H, Rapöhn I, Möhlis K, Strehlau C, Ribas-Latre A, … Weiner J. Myoglobin-mediated lipid shuttling increases adrenergic activation of brown and white adipocyte metabolism and is as a marker of thermogenic adipocytes in humans. Clin Transl Med [Internet]. 2022 Dec;12(12).

33. Willemsen N, Bartelt A. Breathe and burn: Novel roles for myoglobin in thermogenesis. Clin Transl Discov. 2022 Dec;2(4):e153.

34. Cypess AM, Lehman S, Williams G, Tal I, Rodman D, Goldfine AB, … Kahn CR. Identification and Importance of Brown Adipose Tissue in Adult Humans. N Engl J Med. 2009 Apr 9;360(15):1509–17.

35. Van Marken Lichtenbelt WD, Vanhommerig JW, Smulders NM, Drossaerts JMAFL, Kemerink GJ, Bouvy ND, Schrauwen P, Teule GJJ. Cold-Activated Brown Adipose Tissue in Healthy Men. N Engl J Med. 2009 Apr 9;360(15):1500–8.

36. Becher T, Palanisamy S, Kramer DJ, Eljalby M, Marx SJ, Wibmer AG, … Cohen P. Brown adipose tissue is associated with cardiometabolic health. Nat Med. 2021 Jan;27(1):58–65.

37. Fernández-Verdejo R, Marlatt KL, Ravussin E, Galgani JE. Contribution of brown adipose tissue to human energy metabolism. Mol Aspects Med. 2019 Aug;68:82–9.

38. Carpentier AC, Blondin DP, Virtanen KA, Richard D, Haman F, Turcotte ÉE. Brown Adipose Tissue Energy Metabolism in Humans. Front Endocrinol. 2018 Aug 7;9:447.

39. Geerling JJ, Boon MR, Van Der Zon GC, Van Den Berg SAA, Van Den Hoek AM, Lombès M, … Guigas B. Metformin Lowers Plasma Triglycerides by Promoting VLDL-Triglyceride Clearance by Brown Adipose Tissue in Mice. Diabetes. 2014 Mar 1;63(3):880–91.

40. U Din M, Saari T, Raiko J, Kudomi N, Maurer SF, Lahesmaa M, … Virtanen KA. Postprandial Oxidative Metabolism of Human Brown Fat Indicates Thermogenesis. Cell Metab. 2018 Aug;28(2):207-216.e3.

41. Liu X, Wang S, You Y, Meng M, Zheng Z, Dong M, … Jin W. Brown Adipose Tissue Transplantation Reverses Obesity in Ob/Ob Mice. Endocrinology. 2015 Jul 1;156(7):2461–9.

42. Bel JS, Tai TC, Khaper N, Lees SJ. Mirabegron: The most promising adipose tissue beiging agent. Physiol Rep [Internet]. 2021 Mar;9(5).

43. Wang Q, Zhang M, Xu M, Gu W, Xi Y, Qi L, Li B, Wang W. Brown Adipose Tissue Activation Is Inversely Related to Central Obesity and Metabolic Parameters in Adult Human. PLOS ONE. 2015 Apr 20;10(4):e0123795.

44. Lemmer IL, Willemsen N, Hilal N, Bartelt A. A guide to understanding endoplasmic reticulum stress in metabolic disorders. Mol Metab. 2021 Jan;101169.

45. Pohl C, Dikic I. Cellular quality control by the ubiquitin-proteasome system and autophagy. Science. 2019 Nov 15;366(6467):818–22.

46. Finley D. Recognition and Processing of Ubiquitin-Protein Conjugates by the Proteasome. Annu Rev Biochem. 2009 Jun 1;78(1):477–513.

47. Coux O, Tanaka K, Goldberg AL. STRUCTURE AND FUNCTIONS OF THE 20S AND 26S PROTEASOMES. Annu Rev Biochem. 1996 Jun;65(1):801–47.

48. Tanaka K. The proteasome: Overview of structure and functions. Proc Jpn Acad Ser B. 2009;85(1):12–36.

49. Oh E, Akopian D, Rape M. Principles of Ubiquitin-Dependent Signaling. Annu Rev Cell Dev Biol. 2018 Oct 6;34(1):137–62.

50. Hoeller D, Crosetto N, Blagoev B, Raiborg C, Tikkanen R, Wagner S, … Dikic I. Regulation of ubiquitin-binding proteins by monoubiquitination. Nat Cell Biol. 2006 Feb;8(2):163–9.

51. Collins GA, Goldberg AL. The Logic of the 26S Proteasome. Cell. 2017 May;169(5):792–806.

52. Lu Y, Lee B hoon, King RW, Finley D, Kirschner MW. Substrate degradation by the proteasome: A single-molecule kinetic analysis. Science. 2015 Apr 10;348(6231):1250834.

53. Braten O, Livneh I, Ziv T, Admon A, Kehat I, Caspi LH, … Ciechanover A. Numerous proteins with unique characteristics are degraded by the 26S proteasome following monoubiquitination. Proc Natl Acad Sci [Internet]. 2016 Aug 9;113(32).

54. Peth A, Uchiki T, Goldberg AL. ATP-Dependent Steps in the Binding of Ubiquitin Conjugates to the 26S Proteasome that Commit to Degradation. Mol Cell. 2010 Nov;40(4):671–81.

55. Peth A, Kukushkin N, Bossé M, Goldberg AL. Ubiquitinated proteins activate the proteasomal ATPases by binding to Usp14 or Uch37 homologs. J Biol Chem. 2013 Mar 15;288(11):7781–90.

56. Radhakrishnan SK, Lee CS, Young P, Beskow A, Chan JY, Deshaies RJ. Transcription Factor Nrf1 Mediates the Proteasome Recovery Pathway after Proteasome Inhibition in Mammalian Cells. Mol Cell. 2010 Apr;38(1):17–28.

57. Steffen J, Seeger M, Koch A, Krüger E. Proteasomal degradation is transcriptionally controlled by TCF11 via an ERAD-dependent feedback loop. Mol Cell. 2010 Oct 8;40(1):147–58.

58. Koizumi S, Irie T, Hirayama S, Sakurai Y, Yashiroda H, Naguro I, Ichijo H, Hamazaki J, Murata S. The aspartyl protease DDI2 activates Nrf1 to compensate for proteasome dysfunction. eLife. 2016 Aug 16;5:e18357.

59. Lehrbach NJ, Breen PC, Ruvkun G. Protein Sequence Editing of SKN-1A/Nrf1 by Peptide:N-Glycanase Controls Proteasome Gene Expression. Cell. 2019 Apr;177(3):737-750.e15.

60. Northrop A, Byers HA, Radhakrishnan SK. Regulation of NRF1, a master transcription factor of proteasome genes: implications for cancer and neurodegeneration. Mol Biol Cell. 2020 Sep 15;31(20):2158–63.

61. Sha Z, Goldberg AL. Proteasome-Mediated Processing of Nrf1 Is Essential for Coordinate Induction of All Proteasome Subunits and p97. Curr Biol. 2014 Jul;24(14):1573–83.

62. Griffin TA, Nandi D, Cruz M, Fehling HJ, Kaer LV, Monaco JJ, Colbert RA. Immunoproteasome Assembly: Cooperative Incorporation of Interferon γ (IFN-γ)–inducible Subunits. J Exp Med. 1998 Jan 5;187(1):97–104.

63. Kloetzel PM, Ossendorp F. Proteasome and peptidase function in MHC-class-I-mediated antigen presentation. Curr Opin Immunol. 2004 Feb;16(1):76–81.

64. Cui Z, Hwang SM, Gomes AV. Identification of the Immunoproteasome as a Novel Regulator of Skeletal Muscle Differentiation. Mol Cell Biol. 2014 Jan 1;34(1):96–109.

65. Abi Habib J, De Plaen E, Stroobant V, Zivkovic D, Bousquet MP, Guillaume B, … Van Den Eynde BJ. Efficiency of the four proteasome subtypes to degrade ubiquitinated or oxidized proteins. Sci Rep. 2020 Sep 25;10(1):15765.

66. Sahu I, Mali SM, Sulkshane P, Xu C, Rozenberg A, Morag R, … Glickman MH. The 20S as a standalone proteasome in cells can degrade the ubiquitin tag. Nat Commun. 2021 Dec;12(1):6173.

67. Ustrell V. PA200, a nuclear proteasome activator involved in DNA repair. EMBO J. 2002 Jul 1;21(13):3516–25.

68. Rechsteiner M, Hill CP. Mobilizing the proteolytic machine: cell biological roles of proteasome activators and inhibitors. Trends Cell Biol. 2005 Jan;15(1):27–33.

69. Raynes R, Pomatto LCD, Davies KJA. Degradation of oxidized proteins by the proteasome: Distinguishing between the 20S, 26S, and immunoproteasome proteolytic pathways. Mol Aspects Med. 2016 Aug;50:41–55.

70. Huber EM, Groll M. The Mammalian Proteasome Activator PA28 Forms an Asymmetric α4β3 Complex. Structure. 2017 Oct;25(10):1473-1480.e3.

71. Pickering AM, Koop AL, Teoh CY, Ermak G, Grune T, Davies KJA. The immunoproteasome, the 20S proteasome and the PA28αβ proteasome regulator are oxidative-stress-adaptive proteolytic complexes. Biochem J. 2010 Dec 15;432(3):585–95.

72. Seifert U, Bialy LP, Ebstein F, Bech-Otschir D, Voigt A, Schröter F, … Krüger E. Immunoproteasomes Preserve Protein Homeostasis upon Interferon-Induced Oxidative Stress. Cell. 2010 Aug;142(4):613–24.

73. Burris A, Waite KA, Reuter Z, Ockerhausen S, Roelofs J. Proteasome activator Blm10 levels and autophagic degradation directly impact the proteasome landscape. J Biol Chem. 2021 Jan;296:100468.

74. Yazgili AS, Ebstein F, Meiners S. The Proteasome Activator PA200/PSME4: An Emerging New Player in Health and Disease. Biomolecules. 2022 Aug 20;12(8):1150.

75. Chan JY. Targeted disruption of the ubiquitous CNC-bZIP transcription factor, Nrf-1, results in anemia and embryonic lethality in mice. EMBO J. 1998 Mar 16;17(6):1779–87.

76. Shi CX, Zhu YX, Bruins LA, Bonolo De Campos C, Stewart W, Braggio E, Stewart AK. Proteasome Subunits Differentially Control Myeloma Cell Viability and Proteasome Inhibitor Sensitivity. Mol Cancer Res. 2020 Oct 1;18(10):1453–64.

77. Torrelo A, Patel S, Colmenero I, Gurbindo D, Lendínez F, Hernández A, … Paller AS. Chronic atypical neutrophilic dermatosis with lipodystrophy and elevated temperature (CANDLE) syndrome. J Am Acad Dermatol. 2010 Mar;62(3):489–95.

78. Ebstein F, Poli Harlowe MC, Studencka-Turski M, Krüger E. Contribution of the Unfolded Protein Response (UPR) to the Pathogenesis of Proteasome-Associated Autoinflammatory Syndromes (PRAAS). Front Immunol. 2019 Nov 26;10:2756.

79. Kanazawa N. Nakajo-Nishimura Syndrome: An Autoinflammatory Disorder Showing Pernio-Like Rashes and Progressive Partial Lipodystrophy. Allergol Int. 2012;61(2):197–206.

80. Papendorf JJ, Ebstein F, Alehashemi S, Piotto DGP, Kozlova A, Terreri MT, … Krüger E. Identification of eight novel proteasome variants in five unrelated cases of proteasome-associated autoinflammatory syndromes (PRAAS). Front Immunol. 2023 Aug 4;14:1190104.

81. Kitamura A, Maekawa Y, Uehara H, Izumi K, Kawachi I, Nishizawa M, … Yasutomo K. A mutation in the immunoproteasome subunit PSMB8 causes autoinflammation and lipodystrophy in humans. J Clin Invest. 2011 Oct 3;121(10):4150–60.

82. Brehm A, Liu Y, Sheikh A, Marrero B, Omoyinmi E, Zhou Q, … Goldbach-Mansky R. Additive loss-of-function proteasome subunit mutations in CANDLE/PRAAS patients promote type I IFN production. J Clin Invest. 2015 Oct 20;125(11):4196–211.

83. Arima K, Kinoshita A, Mishima H, Kanazawa N, Kaneko T, Mizushima T, … Yoshiura K ichiro. Proteasome assembly defect due to a proteasome subunit beta type 8 (PSMB8) mutation causes the auto-inflammatory disorder, Nakajo-Nishimura syndrome. Proc Natl Acad Sci. 2011 Sep 6;108(36):14914–9.

84. Boyadzhiev M, Marinov L, Boyadzhiev V, Iotova V, Aksentijevich I, Hambleton S. Disease course and treatment effects of a JAK inhibitor in a patient with CANDLE syndrome. Pediatr Rheumatol. 2019 Dec;17(1):19.

85. Bartelt A, Widenmaier SB, Schlein C, Johann K, Goncalves RLS, Eguchi K, … Hotamisligil GS. Brown adipose tissue thermogenic adaptation requires Nrf1-mediated proteasomal activity. Nat Med. 2018 Mar;24(3):292–303.

11. Acknowledgements

12. Curriculum vitae

Personal Information

Name: Nienke Willemsen

Phone:

Date of birth: 09-07-1995

Email: nienke.willemsen@med.uni-muenchen.de

Nationality: Dutch

LinkedIn: https://linkedin.com/in/nienke-w-778108103/

Research

Jan. 2020 – ongoing   **Ludwig-Maximilians-Universität München Hospital**,
Munich (Germany)

PhD candidate at the Institute for Cardiovascular Prevention (IPEK)

Supervisor: Prof. Dr. Alexander Bartelt

Project: "Dynamic regulation of the brown adipose tissue proteasome"

2019 (6 months)   **University of Copenhagen**, Copenhagen (Denmark)

Research internship at the Center for Basic Metabolic Research

Supervisor: Dr. Zach Gerhart-Hines

Project: "Alternative activation of brown adipocytes through a novel G-protein-coupled-receptor"

2018 (6 months)   **University of Amsterdam**, Amsterdam (the Netherlands)

Research internship at the Laboratory for Genetic Metabolic Diseases.

Supervisor: Prof. Dr. Riekelt Houtkooper

Project: "Designing a high-fat diet for ageing research in *C. elegans*"

Education

Sep. 2017 – Oct. 2019 Leiden University, Leiden (the Netherlands)

Master of Science: Biomedical Sciences

Sep. 2013 – Aug. 2016 Amsterdam University College, Amsterdam (the Netherlands)

Bachelor of Science: Liberal Arts & Sciences, *cum laude*

List of publications

Publications that are part of the thesis:

Willemsen N, Arigoni I, Studencka-Turski M, Krüger E, Bartelt A. Proteasome dysfunction disrupts adipogenesis and induces inflammation via ATF3. *Mol. Metab*. May 2022, 101518.

Koçberber Z*, Willemsen N*, Bartelt A. The role of proteasome activators PA28αβ and PA200 in brown adipocyte differentiation and function. *Frontiers in Endocrinology*. May 2023, 2;14:1176733.

Additional research articles:

Kotschi S, Jung A, <u>Willemsen N</u>, Ofoghi A, Proneth B, Conrad M, Bartelt A. NFE2L1-mediated proteasome function protects from ferroptosis. *Mol. Metab*. Jan 2022; 101436.

Sveidahl Johansen O, Ma T, Hansen JB, Markussen LK, Schreiber R, Reverte-Salisa L, -Dong H, Christensen PD, Sun W, Gnad TH, Karavaeava I, Nielsen TS, Kooijman S, Cero C, Dmytriyeva O, Shen Y, Razzoli M, O'Brien SL, Kuipers EN, Nielsen CH, Orchard W, <u>Willemsen N</u>, Jespersen NZ, Lundh M, Sustarsic EG, Hallgren CM, Frost M, McGonigle S, Isidor MS, Broholm C, Pedersen O, Hansen JB, Grarup N, Nielsen S, Rydén M, Soccio R, Rensen PCN, Treebak JT, Schwartz TW, Emanuelli B, Bartolomucci A, Pfeifer A, Zechner R, Scheele C, Mandrup S, Gerhart-Hines Z. Lipolysis drives expression of the constitutively active receptor GPR3 to induce adipose thermogenesis. *Cell*. 2021 Jun; 184(13):3502-3518.e33

Reviews and comments:

<u>Willemsen N</u>, Bartelt A. Breathe and burn: Novel roles for myoglobin in thermogenesis. *Clinical and Translational Discover*. Dec 2022; 2 (4), e153.

<u>Willemsen N</u>*, Kotschi S*, Bartelt A. Fire up the pyre: inosine thermogenic signalling for obesity therapy. *STTT*. Dec 2022; 7(1), 1-2.

Lemmer IL*, <u>Willemsen N</u>*, Hilal N, Bartelt A. A guide to understanding endoplasmic reticulum stress in metabolic disorders. *Mol Metab*. 2021 Jan;101169

Pre-prints:

Ofoghi A, Kotschi S, Lemmer IL, Haas DT, <u>Willemsen N</u>, Bayer B, Moeller S, Haberecht-Mueller S, Krueger E, Krahmer N, Bartelt A. Activating the NFE2L1-ubiquitin-proteasome system by DDI2 protects from ferroptosis. *bioRxiv*, 2023.07. 04.547652

Lemmer IL, Haas DT, <u>Willemsen N</u>, Kotschi S, Toksoez I, Gjika E, Khani S, Rohm M, Diercksen N, Nguyen PBH, Menden MP, Egu DT, Waschke J, Larsen S, Ma T, Gerhart-Hines Z, Herzig S, Dyar K, Krahmer N, Bartelt A. Nfe2l1-mediated proteasome function controls muscle energy metabolism in obesity. *bioRxiv*, 2023.04. 20.537611

*shared first authorship

Conference talks

2023   Helmholtz Diabetes Conference (Munich, Germany)

        Dutch Translational Metabolism Conference (Wageningen, the Netherlands)

2021   XXII Lipid Meeting (Leipzig, Germany – virtual)

2020   European Lipoprotein Club (Tutzing, Germany)

Conference poster presentations

2022   European Lipoprotein Club (Tutzing, Germany) (*winner poster prize*)

        Keystone: Adipose Tissue and Metabolic Health (Whistler, Canada)

        CPH BAT (Copenhagen, Denmark)

        Ubiquitin & Friends (Würzburg, Germany)

        GRK2243 on Ubiquitin (Vienna, Austria)

2021   European Lipoprotein Club (Tutzing, Germany)

Parameters of esteem

2022   ELC Young Investigator Poster Award

2019   Amsterdam Gastroenterology & Metabolism International Student Fellowship

Certifications

2018   FELESA B Animal handling certificate